Functional Analysis of Notch Signaling during Vertebrate Retinal Development

Advisor: Constance L. Cepko Karolina Mizeracka

Functional analysis of Notch signaling during vertebrate retinal development

Abstract

The process of cell fate determination, which establishes the vastly diverse set of neural cell types found in the central nervous system, remains poorly understood. During retinal development, multipotent retinal progenitor cells generate seven major cell types, including photoreceptors, interneurons, and glia, in an ordered temporal sequence. The behavior of these progenitor cells is influenced by the Notch pathway, a widely utilized signal during embryogenesis which can regulate proliferation and cell fate decisions. To examine the underlying genetic changes that occur when *Notch1* is removed from individual retinal cells, microarray analysis of single cells from wild type or *Notch1* conditional knockout retinas was performed. *Notch1* deficient cells downregulated progenitor and cell cycle marker genes, while robustly upregulating genes associated with rod genesis. Single wild type cells expressed markers of both rod photoreceptors and interneurons, suggesting that these cells were in a transitional state.

In order to examine the role of Notch signaling in cell fate specification separate from its role in proliferation, *Notch1* was genetically removed specifically from newly postmitotic cells. *Notch1* deficient cells preferentially became cone photoreceptors at embryonic stages, and rod photoreceptors at postnatal stages. In both cases, this cell fate change occurred at the expense of the other cell types normally produced at that time. In addition, single cell profiling revealed that *Inhibitor of differentiation 1* and *3* genes were robustly downregulated in *Notch1* deficient cells. Ectopic expression of these genes during postnatal development in wild type retinas was sufficient to drive production of

progenitor/Müller glial cells. Moreover, *Id1* and *3* partially rescued the production of Müller glial cells and bipolar cells in the absence of *Notch1,* even in newly postmitotic cells. We propose that after cell cycle exit, retinal precursor cells transition through a period in which they express marker genes of several different cell types as they commit to a fate, likely endowed by their progenitor cell. Specifically, cells that will become bipolars or Müller glia depend on Id-mediated Notch signaling during this transitional state to take on their respective fates.

This work is dedicated to my family:

My grandparents, my parents, and Raphael

Acknowledgements

I would like to thank all the members of the Cepko-Tabin and Dymecki labs for their scientific advice, emotional support, and constant supply of hilarity and fun during my graduate school years.

Connie Cepko has been an amazing mentor for me. All of our interactions made it clear that she was greatly invested in my progress, partly because my project was a mix of her favorite things: retinal progenitor cells, Notch signaling, viruses, and single cell profiling, but also because she cared about my development as a scientist on a personal level. A deep-thinking, rigorous, and creative scientist, she is a rare example of a very successful, but grounded researcher.

I would like to thank Cliff Tabin, the head of the Genetics department, for creating such an amazing environment for doing research. Also, I would like to thank Susan Dymecki for all her support over the years.

I would like extend my gratitude to Tim Cherry and Jeff Trimarchi for being my friends and mentors when I first started in the lab. Also, I would like to thank all the wonderful Bay 3 members who made day-to-day life in the lab so enjoyable. These include: Laura Weiser, Christina Demaso, Didem Goz, and Patrick Allard. Patrick and I overlapped in the bay for a long time and spent many an evening talking about ridiculous things or loudly singing.

I would like to thank all the members of the Cepko lab, and in particular: Nate Billings, Santiago Rompani, Mark Emerson, Takahiko Matsuda, Sui Wang, Wenjun Xiong, Natalia Surzenko, and Wenjia You. And of course, I have to acknowledge and

thank the wonderful Ladies in the Tabin lab that are my very dear friends: Yana Kamberov, Jessica Lehoczky, Jenna Galloway, and Eddy McGlinn. These wonderful women have advised me both scientifically and personally, made the lab always an entertaining place, and are all fiercely talented scientists!! In addition, I would like to thank my amazing friends, Amanda Nottke (my twin!) and Jimmy Hu, for all their support and friendship. Tabin grad students, Tamar Katz, Amy Shyer, Alan Rodrigues, Aysu Ugur, and Matt Schwartz have made social life in the lab so much fun.

I would like to thank my favorite classmates: Dan O'Connell, Joyce Tse O'Connell, Simon Trevino, Dave Shore, Mike Alpert, and Dana Christofferson. They have made my time in graduate school very memorable: full of delicious dinner parties, travel adventures, and ridiculous parties. Together, we went from the "G1 party group" to more "mature" adults. I will always cherish these amazing friends from grad school.

I would like to thank my parents for their unending support. They have always put my education first, and have taught me directly, as well as by example, how to lead a fulfilling life. They had to overcome many adverse situations as immigrants in a new land, yet became successful because of their intelligence, good humor, discipline, and hard work. Their achievements serve as constant inspiration for my life.

I also want to extend a big thank you to my wonderful grandparents, a team of superstars: Babcia Basia, Dziadek Gienek, Babcia Krysia, Dziadek Bolek. Despite having lived their lives in a difficult time and place, my grandparents are accomplished, generous, quick-witted, and warm people. They know a surprising amount about modern biology, keep close tabs on my life and work, and always make me feel incredibly supported. They are very special to me.

I would also like to thank my amazing husband, Raphael Bruckner, for all his support over the years. Rafi has enriched my life in more ways than I can count or fully appreciate. He is the smartest person I know, kind, hard-working, fun, talented, and hilarious. As it turns out, you can meet your very best friend and life companion at a BBS retreat.

Table of Contents

Chapter 1. Introduction……...…….……1

Chapter 2. Analysis of gene expression in wild type and Notch1 mutant retinal cells by single cell profiling……..……43

Chapter 3. Notch1 and downstream factors are required in newly postmitotic cells to inhibit the rod photoreceptor fate……..81

Chapter 4. Notch1 is required in embryonic newly postmitotic cells to inhibit the photoreceptor fate……..…..118

Chapter 5. Discussion…….131

Appendix 1. Table of upregulated genes in Notch1 deficient cells……..…….....148

Appendix 2. Table of downregulated genes in Notch1 deficient cells……...168

Appendix 3. Gene identities……176

Appendix 4. Transcriptional role of cyclin D1 in development revealed by a genetic-proteomic screen……...…180

Chapter 1

Introduction

Retinal development and Notch signaling

The retina

In examining the vertebrate eye, perhaps not too surprisingly, Charles Darwin found this organ "absurd in the highest possible degree" and deemed it impossible to have evolved through natural selection. To this day, the eye, and especially its neural component, the retina, continue to be fascinating structures that function more effectively than the most impressive manmade camera. The retina is a light sensitive tissue that lines the back of the eye. This highly specialized organ receives visual input from the outside environment, processes this information, and relays it to higher order visual processing centers in the brain. In understanding the function and development of the retina, we gain insight into how neural systems translate visual input into electrical impulses and how neural systems form during development. Although it still harbors mysteries, the retina is simpler in its neuroanatomy from the brain, thus making it an approachable part of the central nervous system in which to study neurogenesis.

Over a hundred years ago, the neuroanatomist Santiago Ramon y Cajal and others, performed Golgi staining on retinal tissue, revealing its architecture, circuitry, and diverse set of neural cell types. The ultrastructure of the retina consists of three nuclear layers and two plexiform layers. The cell bodies of rod and cone photoreceptors are located in the outer nuclear layer (ONL). These cells protrude segments, which consist of both inner and outer components (OS and IS), into the subretinal space where they interact with the pigmented epithelium (RPE). Photoreceptor cells synapse with bipolar cells and horizontal cells in the outer plexiform layer (OPL). Below the OPL, bipolar, horizontal, and amacrine cell bodies comprise the inner nuclear layer (INL). Bipolar and

amacrine cells synapse with ganglion cell dendrites in the inner plexiform layer (IPL). Ganglion cells, the relay neurons of the retina, reside in the ganglion cell layer (GCL) along with displaced amacrine cells. The cell bodies of Müller glial cells are also located in the INL, with long processes that extend from the scleral side of the ONL to the fiber layer inside of the ganglion cell layer (GCL) (Figure 1.1).

The positions of the different cell types within the structure of the retina form the basis of its circuitry and function. Only the apical positioning of photoreceptors in the retina seems counterintuitive, as light must pass through all the layers to reach photosensitive pigments in the outer segments of photoreceptors. Remarkably, this occurs with minimal light scattering, due in part to the tight packing of the layers. Moreover, Müller glial cells serve as living optical fibers and help to transmit light through the thickness of the retina (Franze et al., 2007).

Light signal is translated to an electrical signal in photoreceptor cells, which consist of two major types. Rod photoreceptors are exquisitely sensitive to light and can be activated by just one photon (Dunn and Rieke, 2008). Because of this ability, these cells are used almost exclusively under low light conditions. Humans have three different types of cone photoreceptors, each of which expresses a different opsin protein (sensitive to short, medium, or long wavelength light). Mice have two different types of opsin proteins, expressed at varying levels in cones. However, due to their nocturnal nature, the majority of photoreceptors (97%) in the rodent retina are rods (Carter-Dawson and LaVail, 1979). Opsin proteins are G-protein coupled receptors, which become activated upon photon absorption. Activation of the opsin molecule initiates a cascade of

Figure 1.1. Structure of the eye and adult retina

A schematic cross section of the eye. The retina is a thin, light sensitive tissue that lines the back of the eye (A) (adapted with permission from Kolb et al., http://www.webvision.med.utah.edu). The ultrastructure of the retina consists of three nuclear layers and two plexiform layers. The outer nuclear layer (ONL) consists of the cell bodies of rod and cone photoreceptors. These cells extend segments into the subretinal space, which consist of both inner and outer components (OS and IS, not denoted). Photoreceptor cells synapse with bipolar cells and horizontal cells in the outer plexiform layer (OPL). The inner nuclear layer (INL) consists of bipolar, horizontal, and amacrine cell bodies. Bipolar and amacrine cells synapse with ganglion cell dendrites in the inner plexiform layer (IPL). Ganglion cells comprise the ganglion cell layer (GCL) along with displaced amacrine cells. The cell bodies of Müller glial cells are also located in the INL, with long processes that extend from the width of the retina (B).

Figure 1.1 continued

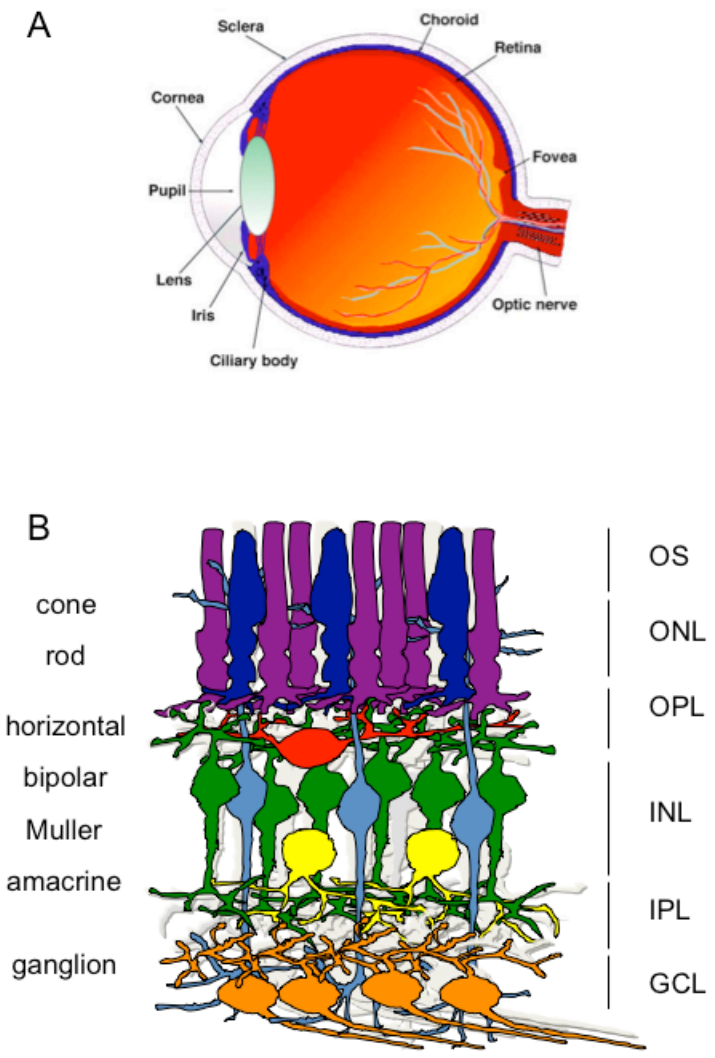

Figure 1.1

biochemical reactions, which ultimately lead to graded hyperpolarization of the photoreceptor cell.

Next, the impulse triggered by light is transmitted to interneurons located in the INL. Bipolar cells extend dendrites into the OPL and synapse with either cone or rod photoreceptors. Consequently, this class of cells can be split into two major groups: cone and rod bipolars. Within these two categories, bipolar cells can also be categorized as ON or OFF, depending on how they respond to the light signal, which in turn is contingent on whether they express the metabotropic receptor, mGluR6. Photoreceptors communicate with bipolars cells by constantly releasing the neurotransmitter, glutamate. When activated by light, photoreceptors become hyperpolarized and release less glutamate. If a bipolar expresses mGluR6, it depolarizes in response to the incoming light signal. This type of bipolar is classified as ON. Bipolars that do not express mGluR6 and hyperpolarize in response to light signal are called OFF bipolars. Bipolar cells extend a single axon to the IPL where they synapse with ganglion and amacrine cells. Importantly, different types of bipolar cells project to different laminations in the IPL. Likewise, ganglion cells extend dendrites to discrete layers. Specificity in ramification of synaptic partners results in specificity of connections that result in the extraction of useful information, e.g. the direction of motion. Upon receiving input from bipolar calls, ganglion cells, which are projection neurons, relay the processed signals to the brain. Their long axons are bundled to form the optic nerve and project to the midbrain, thalamus, hypothalamus, and other locations.

Transmission from photoreceptor to bipolar to ganglion cell comprises the vertical circuit of light detection. In addition to these connections, two types of inhibitory

interneurons located in the INL play an important role in modulating signal transmission. Horizontal cells are located in the upper part of the INL and extend processes into the OPL. Their role is to provide negative feedback onto an activated photoreceptor in order to restrict the field of cells that becomes activated near that cell. Amacrine cells are another type of interneuron found in the INL and GCL with processes extending to discrete ramifications in the IPL. This class of cells is highly diverse and is thought to have a wide array of functions, both inhibiting and stimulating light signal transmission depending on the type of the amacrine cell and its location.

In addition to acting as optical fibers, Müller glial cells play other supportive roles in the retina. In lower vertebrates, Müller glial cells function as adult stem cells. They become activated upon tissue injury and can divide to give rise to neurons well after the end of embryogenesis (Bernardos et al., 2007). However, this ability seems to have been lost in the rodent and human retina.

The composition of the adult rodent retina consists of 72.3% rod photoreceptors, 10.3% bipolar cells, 8.4% amacrine cells, 2.7% Müller glial cells, 2.5% cone photoreceptors, and 0.3% horizontal cells (Young, 1985a). The cells that comprise each class are predominantly classified together due to their similarity in function, location in the retina, and morphology. However, within each class, cells can be further subdivided into a number of cell types due to their expression of unique marker gene sets or distinct morphology. Over the years, it has become evident that the retina actually consists of over 60 different cell types, with the amacrine class being the most diverse with 29 distinguishable types known currently (Masland, 2011).

In addition to its well-defined structure and thorough cataloging of cell types, the retina is the only part of the CNS that is readily accessible for experimentation *in vivo* during development. Retinas can be cultured *ex vivo* for several weeks. All these features make the developing retina an excellent model for dissecting how cell fate decisions are made during neurogenesis.

DEVELOPMENT OF THE RETINA

Early retinal patterning

During mouse embryogenesis, the incipient eye, or eye field, is a group of cells in the anterior neural plate that are patterned from ectoderm and are a part of the neural tube. This tissue undergoes a series of structural changes as it gives rise to the neural retinal and the pigmented retinal epithelium (RPE). After 9.5 days of gestation (E9.5) in the mouse, the eye field separates into two lateral optical vesicles, which evaginate from the neural tube. The optic vesicle interacts with the overlying ectoderm, which causes it to invaginate and form a double-layered optic cup. The layer inside of the optic cup becomes the neural retina and the outside becomes the RPE.

After the formation of the optic cup, the one-cell thick layer that will become the neural retina proliferates to form a neuroepithelium. Initially, this epithelium constitutes only cycling RPCs that divide symmetrically to give rise to more RPCs. As development progresses, neurogenesis begins when most RPCs divide asymmetrically to produce a RPC and a newly born neuron, which migrates to the vitreal side of the retina. Some symmetrical divisions that give rise to two neurons do also occur at this time. Two appreciable layers form with newly born neurons constituting the inner neuroblastic layer

(INBL), and RPCs comprising the outer neuroblastic layer (ONBL). At late stages of neurogenesis, RPCs divide symmetrically to generate two postmitotic cells that differentiate into neurons. About a week after the birth of a mouse pup, the progenitor pool becomes extinguished and the retina consists of neurons at various stages of differentiation.

Features of RPCs

RPCs are radial cells that extend processes from the scleral to the vitreal sides of the retina. They undergo interkinetic nuclear migration as they progress through the cell cycle. The soma of RPCs is located close to the vitreal side of the ONBL during S phase, close to the scleral side during M phase, and in between during G1 and G2 (reviewed in Baye and Link, 2008).

Cell cycle length has been measured in the developing rat retina. At E14, cell cycle length is between 14 and 15 hours, with an S-phase of about 5 hours. As development progresses, the length of the cell cycle and S-phase increases, such that at P0 cell cycle length is over 30 hours and the duration of S-phase is about 20 hours (Alexiades and Cepko, 1996). Additionally, the cell cycles of individual RPCs are not synchronized, such that at a given time, different cells are at different stages of the cell cycle.

Birthdating of retinal neurons

A neurons's birthday is defined to be the moment at which it exits the cell cycle. Birthdating experiments are performed by labeling a tissue with [H^3]-thymidine, which is

taken up by cells and incorporated into the DNA of a dividing cell during S-phase. If the labeled cell continues to divide, it will dilute the concentration of labeled nucleotides in its genome, resulting in daughter cells with low signal. However, if a labeled cell exits the cell cycle shortly after incorporating [H^3]-thymidine, it will contain a high concentration of radio-labeled nucleotides in its genome and can be detected by autoradiography. Birthdating experiments in a number of different organisms determined that there is a conserved order during retinal cell type genesis that occurs in a central-to-peripheral gradient (Young, 1985b; Rapaport et al., 2004). Ganglion cells are born first, followed by cone photoreceptors and horizontal cells. Amacrine cells and rod photoreceptors are born during both embryonic and postnatal stages. Finally, at postnatal stages, bipolar and Müller glial cells are produced (Figure 1.2).

Retinal progenitor competence

Birthdating experiments determined that there is conserved, temporal order in which retinal cell types get produced. In addition, these studies indicated that there is significant overlap in the time windows these different cells are produced. Moreover, lineage tracing experiments with replication incompetent viruses provided evidence that RPCs are multipotent. A single clone marked by a virus early in development could comprise a large number, or all, of the cell types found in the adult (Turner et al., 1990).

Due to these observations and some others described below, the competence model was put forth to describe how RPCs generate the many different cell types of the retina. This model states that RPCs progress through distinct, but overlapping, temporal windows during which they are competent to produce certain types of retinal neurons.

Figure 1.2. Percentages of neurons born throughout rat retinal development

The percentage of each retinal cell type born is plotted over the course of rat retinal development. Ganglion cells, horizontal cells, and cone photoreceptors are all mostly born during embryonic stages. Rod photoreceptor and amacrine cell productions spans embryonic and postnatal stages. Bipolar and Müller glial cells are born postnatally. E-embryonic day, P-postnatal day. Adapted from Rapaport et al., 2004.

Figure 1.2 continued

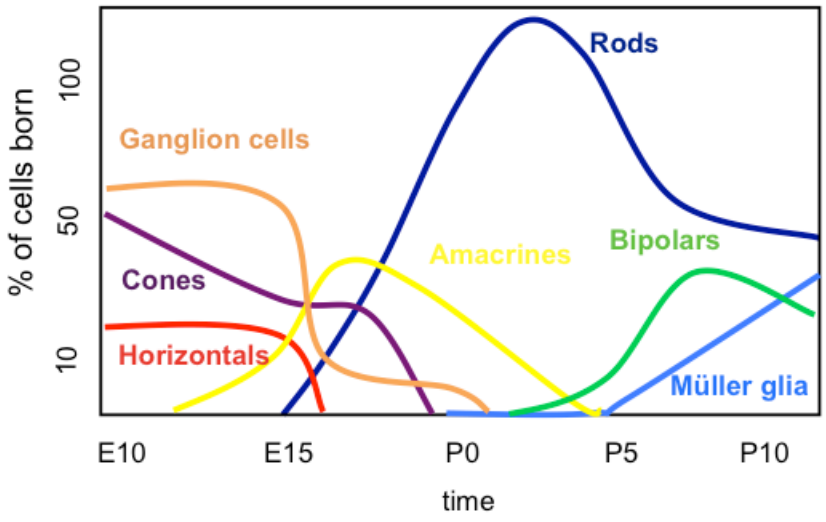

Figure 1.2

This concept of changes in competency over time accommodates the observation that different cell types have distinct birthdates, but a single, multipotent RPC can give rise to a number of different cell types, even those born at very different time points (Cepko et al., 1996; Livesey and Cepko, 2001) (Figure 1.3, A).

Specification of cell fate

During the development of the CNS, a relatively small number of progenitor cells give rise to a vastly diverse set of neurons. The progenitor cells of the cerebral cortex, retina, hindbrain, and spinal cord produce a series of different cell types in a sequential and reproducible manner. The progression of temporal changes in progenitor competence is due either to extrinsic cues in the environment, an intrinsic program, or a combination of both effects. The relative contribution of these two influences remains a major question in the field of developmental neurobiology.

Intrinsic factors

In order to test the importance of intrinsic and extrinsic cues on RPC competence, RPCs from different developmental time points were cultured together in aggregates. E16 RPCs were cultured with an excess of postnatal cells and the cell fate of the produced neurons was assayed. In the presence of postnatal cells, E16 RPCs produced more cones and fewer amacrines than normal. This suggested that environmental cues altered the proportion of a particular cell type produced at a given time, but could not force RPCs to produce a temporally inappropriate cell type (Belliveau and Cepko, 1999). Because extrinsic factors could not change the fate of the cells, it was surmised that RPCs were

intrinsically programmed to produce temporally restricted cell types. Culturing postnatal cells in an environment of embryonic cells yielded similar results (Belliveau et al., 2000).

In the heterochronic mixing experiments described above, RPCs were cultured with either younger or older retinal cells in aggregate and produced temporally appropriate progeny. Furthermore, RPCs can be cultured in completely non-retinal environments and still produce the correct cell types. In order to test this, late embryonic rat RPCs were dissociated and cultured at clonal density. Interestingly, the amount of divisions these cells underwent, the particular cell types they produced, and the order in which their progeny were produced were remarkably similar to those of cells observed in comparable explant cultures (Cayouette et al., 2003). These culture experiments, in which extracellular signals are either absent or different from the normal environment, reveal that the intrinsic state of an RPC is sufficient for specifying the temporal identity of its daughter cells.

What does it mean for progeny of RPCs to be intrinsically determined? This observation would suggest that the fate decision is made by the cycling mother RPC and then passed on to its daughter cells. When this cell divides, it passes on fate determinants (either by chromatin marks or proteins or RNAs) to its two daughter cells and this decision is invariant. Once made, these postmitotic daughter cells will carry out the program endowed by their mother cell and begin to differentiate into predetermined cell types. In support of this notion, transplantation experiments in the developing cortex provided evidence that cell fate is specified just prior to a neuron's last division (McConnell and Kaznowski, 1991).

The specification of neuroblasts in the *Drosophila* ventral nerve cord is an example of a well-defined intrinsic program that instructs cell fate. The *Drosophila* CNS develops from an array of neuroblasts, which delaminate from the neuroectoderm at a specific time and position. Neuroblasts divide asymmetrically to produce another neuroblast and a ganglion mother cell (GMC) (reviewed in Pearson and Doe). GMCs divide only once, producing either neurons or glia. Due to the highly stereotyped manner of these divisions in space and time, neuroblasts, GMCs, and the resultant progeny cells can be readily tracked during this process. A number of studies have determined that a series of transcription factors, Hunchback, Kruppel, pdm1, and castor, are expressed in neuroblasts, GMCs, and newly produced neurons in a temporal order (Kambadur et al., 1998; Isshiki et al., 2001). Moreover, Hunchback and Kruppel, in conjunction with some yet unknown clock mechanism, regulate the intrinsic state of the neuroblast and its lineage. Genetic removal of Hunchback or Kruppel resulted in a loss of the early-born neurons, and normal production of later born neurons. Conversely, when Hunchback expression was ectopically extended in neuroblasts, these cells produced an excess of early born neurons (Isshiki et al., 2001; Novotny et al., 2002). Moreover, misexpression of Hunchback after it had already been turned off in late neuroblasts resulted in production of early born neurons (Pearson and Doe, 2003). It is unclear if the later expressed factors are as potent as Hunchback and Kruppel, but these results demonstrate how an intrinsic factor can modulate temporal identity of progenitor cells in the *Drosophila* CNS.

The production of neurons from neuroblasts also serves as a model for how asymmetric inheritance of certain factors can produce two non-equivalent cells. In the

Drosophila CNS, *Prospero* encodes a protein that is asymmetrically segregated during neuroblast division such that it is only inherited by the GMC daughter and not the neuroblast daughter (Spana and Doe, 1995). Prospero functions to limit the proliferative potential of the GMC, such that this cell only undergoes one round of division. Interestingly, Prox1, an ortholog in mice, also drives RPCs out of the cell cycle during retinal development (Dyer et al., 2003). Another intrinsic mechanism for generating non-equivalent sibling daughter cells is the asymmetric localization of the determinant, Numb. During GMC division, Numb is segregated directionally to one daughter cell, where it antagonizes Notch-Delta signaling (described in greater detail below). In the absence of Numb, both daughter cells take on the same neuronal fate (Spana and Doe, 1996).

Does a similar cascade of sequential gene expression direct cell fate during retinal development? A study determined that *Ikaros*, a mouse ortholog of *Hunchback*, is expressed in almost all embryonic RPCs, but not in postnatal RPCs. Similar to the ability of Hunchback, temporally inappropriate expression of *Ikaros* in late RPCs resulted in the production of horizontal cells, which are normally produced early in retinal development (Elliott et al., 2008). However, even though misexpression of *Ikaros* induced the production of a cell type not normally produced at postnatal stages, it is difficult to definitively determine if the competence state of the transduced RPC was indeed pushed back to an earlier state, or merely directed to take on this particular fate. Other early born cell types, such as ganglion cells and cone photoreceptors, were not observed.

In many cases, the genetic mechanisms underlying an intrinsically programmed cell are not elucidated, but the committed progenitor can be marked and its progeny

followed. For example, it was shown that RPCs which are positive for the factor VC1.1 give rise to horizontal cells and amacrine cells, but not cone photoreceptors, a cell type produced concomitantly (Alexiades and Cepko, 1997). In another set of experiments, lentiviral marking of single RPCs in the developing chicken retina led to the discovery of a bias in progeny production. The chicken retina is comprised of three different types of horizontal cells, H1, H2, and H3. Clones which contained two horizontal cells had only cells of the same subtype, H1 or H3 (Rompani and Cepko, 2008). Interestingly, this did not extend to H2, which showed no production in pairs. This suggested that a multipotent RPC gives rise to a committed RPC, which will then divide symmetrically to make two neurons of the same subtype. Similarly, live imaging in the developing zebrafish retina revealed mitotic precursor cells that were dedicated solely to the production of horizontal cells. These horizontal precursor cells expressed horizontal marker genes and divided in the horizontal cell layer (Godinho et al., 2007). Recent work from our lab has determined that expression of the transcription factor, *Olig2*, marks RPCs which only give rise to specific cell fates. In these studies, embryonic Olig2+ RPCs, unlike randomly marked RPCs, produced small clones comprised of horizontal cells and cone photoreceptors and not the other cell types produced at this time (Hafler et al., in press). At postnatal stages, Olig2+ RPCs only produced amacrine cells and rod photoreceptors, and not bipolar cells and Müller glial cells. These discoveries point to the existence of committed RPCs that produce progeny biased to become only certain cell types (Figure 1.3, B).

Figure 1.3 Retinal competence and clonal analysis

Retinal progenitor cells pass through competence states during which they are restricted to generate only certain types of retinal neurons (A). Adapted from Cepko et al., 1996, Livesey and Cepko, 2001. An example of a large, hypothetical embryonic clone. Progenitor cells (blue) divide to give rise to more progenitor cells and/or neurons. Some progenitor cells (green) are more restricted and divide to produce two stereotyped neurons (B).

Figure 1.3 continued

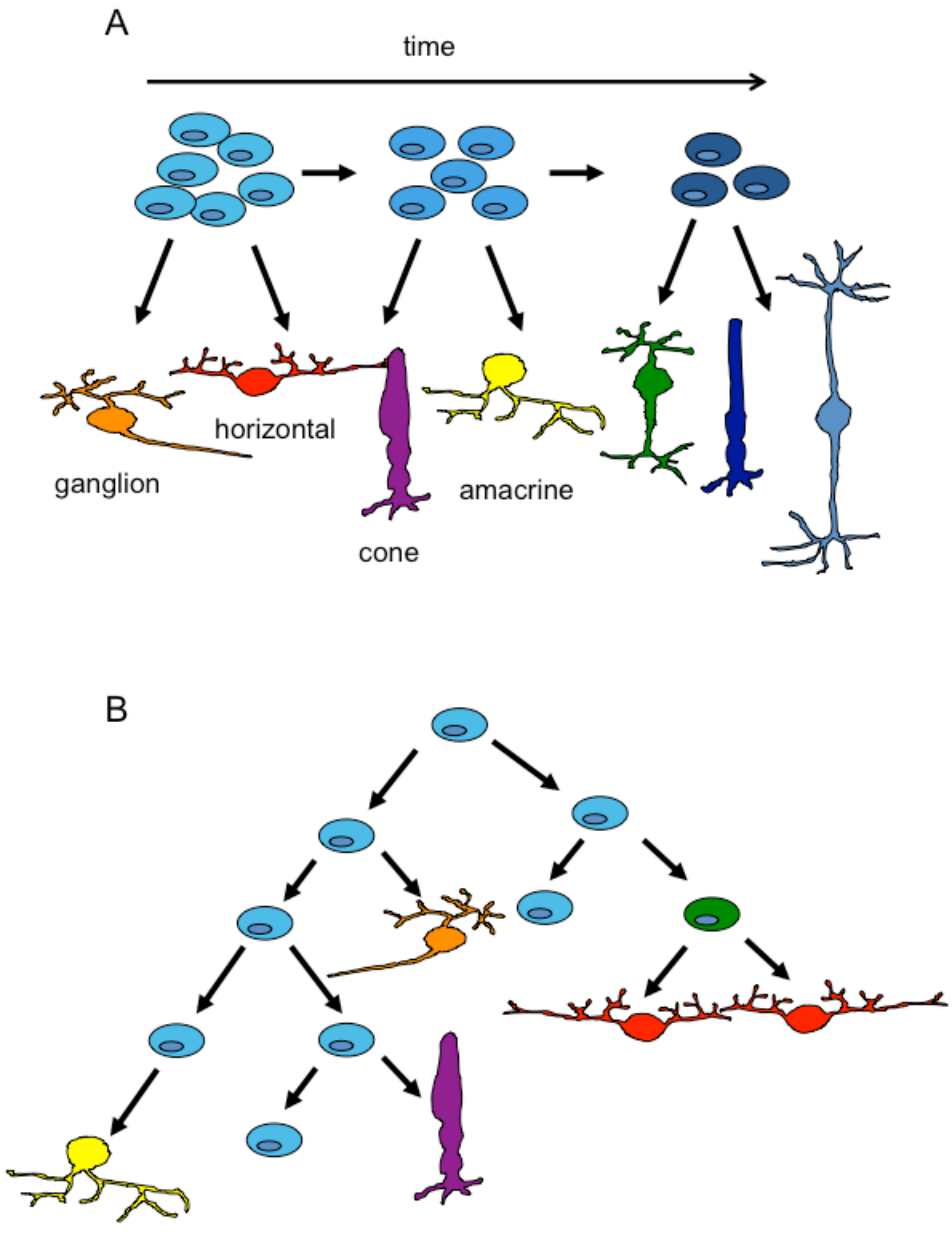

Figure 1.3

Extrinsic factors

Although there is strong evidence that intrinsic factors determine cell identity in the developing retina, an unbiased approach of single cell profiling yielded surprising results. Single cells from different stages of retinal development were isolated by dissociation and profiled on microarrays. The identity of these cells was determined post hoc, and in total, the transcriptional profiles of 42 RPCs were examined. A clear result from this large scale analysis was that gene expression in RPCs was vastly heterogeneous (Trimarchi et al., 2008). Even cells harvested from a similar time point expressed different gene sets, and only a few genes could be ascribed to early versus late RPCs. This suggests that the majority of RPCs are different from one another, which may be a reflection of the ultimate heterogeneity of the mature retina.

Furthermore, in addition to the heterochronic mixing experiments described above, several other studies point to the possibility that extracellular factors that can change the fate of RPCs or even newly born neurons. For example, culturing young RPCs, which produce ganglion cells, with retinal cells from increasingly older retinas resulted in the inhibition of ganglion cell production (Waid and McLoon, 1998). This inhibitory signal may be Notch, as knockdown of Notch with antisense oligonucleotides in the chicken retina resulted in overproduction of ganglion cells, whereas ectopic Notch signal resulted in fewer ganglion cells (Austin et al., 1995). In another study, the addition of ciliary neurotrophic factor (CNTF) to rat retinal explants resulted in a reduced production of rod photoreceptors. Concomitantly, a larger number of bipolar cells, amacrine cells, and Müller glial cells were generated. CNTF could induce a cell fate change in newly postmitotic rods until they were differentiated enough to express opsin

proteins (Ezzeddine et al., 1997). However, these experiments do not definitively prove that extrinsic signals are involved during normal development.

In summary, intrinsic, and potentially extrinsic factors, are important in dictating temporal identity and cell fate decisions in the developing retina. Most likely, RPCs endow a network of genes to their daughter cells, giving them an inherent bias in terms of fate choice. However, commitment to that particular fate takes time, and extracellular factors can alter the outcome of the intrinsic program during this "plastic" period.

BHLH and homeobox transcription factors

Two major families of transcription factors are involved in specifying cell identity in the retina: the homeobox transcription factors and bHLH transcription factors.

Pax6, a homeobox transcription factor conserved in almost all metazoans, is a master regulator of eye development (Gehring and Ikeo, 1999). Its expression in some non-retinal tissues is sufficient to induce formation of the eye in *Drosophila* (Halder et al., 1995). Mice null for *Pax6* do not develop eyes, and humans with non-lethal mutations have smaller sized eyes (Hogan et al., 1986, 1988). *Pax6* is expressed in RPCs during development and is necessary for promoting proliferation. Like a number of other transcription factors which play a role in RPCs, it continues to be expressed after cell cycle exit, but only in a subset of cell types. In this case, *Pax6* is expressed at low levels in Müller glial cells and robustly in amacrine cells. Conditional removal of this factor during retinal development causes RPCs to exit the cell cycle and, surprisingly, to produce a subset of amacrine cells (Marquardt et al., 2001). *Rax*, another member of the

homeobox transcription factor family, is responsible for patterning the incipient eye field. Later in retinal development, it promotes RPC proliferation and the generation of Müller glial cells (Mathers et al., 1997; Furukawa et al., 2000). *Chx10* is expressed in RPCs and later in differentiated bipolar cells. *Chx10* mutants exhibit reduced proliferation and lack bipolar cells (Burmeister et al., 1996).

Otx2 and *Crx* are two homeobox transcription factors that are important regulators of the photoreceptor cell fate. *Otx2* misexpression induces overproduction of photoreceptors, and its removal results in an excess of amacrine cells produced at the expense of photoreceptors (Chen et al., 1997; Furukawa et al., 1997; Nishida et al., 2003). *Crx* mutants display a relatively mild phenotype in that the outer segments of photoreceptors do not develop normally (Morrow et al., 2005).

Basic helix-loop-helix (bHLH) transcription factors are another family of important fate regulators in the retina. These can be generally characterized as either repressors or activators of neuronal fate. Hes genes, homologs of *Drosophila hairy* and *Enhancer of split*, are transcriptional repressors that maintain cells in an undifferentiated state (Sasai et al., 1992). RPCs in the *Hes1* null retina exhibit impaired proliferation and prematurely exit the cell cycle (Ishibashi et al., 1995; Tomita et al., 1996; Takatsuka et al., 2004). *Hes5* is also expressed in the retina, and loss of this factor results in a decrease of Müller glial cells (Deneen et al., 2006). Concurrently, overexpression of *Hes5* induces Müller glial production (Hojo et al., 2000). The misexpression of *Hesr2*, another family member, also results in the overproduction of Müller glial cells. *Hes1*, *Hes5*, and *Hesr2* are all direct targets of Notch signaling, which is discussed below. In addition to other

roles, one function of Hes family members is to repress the transcription of pro-neurogenic bHLH transcription factors.

Math5, an ortholog of *Drosophila atonal*, is expressed in cycling progenitor cells and in newly postmitotic cells. *Math5* conditional knockout retinas fail to produce ganglion cells, the first cell type to be produced during development (Brown et al., 2001; Wang et al., 2001). Misexpression of *Math5* results in the promotion of ganglion production (Yao et al., 2007). Fate mapping experiments have revealed that Math5-expressing cells give rise to not only ganglion cells, but also cone and rod photoreceptors, horizontal cells, and amacrine cells (Yang et al., 2003; Feng et al., 2010).

NeuroD1 is expressed throughout retinal development and has a number of roles yet to be fully determined in the developing retina. It was observed that ectopic expression of *NeuroD1* leads to an increase in production of rod photoreceptors in one study (Inoue et al., 2002), and an increase in amacrine cells in another study (Morrow et al., 1999). Removal of *NeuroD1* results in the overproduction of Müller glial cells. In general, pro-neurogenic bHLH transcription factors, such as *Math5*, *NeuroD1*, *Mash1*, *Math3*, and *Ngn2*, seem to play redundant roles. Frequently, compound mutants have to be generated or combinations of homeobox and bHLH factors have be to misexpressed in order to observe any appreciable or predictable phenotypes. For example, only the triple compound knockout, *Mash1*$^{-/-}$*;Math3*$^{-/-}$*;NeuroD1*$^{-/-}$, produces significantly fewer rod photoreceptors (Akagi et al., 2004). Together, homeobox and bHLH transcription factors, in conjunction with many other transcriptional regulators not mentioned here, direct cell fate in the developing retina. A major goal of future studies is to assemble combinatorial networks that take into account this myriad of important regulatory proteins.

NOTCH SIGNALING

The Notch pathway is a highly conserved signal transduction cascade that is utilized throughout embryogenesis and in stem cells of the adult organism (Artavanis-Tsakonas et al., 1999). *Drosophila* possess one Notch receptor and *C. elegans* have two paralogs. In higher vertebrates, there are four receptors, *Notch1-4*. In the mouse, Notch pathway ligands include *Delta-like1,3,4* and *Jagged1,2*. Although it is an extrinsic signal in most cases, the readout for this pathway's input will be interpreted depending on the intrinsic state of the cell receiving the signal. Because of this, Notch signaling has been implicated in promoting or suppressing proliferation, cell death, differentiation, and in the achievement of a multitude of cell fate decisions in most developmental systems.

Notch was initially discovered in 1914 when John Dexter observed mutant flies that had a characteristic notched wing phenotype. Unlike other developmental pathways, canonical *trans* Notch signaling occurs at short range, between two adjacent cells, as both the receptor and the ligand are single pass, transmembrane proteins (Wharton et al., 1985; Kidd et al., 1986). Pathway activation occurs through proteolysis of the receptor at the cell membrane following ligand interaction. After this cleavage event, the Notch intracellular domain, NICD, translocates into the nucleus where it associates with a transcriptional complex to activate downstream target genes (Figure 1.4).

Figure 1.4. The canonical Notch signaling pathway

A schematic representation of two adjacent cells undergoing Notch signal activation. The Notch receptor undergoes several post-translational modifications, including glycosylation and site 1 (S1) cleavage by furin shortly after translation. The resultant heterodimer is targeted to the cell membrane. The receptor interacts with a ligand presented on an adjacent cell. It is postulated that endocytosis of the ligand results in a mechanical force that pulls on the Notch receptor exposing it to site 2 (S2) cleavage by ADAM metalloproteases. Next, γ-secretase cleaves the Notch transmembrane domain from site 3 (S3) to site 4 (S4), thereby releasing the Notch intracellular domain (NICD). NICD translocates into the nucleas where it interacts with CSL (CBF1/RBP-J/Su(H)/Lag-1). In the absence of NICD, CSL is a transcriptional repressor. Upon binding, NICD, CSL, and Mastermind (Mam), along with other coactivators, activate the transcription of downstream Notch target genes (reviewed in Kopan and Ilagan, 2009).

Figure 1.4 continued

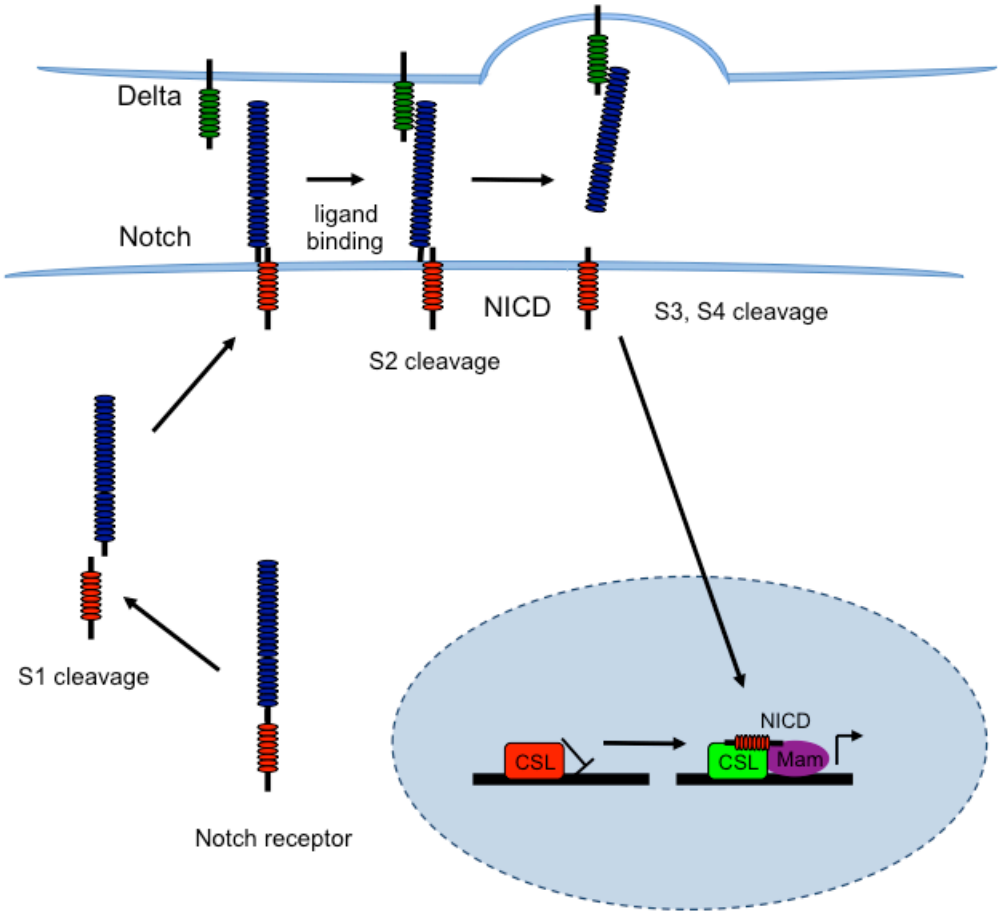

Figure 1.4

Canonical pathway activation

Since the initial discovery of the core components of the Notch pathway, studies in a variety of organisms have identified a myriad of regulators and additional pathway components, revealing an underlying complexity of how the Notch receptor matures, undergoes several proteolytic events, regulates transcription in the nucleus, and ultimately gets targeted for degradation (reviewd in Bray, 2006; Kopan and Ilagan, 2009). The Notch receptor undergoes four cleavage events during activation at four disparate sites on the mature protein (S1-S4). After translation, the Notch receptor is glycosylated by O-fucosyltransferase (Ofut1) and Rumi. Next, furin-like convertase cleaves the receptor at cleavage site S1, producing two separate domains, the Notch extracellular domain (NECD) and the Notch transmembrane and intracellular domain (NTMIC). Noncovalent interactions hold these two domains together and the resultant heterodimer is trafficked to the cell membrane. The Fringe family of glycosyltransferases can further modify the mature receptor, changing its ability to interact with ligands (Moloney et al., 2000).

Upon ligand binding via EGF repeats on the NECD, the Notch receptor becomes activated and undergoes a conformational change. This is thought to be due in part to ligand endocytosis which "pulls" on the receptor and exposes the S2 cleavage site. ADAM metalloproteases cleave the intracellular part of the Notch receptor right before the transmembrane domain (S2), resulting in a membrane-tethered Notch extracellular truncation fragment (NEXT). The NECD is shed from the membrane surface. The NEXT domain is a substrate for γ-secretase, a complex of proteases that cleave at the cell membrane (Selkoe and Wolfe, 2007). ϒ-secretase cleaves the NEXT domain at S3 and

S4, both within the transmembrane domain, and releases the intracellular domain, NICD. This cleavage event can occur at the cell membrane or within an endosome.

After release from the cell membrane, NICD translocates to the nucleus where it interacts with the DNA-binding protein, CSL (CBF1/RBPJ/Su(H)/Lag-1). In the absence of NICD, CSL acts as a transcriptional repressor. However, upon binding NICD, CSL becomes a transcriptional activator, forms a complex with Mastermind, and in conjunction with other co-factors turns on downstream target genes (Gordon et al., 2008; Kovall, 2008). A consensus DNA binding site for CSL has been defined (Bailey and Posakony, 1995) and a number of targets have been identified experimentally or predicted by a computational approach (Rebeiz et al., 2002). The most well characterized downstream target genes of this pathway comprise the members of the Hes family of transcription factors (Lecourtois and Schweisguth, 1995)(described above). Indubitably, a number of not yet characterized target genes, that become activated in a context dependent manner, mediate the observed pleiotropic effects of this pathway.

Regulation of Notch activity

Because the cleavage of a single Notch receptor results in a moiety that activates transcription, the amount of Notch receptor on the cell surface is tightly controlled by endocytosis. Therefore, regulation of the amount of Notch receptors by endocytosis is an important component of signal strength modulation (reviewed in Yamamoto et al., 2010). In addition, E3 ubiquitin ligases such as Deltex, Nedd4, Su(Dx)/Itch and others have been identified as regulators of Notch signaling (reviewed in Kopan and Ilagan, 2009).

Nrarp is a Notch inhibitor, which contains a similar ankyrin repeat found in the Notch receptor. It functions by binding the NICD/CSL/Mastermind complex, and this activity is thought to prevent downstream target activation (Lamar et al., 2001). *Nrarp* itself is a downstream target of Notch activation, thus its expression may result in a negative feedback loop that shuts off the Notch signal (Krebs et al., 2001). Another negative Notch regulator that plays a role in asymmetric cell division is Numb (Zhong et al., 1996). This protein is inherited asymmetrically during divisions that will yield two non-equivalent daughter cells. Numb antagonizes Notch activity in the daughter cell that inherited it, thus differentiating it from its sister cell. Numb action is specific to dividing cells, as recently it has been shown that it must interact with a Golgi restricted protein, ACBD3, to function. Golgi fragmentation during mitosis enables the interaction between ACBD3 and Numb, thus activating Numb and inhibiting Notch (Zhou et al., 2007). Recently, it has been demonstrated that Numb antagonizes Notch signaling by increasing endocytosis in the cell (Couturier et al., 2012).

Notch ligands are also highly regulated via transcription, post-translational modifications, and presentation on the cell surface. The canonical paradigm of Notch signal transduction holds that Delta/Serrate/Jagged ligands are transmembrane proteins presented on cells adjacent to those expressing the Notch receptor. Endocytosis of presented ligands plays a key role in activating Notch signaling, as the mechanical force leveraged by the endocytosed ligand exposes the cleavage site on the Notch receptor (Nichols et al., 2007). Endocytosis of ligands is initiated by the E3 ubiquitin ligases, Neuralized and Mindbomb (Le Borgne, 2006). However, studies in *C. elegans* have determined that half of the ligands are diffusible (Chen and Greenwald, 2004; Komatsu et

al., 2008). More studies have to be performed to fully understand how predominant Notch activation by diffusible ligands is in vertebrates and how it occurs without the mechanical force of endocytosis.

In addition to non-canonical receptor activation by diffusible ligands, *cis* activation has also been observed. The interaction between ligand and receptor in the same cell mostly results in inhibition of the pathway (Cordle et al., 2008). However, recent studies in *Drosophila* reveal that the pathway can also *cis*-activate. This mechanism is described further below.

Notch signaling during *Drosophila* nervous system development

Classical experiments in the fly have defined a paradigm for Notch signal activation and function. Because Notch signaling occurs between adjacent cells, it is commonly recruited during embryogenesis to direct cell fate changes among initially equivalent cells. This mechanism, called lateral inhibition, is described below.

The development of the *Drosophila* macrochaetae, a part of the peripheral nervous system responsible for mechanoreception, serves as an excellent model for how lateral inhibition can be exerted in a repetitive and pleiotropic manner. During the development of this organ, Notch signaling initially prevents neurogenesis, later acts to select the fate of one cell amongst a population of identical cells, and finally mediates a binary choice between two cell fates. Initially, proneural clusters of equivalent cells form in a uniform layer of ectodermal cells. These cells homogenously express Notch and Delta, until one cell stochastically upregulates Delta. This results in activation of Notch

signaling in its neighbors and serves as a classical example of lateral inhibition (Heitzler et al., 1996). The high Delta expressing cell becomes the Sensory Organ Precursor (SOP) cell, which divides asymmetrically to give rise to two non-equivalent daughter cells, the pIIa and pIIb cell. The binary choice between these two fates is mediated by the asymmetric inheritance and expression of Notch, Delta, and pathway regulators. Numb protein is asymmetrically passed on to the pIIb cell, where it antagonizes Notch activity. This cell also expresses Delta and activates the Notch receptor expressed by the pIIa cell (Furman and Bukharina, 2011). Thus, initial differences passed on by the SOP are amplified as the pIIa cell receives input from Notch signal transduction while the pIIb cell does not. Recently, an even earlier mechanism that exposes the emerging pIIa cell to Notch signal has been uncovered. During SOP cell mitosis, Notch and Delta proteins are asymmetrically trafficked to the incipient pIIa cell via special endosomes (Coumailleau et al., 2009). Due to the inheritance of both ligand and receptor, active Notch signaling is observed in the pIIa cell shortly after mitosis and presumably directs the fate of this cell. This observation is one of the first examples of Notch *cis*-activation and the Notch-Delta interaction likely occurs inside an endosome. Later in development, the pIIa cell divides to produce a hair and socket cell, whereas the pIIb cells divides to produce a sheath cell and a neuron. This is just one example of a developmental system in which thorough investigation of Notch signaling clearly demonstrates how it can be used repetitively to drive cell fate specification.

Notch signaling in the central nervous system

The roles of Notch signaling in the vertebrate CNS are consistent with the findings of classical experiments in the fly. Broadly, Notch signaling performs three major functions (exemplified in the SOP system above): 1.) maintenance of cells in an undifferentiated state 2.) induction of glial cell fate 3.) mediation of binary cell fate choices.

Constitutive activation of Notch, achieved by the overexpression of the intracellular form of the receptor (NICD), in the developing mouse forebrain resulted in the production of radial glial cells (Gaiano et al., 2000). In a similar manner, hyperactivation of Notch signaling in the retina generated cells that resembled glial cells. These results have been observed in *Xenopus*, zebrafish, and rodents (Dorsky et al., 1995; Furukawa et al., 2000; Scheer et al., 2001). Retroviral expression of NICD in the postnatal rodent retina resulted in clones that were larger than control infections, suggesting that NICD drives proliferation in infected RPCs (Bao and Cepko, 1997; Furukawa et al., 2000). Marked cells had abnormal morphology and expressed Müller glial marker genes (Furukawa et al., 2000). Similar results were observed when NICD was ectopically expressed in embryonic RPCs via a conditional genetic cross (Jadhav et al., 2006a), however excessive proliferation was not observed. These retinas exhibited an expanded INL that contained a large amount of Müller glial-like cells. Furthermore, NICD expressing cells were profiled on microarrays at early (E13.5) and late (P10) time points. At early stages, these mutant cells expressed Notch target genes and early progenitor marker genes. At P10, NICD cells also expressed Notch target genes, but also marker genes of late progenitor cells and Müller glial cells. These results provided

evidence that NICD-expressing cells are capable of transitioning from early progenitors to late, glial-like cells even though they did not produce neurons. In addition, a different genetic cross was utilized to misexpress NICD in newly postmitotic cells. In the presence of constitutively active Notch signaling, a population of postmitotic cells were induced to become Müller glial cells (Jadhav et al., 2006a). These studies underscore the potency of activated Notch in the developing retina.

Activation of Notch ligands converges on the transcriptional regulator, *CSL* (also known as RBP-J). Conditional deletion of this factor in the developing cortex resulted in depletion of the progenitor pool and precocious neurogenesis (Imayoshi et al., 2010). In a similar manner, conditional knockout of *CSL* from the retina disrupted proliferation, induced differentiation, and caused gross morphological abnormalities. After exit from cell cycle, $CSL^{-/-}$ cells preferentially became ganglion cells and cone photoreceptors (Riesenberg et al., 2009).

Analysis of retinas in which *Notch1* was removed early in development, was similar but not identical to the phenotypes observed when CSL was conditionally deleted. Wherein activation of Notch signaling results in overproliferation and induction of a progenitor/Müller glial cell state, removal of *Notch1* during early retinal development resulted in precocious exit from cell cycle (Yaron et al., 2006; Jadhav et al., 2006b). In addition, *Notch1* mutant retinas were smaller and exhibit disrupted laminar morphology. Because RPCs that lack *Notch1* exit the cell cycle prematurely, it would be expected that an overproduction of early cell types, such as ganglion cells, cone photoreceptors, and horizontal cells would be observed. Interestingly, when *Notch1* mutant RPCs exit the cell cycle, they produce an excess of cone photoreceptors at the expense of the other early cell

types (Yaron et al., 2006; Jadhav et al., 2006b). This cell fate change does not appear to be due to cell death, as only a slight increase in TUNEL+ cells is observed (Yaron et al., 2006). Microarray analysis of E13.5 retinas revealed upregulation of genes associated with cone genesis, including *Crx*, *Otx2*, *Math3*, *thyroid hormone receptor-β*, and *NeuroD1*. In addition, a similar phenotype was observed when *Notch1* was conditionally removed from postnatal RPCs by viral transduction. In this assay, *Notch1* mutant cells preferentially became rod photoreceptors at the expense of the other cell types produced postnatally. Taken together, these studies show that Notch signaling maintains the progenitor state during retinal development. In addition, *Notch1* inhibits the photoreceptor fate at embryonic and postnatal stages.

Open questions

Notch signaling is an important and commonly utilized mode of communication between cells during development. Questions as to how this pathway exerts specific effects in so many different developmental systems are still unanswered. However, because Notch signaling is involved in so many processes, a better understanding of how this pathway functions provides us with important insight into some of the most fundamental aspects of development.

In the developing retina, Notch signaling maintains RPCs in a proliferative state and inhibits photoreceptor cell fate. One question that arises from these observations is whether these two roles can be separated. By manipulating Notch signaling in newly

postmitotic cells, we can start to dissect the many roles of this pathway during retinal development.

Another major question is what downstream target genes change when Notch signaling is depleted during neurogenesis. The novel approach of single cell profiling makes it possible to investigate changes in gene expression at the resolution of individual cells, as opposed to global changes in the whole tissue. Profiling cells lacking Notch will lead to a better understanding of the genetic programs that underlie cell fate specification and can reveal candidate factors which regulate this process downstream of Notch signaling.

REFERENCES

Bessho, Y., Takahashi, M., Lee, J.E., Guillemot, F., and Kageyama, R. (2004). Requirement of multiple basic helix-loop-helix genes for retinal neuronal subtype specification. J. Biol. Chem *279*, 28492–28498.

Alexiades, M.R., and Cepko, C. (1996). Quantitative analysis of proliferation and cell cycle length during development of the rat retina. Dev. Dyn *205*, 293–307.

Alexiades, M.R., and Cepko, C.L. (1997). Subsets of retinal progenitors display temporally regulated and distinct biases in the fates of their progeny. Development *124*, 1119–1131.

Artavanis-Tsakonas, S., Rand, M.D., and Lake, R.J. (1999). Notch signaling: cell fate control and signal integration in development. Science *284*, 770–776.

Austin, C.P., Feldman, D.E., Ida, J.A., Jr, and Cepko, C.L. (1995). Vertebrate retinal ganglion cells are selected from competent progenitors by the action of Notch. Development *121*, 3637–3650.

Bailey, A.M., and Posakony, J.W. (1995). Suppressor of hairless directly activates transcription of enhancer of split complex genes in response to Notch receptor activity. Genes Dev. *9*, 2609–2622.

Bao, Z.Z., and Cepko, C.L. (1997). The expression and function of Notch pathway genes in the developing rat eye. J. Neurosci *17*, 1425–1434.

Baye, L.M., and Link, B.A. (2008). Nuclear migration during retinal development. Brain Res. *1192*, 29–36.

Belliveau, M.J., and Cepko, C.L. (1999). Extrinsic and intrinsic factors control the genesis of amacrine and cone cells in the rat retina. Development *126*, 555–566.

Belliveau, M.J., Young, T.L., and Cepko, C.L. (2000). Late retinal progenitor cells show intrinsic limitations in the production of cell types and the kinetics of opsin synthesis. J. Neurosci. *20*, 2247–2254.

Bernardos, R.L., Barthel, L.K., Meyers, J.R., and Raymond, P.A. (2007). Late-stage neuronal progenitors in the retina are radial Müller glia that function as retinal stem cells. J. Neurosci. *27*, 7028–7040.

Le Borgne, R. (2006). Regulation of Notch signalling by endocytosis and endosomal sorting. Curr. Opin. Cell Biol. *18*, 213–222.

Bray, S.J. (2006). Notch signalling: a simple pathway becomes complex. Nat. Rev. Mol. Cell Biol. *7*, 678–689.

Brown, N.L., Patel, S., Brzezinski, J., and Glaser, T. (2001). Math5 is required for retinal ganglion cell and optic nerve formation. Development *128*, 2497–2508.

Burmeister, M., Novak, J., Liang, M.Y., Basu, S., Ploder, L., Hawes, N.L., Vidgen, D., Hoover, F., Goldman, D., Kalnins, V.I., et al. (1996). Ocular retardation mouse caused by Chx10 homeobox null allele: impaired retinal progenitor proliferation and bipolar cell differentiation. Nat. Genet. *12*, 376–384.

Carter-Dawson, L.D., and LaVail, M.M. (1979). Rods and cones in the mouse retina. I. Structural analysis using light and electron microscopy. J. Comp. Neurol. *188*, 245–262.

Cayouette, M., Barres, B.A., and Raff, M. (2003). Importance of intrinsic mechanisms in cell fate decisions in the developing rat retina. Neuron *40*, 897–904.

Cepko, C.L., Austin, C.P., Yang, X., Alexiades, M., and Ezzeddine, D. (1996). Cell fate determination in the vertebrate retina. Proc. Natl. Acad. Sci. U.S.A. *93*, 589–595.

Chen, N., and Greenwald, I. (2004). The lateral signal for LIN-12/Notch in C. elegans vulval development comprises redundant secreted and transmembrane DSL proteins. Dev. Cell *6*, 183–192.

Cordle, J., Johnson, S., Tay, J.Z.Y., Roversi, P., Wilkin, M.B., de Madrid, B.H., Shimizu, H., Jensen, S., Whiteman, P., Jin, B., et al. (2008). A conserved face of the Jagged/Serrate DSL domain is involved in Notch trans-activation and cis-inhibition. Nat. Struct. Mol. Biol. *15*, 849–857.

Coumailleau, F., Fürthauer, M., Knoblich, J.A., and González-Gaitán, M. (2009). Directional Delta and Notch trafficking in Sara endosomes during asymmetric cell division. Nature *458*, 1051–1055.

Couturier, L., Vodovar, N., and Schweisguth, F. (2012). Endocytosis by Numb breaks Notch symmetry at cytokinesis. Nat. Cell Biol. *14*, 131–139.

Deneen, B., Ho, R., Lukaszewicz, A., Hochstim, C.J., Gronostajski, R.M., and Anderson, D.J. (2006). The transcription factor NFIA controls the onset of gliogenesis in the developing spinal cord. Neuron *52*, 953–968.

Dorsky, R.I., Rapaport, D.H., and Harris, W.A. (1995). Xotch inhibits cell differentiation in the Xenopus retina. Neuron *14*, 487–496.

Dunn, F.A., and Rieke, F. (2008). Single-photon absorptions evoke synaptic depression in the retina to extend the operational range of rod vision. Neuron *57*, 894–904.

Dyer, M.A., Livesey, F.J., Cepko, C.L., and Oliver, G. (2003). Prox1 function controls progenitor cell proliferation and horizontal cell genesis in the mammalian retina. Nat. Genet. *34*, 53–58.

Elliott, J., Jolicoeur, C., Ramamurthy, V., and Cayouette, M. (2008). Ikaros confers early temporal competence to mouse retinal progenitor cells. Neuron *60*, 26–39.

Ezzeddine, Z.D., Yang, X., DeChiara, T., Yancopoulos, G., and Cepko, C.L. (1997). Postmitotic cells fated to become rod photoreceptors can be respecified by CNTF treatment of the retina. Development *124*, 1055–1067.

Franze, K., Grosche, J., Skatchkov, S.N., Schinkinger, S., Foja, C., Schild, D., Uckermann, O., Travis, K., Reichenbach, A., and Guck, J. (2007). Müller cells are living optical fibers in the vertebrate retina. Proc. Natl. Acad. Sci. U.S.A. *104*, 8287–8292.

Furman, D.P., and Bukharina, T.A. (2011). Drosophila mechanoreceptors as a model for studying asymmetric cell division. Int. J. Dev. Biol. *55*, 133–141.

Furukawa, T., Mukherjee, S., Bao, Z.Z., Morrow, E.M., and Cepko, C.L. (2000). rax, Hes1, and notch1 promote the formation of Müller glia by postnatal retinal progenitor cells. Neuron *26*, 383–394.

Gaiano, N., Nye, J.S., and Fishell, G. (2000). Radial glial identity is promoted by Notch1 signaling in the murine forebrain. Neuron *26*, 395–404.

Gehring, W.J., and Ikeo, K. (1999). Pax 6: mastering eye morphogenesis and eye evolution. Trends Genet. *15*, 371–377.

Godinho, L., Williams, P.R., Claassen, Y., Provost, E., Leach, S.D., Kamermans, M., and Wong, R.O.L. (2007). Nonapical symmetric divisions underlie horizontal cell layer formation in the developing retina in vivo. Neuron *56*, 597–603.

Gordon, W.R., Arnett, K.L., and Blacklow, S.C. (2008). The molecular logic of Notch signaling--a structural and biochemical perspective. J. Cell. Sci. *121*, 3109–3119.

Halder, G., Callaerts, P., and Gehring, W.J. (1995). Induction of ectopic eyes by targeted expression of the eyeless gene in Drosophila. Science *267*, 1788–1792.

Heitzler, P., Bourouis, M., Ruel, L., Carteret, C., and Simpson, P. (1996). Genes of the Enhancer of split and achaete-scute complexes are required for a regulatory loop between Notch and Delta during lateral signalling in Drosophila. Development *122*, 161–171.

Hogan, B.L., Hirst, E.M., Horsburgh, G., and Hetherington, C.M. (1988). Small eye (Sey): a mouse model for the genetic analysis of craniofacial abnormalities. Development *103 Suppl*, 115–119.

Hogan, B.L., Horsburgh, G., Cohen, J., Hetherington, C.M., Fisher, G., and Lyon, M.F. (1986). Small eyes (Sey): a homozygous lethal mutation on chromosome 2 which affects the differentiation of both lens and nasal placodes in the mouse. J Embryol Exp Morphol *97*, 95–110.

Hojo, M., Ohtsuka, T., Hashimoto, N., Gradwohl, G., Guillemot, F., and Kageyama, R. (2000). Glial cell fate specification modulated by the bHLH gene Hes5 in mouse retina. Development *127*, 2515–2522.

Imayoshi, I., Sakamoto, M., Yamaguchi, M., Mori, K., and Kageyama, R. (2010). Essential roles of Notch signaling in maintenance of neural stem cells in developing and adult brains. J. Neurosci. *30*, 3489–3498.

Inoue, T., Hojo, M., Bessho, Y., Tano, Y., Lee, J.E., and Kageyama, R. (2002). Math3 and NeuroD regulate amacrine cell fate specification in the retina. Development *129*, 831–842.

Ishibashi, M., Ang, S.L., Shiota, K., Nakanishi, S., Kageyama, R., and Guillemot, F. (1995). Targeted disruption of mammalian hairy and Enhancer of split homolog-1 (HES-1) leads to up-regulation of neural helix-loop-helix factors, premature neurogenesis, and severe neural tube defects. Genes Dev *9*, 3136–3148.

Isshiki, T., Pearson, B., Holbrook, S., and Doe, C.Q. (2001). Drosophila neuroblasts sequentially express transcription factors which specify the temporal identity of their neuronal progeny. Cell *106*, 511–521.

Jadhav, A.P., Cho, S.-H., and Cepko, C.L. (2006a). Notch activity permits retinal cells to progress through multiple progenitor states and acquire a stem cell property. Proc. Natl. Acad. Sci. U.S.A *103*, 18998–19003.

Jadhav, A.P., Mason, H.A., and Cepko, C.L. (2006b). Notch 1 inhibits photoreceptor production in the developing mammalian retina. Development *133*, 913–923.

Kambadur, R., Koizumi, K., Stivers, C., Nagle, J., Poole, S.J., and Odenwald, W.F. (1998). Regulation of POU genes by castor and hunchback establishes layered compartments in the Drosophila CNS. Genes Dev. *12*, 246–260.

Kidd, S., Kelley, M.R., and Young, M.W. (1986). Sequence of the notch locus of Drosophila melanogaster: relationship of the encoded protein to mammalian clotting and growth factors. Mol. Cell. Biol. *6*, 3094–3108.

Komatsu, H., Chao, M.Y., Larkins-Ford, J., Corkins, M.E., Somers, G.A., Tucey, T., Dionne, H.M., White, J.Q., Wani, K., Boxem, M., et al. (2008). OSM-11 facilitates LIN-12 Notch signaling during Caenorhabditis elegans vulval development. PLoS Biol. *6*, e196.

Kopan, R., and Ilagan, M.X.G. (2009). The canonical Notch signaling pathway: unfolding the activation mechanism. Cell *137*, 216–233.

Kovall, R.A. (2008). More complicated than it looks: assembly of Notch pathway transcription complexes. Oncogene *27*, 5099–5109.

Krebs, L.T., Deftos, M.L., Bevan, M.J., and Gridley, T. (2001). The Nrarp gene encodes an ankyrin-repeat protein that is transcriptionally regulated by the notch signaling pathway. Dev. Biol *238*, 110–119.

Lamar, E., Deblandre, G., Wettstein, D., Gawantka, V., Pollet, N., Niehrs, C., and Kintner, C. (2001). Nrarp is a novel intracellular component of the Notch signaling pathway. Genes Dev. *15*, 1885–1899.

Lecourtois, M., and Schweisguth, F. (1995). The neurogenic suppressor of hairless DNA-binding protein mediates the transcriptional activation of the enhancer of split complex genes triggered by Notch signaling. Genes Dev. *9*, 2598–2608.
Livesey, F.J., and Cepko, C.L. (2001). Vertebrate neural cell-fate determination: lessons from the retina. Nat. Rev. Neurosci *2*, 109–118.

Masland, R.H. (2011). Cell populations of the retina: the Proctor lecture. Invest. Ophthalmol. Vis. Sci. *52*, 4581–4591.

Mathers, P.H., Grinberg, A., Mahon, K.A., and Jamrich, M. (1997). The Rx homeobox gene is essential for vertebrate eye development. Nature *387*, 603–607.

McConnell, S.K., and Kaznowski, C.E. (1991). Cell cycle dependence of laminar determination in developing neocortex. Science *254*, 282–285.

Moloney, D.J., Panin, V.M., Johnston, S.H., Chen, J., Shao, L., Wilson, R., Wang, Y., Stanley, P., Irvine, K.D., Haltiwanger, R.S., et al. (2000). Fringe is a glycosyltransferase that modifies Notch. Nature *406*, 369–375.

Morrow, E.M., Furukawa, T., Lee, J.E., and Cepko, C.L. (1999). NeuroD regulates multiple functions in the developing neural retina in rodent. Development *126*, 23–36.

Nichols, J.T., Miyamoto, A., Olsen, S.L., D'Souza, B., Yao, C., and Weinmaster, G. (2007). DSL ligand endocytosis physically dissociates Notch1 heterodimers before activating proteolysis can occur. J. Cell Biol. *176*, 445–458.

Novotny, T., Eiselt, R., and Urban, J. (2002). Hunchback is required for the specification of the early sublineage of neuroblast 7-3 in the Drosophila central nervous system. Development *129*, 1027–1036.

Pearson, B.J., and Doe, C.Q. (2003). Regulation of neuroblast competence in Drosophila. Nature *425*, 624–628.

Rapaport, D.H., Wong, L.L., Wood, E.D., Yasumura, D., and LaVail, M.M. (2004). Timing and topography of cell genesis in the rat retina. J. Comp. Neurol *474*, 304–324.

Rebeiz, M., Reeves, N.L., and Posakony, J.W. (2002). SCORE: a computational approach to the identification of cis-regulatory modules and target genes in whole-genome sequence data. Site clustering over random expectation. Proc. Natl. Acad. Sci. U.S.A. *99*, 9888–9893.

Riesenberg, A.N., Liu, Z., Kopan, R., and Brown, N.L. (2009). Rbpj cell autonomous regulation of retinal ganglion cell and cone photoreceptor fates in the mouse retina. J. Neurosci *29*, 12865–12877.

Rompani, S.B., and Cepko, C.L. (2008). Retinal progenitor cells can produce restricted subsets of horizontal cells. Proc. Natl. Acad. Sci. U.S.A *105*, 192–197.

Sasai, Y., Kageyama, R., Tagawa, Y., Shigemoto, R., and Nakanishi, S. (1992). Two mammalian helix-loop-helix factors structurally related to Drosophila hairy and Enhancer of split. Genes Dev. *6*, 2620–2634.

Scheer, N., Groth, A., Hans, S., and Campos-Ortega, J.A. (2001). An instructive function for Notch in promoting gliogenesis in the zebrafish retina. Development *128*, 1099–1107.

Selkoe, D.J., and Wolfe, M.S. (2007). Presenilin: running with scissors in the membrane. Cell *131*, 215–221.

Spana, E.P., and Doe, C.Q. (1995). The prospero transcription factor is asymmetrically localized to the cell cortex during neuroblast mitosis in Drosophila. Development *121*, 3187–3195.

Spana, E.P., and Doe, C.Q. (1996). Numb antagonizes Notch signaling to specify sibling neuron cell fates. Neuron *17*, 21–26.

Takatsuka, K., Hatakeyama, J., Bessho, Y., and Kageyama, R. (2004). Roles of the bHLH gene Hes1 in retinal morphogenesis. Brain Res *1004*, 148–155.

Tomita, K., Ishibashi, M., Nakahara, K., Ang, S.L., Nakanishi, S., Guillemot, F., and Kageyama, R. (1996). Mammalian hairy and Enhancer of split homolog 1 regulates differentiation of retinal neurons and is essential for eye morphogenesis. Neuron *16*, 723–734.

Trimarchi, J.M., Stadler, M.B., and Cepko, C.L. (2008). Individual retinal progenitor cells display extensive heterogeneity of gene expression. PLoS ONE *3*, e1588.

Turner, D.L., Snyder, E.Y., and Cepko, C.L. (1990). Lineage-independent determination of cell type in the embryonic mouse retina. Neuron *4*, 833–845.

Waid, D.K., and McLoon, S.C. (1998). Ganglion cells influence the fate of dividing retinal cells in culture. Development *125*, 1059–1066.

Wang, S.W., Kim, B.S., Ding, K., Wang, H., Sun, D., Johnson, R.L., Klein, W.H., and Gan, L. (2001). Requirement for math5 in the development of retinal ganglion cells. Genes Dev. *15*, 24–29.

Wharton, K.A., Johansen, K.M., Xu, T., and Artavanis-Tsakonas, S. (1985). Nucleotide sequence from the neurogenic locus notch implies a gene product that shares homology with proteins containing EGF-like repeats. Cell *43*, 567–581.

Yamamoto, S., Charng, W.-L., and Bellen, H.J. (2010). Endocytosis and intracellular trafficking of Notch and its ligands. Curr. Top. Dev. Biol. *92*, 165–200.

Yang, Z., Ding, K., Pan, L., Deng, M., and Gan, L. (2003). Math5 determines the competence state of retinal ganglion cell progenitors. Dev. Biol. *264*, 240–254.

Yao, J., Sun, X., Wang, Y., Xu, G., and Qian, J. (2007). Math5 promotes retinal ganglion cell expression patterns in retinal progenitor cells. Mol. Vis. *13*, 1066–1072.

Yaron, O., Farhy, C., Marquardt, T., Applebury, M., and Ashery-Padan, R. (2006). Notch1 functions to suppress cone-photoreceptor fate specification in the developing mouse retina. Development *133*, 1367–1378.

Young, R.W. (1985a). Cell differentiation in the retina of the mouse. Anat. Rec *212*, 199–205.

Young, R.W. (1985b). Cell proliferation during postnatal development of the retina in the mouse. Brain Res *353*, 229–239.

Zhong, W., Feder, J.N., Jiang, M.M., Jan, L.Y., and Jan, Y.N. (1996). Asymmetric localization of a mammalian numb homolog during mouse cortical neurogenesis. Neuron *17*, 43–53.

Zhou, Y., Atkins, J.B., Rompani, S.B., Bancescu, D.L., Petersen, P.H., Tang, H., Zou, K., Stewart, S.B., and Zhong, W. (2007). The mammalian Golgi regulates numb signaling in asymmetric cell division by releasing ACBD3 during mitosis. Cell *129*, 163–178.

Chapter 2

Analysis of gene expression in wild type and Notch1 mutant retinal cells by single cell profiling

Karolina Mizeracka, Jeffrey M. Trimarchi, Michael B. Stadler, and Constance L. Cepko

Contributions: J.M.T assisted in harvesting and profiling of single retinal cells, M.B.S and J.M.T. assisted in performing analysis of microarray data

Summary

The vertebrate retina is comprised of sensory neurons, the photoreceptors, as well as many other types of neurons and one type of glial cell. These cells are generated by multipotent retinal progenitor cells (RPCs) which express *Notch1*. Loss of *Notch1* in RPCs late during retinal development results in the overproduction of rod photoreceptors at the expense of interneurons and glia. To examine the molecular underpinnings of this observation, microarray analysis of single retinal cells from wild type (WT) or Notch1 conditional knockout (N1-CKO) retinas was performed. The majority of N1-CKO cells lost expression of known Notch target genes. These cells also had low levels of RPC and cell cycle genes, and robustly upregulated rod precursor genes. In addition, single WT cells, in which cell cycle marker genes were downregulated, expressed markers of both rod photoreceptors and interneurons. These results demonstrate that individual, newly postmitotic retinal cells can begin to differentiate into more than one cell type, and that this transitional state may be dependent on *Notch1* signaling.

Introduction

The vertebrate retina is an excellent model system for understanding how signaling pathways regulate gene expression during development. It consists of six major neuronal cell types and one glial cell type that can be readily identified by molecular markers, gene expression, and morphology. These cell types arise in a temporal, but overlapping, order from a pool of multipotent RPCs (Livesey and Cepko, 2001). During retinal neurogenesis, ganglion cells are generated first, followed by horizontal cells, cone photoreceptors, and amacrine cells. Rod photoreceptors, bipolar cells, and Müller glial cells are the last cell types to be produced (Young, 1985b; Wong and Rapaport, 2009).

Previous studies have determined that during retinal development, the Notch signaling pathway regulates both cell cycle exit and cell fate specification (Yaron et al., 2006; Jadhav et al., 2006b). Genetic removal of *Notch1* from early RPCs resulted in cell cycle exit and the premature onset of neurogenesis (Yaron et al., 2006; Jadhav et al., 2006b). Furthermore, overproduction of cone photoreceptors at the expense of other cell types was observed in these *Notch1* deficient retinas. Deletion of a conditional allele of *Notch1* by viral delivery of Cre during later, postnatal, stages of retinal development led to the overproduction of rod photoreceptors (Jadhav et al., 2006b), in keeping with the birth order of rod and cone photoreceptor cells. The N1-CKO cells generated in the postnatal environment acquired their phenotype in a cell autonomous manner. Therefore, in individual RPCs and their newly postmitotic daughter cells, Notch signaling is crucial for maintenance of the progenitor state, as well as for the repression of the photoreceptor fate.

Previous lineage analyses of the postnatal retina showed that individual clones of only two cells could be a variety of combinations of two very different cell types. For example, a rod and Müller glial cell, a rod and a bipolar cell or an amacrine cell. Cells may be sorting out their fates as they exit the cell cycle, or perhaps when they enter a newly postmitotic state. Previous single cell gene expression profiles showed that cycling cells are very heterogeneous (Trimarchi et al., 2007, 2008). They must lose this heterogeneity as they transition into differentiated neurons, since even in the WT case, most take on the rod fate. We wished to explore further the newly postmitotic state where these processes were taking place, and exploit the differences among WT and N1-CKO cells for insight into these events. Specifically, we were interested in identifying Notch responsive genes that may regulate or be markers of cell cycle, progenitor state, and cell fate determination. Although microarray studies have been carried out on *Notch1* deficient retinas, an analysis of the transcriptional profile of single *Notch1* conditional knockout (N1-CKO) cells has never been performed (Jadhav et al., 2006b). Single cell profiling of N1-CKO and WT cells would allow an appreciation of these events even among a group of heterogenous cells.

This study led to the identification of a large number of genes that were either up or downregulated in the absence of Notch signaling. By post hoc classification, we were able to identify individual cells at different stages of the progenitor to postmitotic neuron continuum, revealing the transcriptional profile of cells during this transition. Finally, we observed that single WT cells expressed early differentiation genes of both interneurons and photoreceptors. These expression profiles may indicate that there is plasticity

regarding cell fate, and/or that certain types of genes are derepressed transiently during this phase of retinal development.

Results

Profiling single WT and N1-CKO retinal cells

Previous studies have shown that introduction of Cre using a retrovirus vector into a characterized *Notch1*$^{fl/fl}$ strain of mice results in an increased production of rod photoreceptors at the expense of two interneurons (bipolar and amacrine cells), as well as, Müller glial cells (Jadhav et al., 2006b). In order to generate N1-CKO cells for single cell expression profiling, retinas of *Notch1*$^{fl/fl}$ P0 pups were electroporated *in vivo* with plasmids encoding Cre driven by a broadly active promoter, CAG, along with a Cre-responsive GFP reporter, also driven by the CAG promoter (CALNL-GFP). For controls, the retinas of sibling *Notch1*$^{fl/fl}$ pups were electroporated with CAG:GFP. The animals were sacrificed at P3 to allow time for *Notch1* to be genetically removed and downstream gene expression changes to occur. Retinas electroporated with either CAG:Cre and CALNL-GFP or CAG:GFP alone were dissected and dissociated to individual cells, which were then harvested under a dissecting microscope on the basis of their GFP signal. In total, 13 N1-CKO cells and 13 WT were harvested and profiled on Affymetrix microarrays. These methods have been used previously for profiling individual retinal cells, with the results validated by several methods, primarily *in situ* hybridization (Brady and Iscove, 1993; Dulac and Axel, 1995; Iscove et al., 2002; Tietjen et al., 2003; Trimarchi et al., 2007).

Expression levels of Notch target genes in N1-CKO and WT cells

In order to confirm that Notch1 signaling was indeed depleted in N1-CKO cells, the levels of several direct target genes were assessed (Ohtsuka et al., 1999; Iso et al., 2001; Krebs et al., 2001). The levels of *Hes1*, *Hes5*, *Hey1*, and *Nrarp* expression were lower in most N1-CKO cells than in WT cells (Figure 2.1, see N1-CKO cells 4-13 vs. WT cells 1-6). *Hes5* was still detectable in some N1-CKO cells (Figure 1, see N1-CKO cells 4, 6, 9, 12). A few N1-CKO cells expressed more than one Notch target gene, suggesting that these cells had not lost all their Notch signal, while some may have been in the process of downregulating Notch signaling (Figure 2.1, N1-CKO cells 1-3). Some WT cells expressed high levels of Notch targets, presumably because they still had active Notch signaling (Figure 2.1, see WT cells 1-6, 13). As discussed further below, most of these cells were also the ones classified as RPCs (Figure 2.2, see WT cells 2-6). Similar to the majority of the N1-CKO cells, several of the WT cells exhibited low levels of Notch target genes (Figure 2.1, see WT cells 7-12). These WT cells most likely were in a transitional state during which they were downregulating Notch activity to exit the cell cycle, as occurs normally, especially at this time in development (Young, 1985a). Overall, these data indicate that the majority of N1-CKO cells had lost Notch signaling.

Classification of cells using their molecular signatures

One of our goals is to understand the transition that cells undergo as they exit the cell cycle and choose their fate, both in the WT and N1-CKO cells. In order to investigate if there are indications of an eventual fate choice during this transition, we classified each N1-CKO and WT cell according to its expression of cell type-specific markers. The

Figure 2.1. Expression of selected Notch target genes in WT and N1-CKO single cells

Notch1$^{fl/fl}$ retinas were electroporated at P0 *in vivo* with CAG:GFP (to mark WT cells) or CAG:Cre plus CALNL-GFP, a Cre-responsive reporter (to mark N1-CKO cells). At P3, retinas were dissociated to single cells and GFP+ cells were harvested as single cells. Cells were then subjected to reverse transcription and PCR, with the resulting probes hybridized to Affymetrix arrays. The signal levels for different genes are shown as a histogram.

Figure 2.1 continued

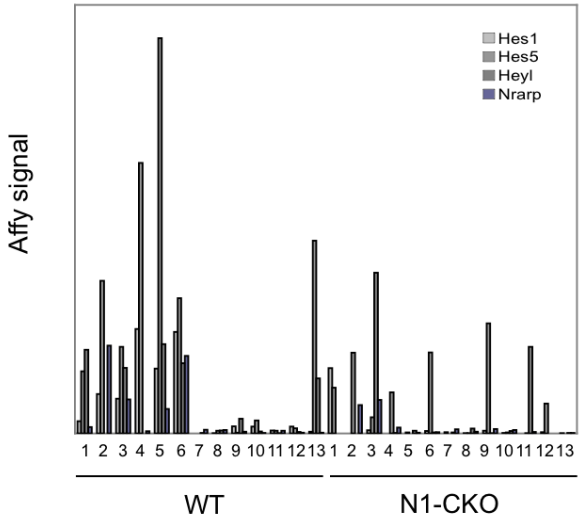

Figure 2.1.

classification scheme, as devised previously, is based upon the normalized values of genes co-expressed with known markers of each of the retinal cell types (Trimarchi et al., 2007, 2008). As an example, in order to determine if a cell has characteristics of an amacrine cell, an analysis was carried out to determine which genes serve as markers of the amacrine fate. We used the microarray data from cells profiled previously to identify genes whose expression was strongly associated with the expression of the known amacrine-specific genes, *Tcfap-2β, Gad1,* and *Glyt1*. The associations were derived from 194 single retinal cells that were profiled in our lab and which encompassed most retinal cell types (Trimarchi et al., 2007, 2008; Kim et al., 2008b; Roesch et al., 2008; Cherry et al., 2009). A Fisher's exact test was used to determine the p-value for correlations between any given gene and *Tcfap-2β, Gad1,* and *Glyt1*. Only associated genes that had p-values of 10^{-3} or lower were considered to be highly associated. The relative expression level for each associated gene in each P3 N1-CKO or WT cell was calculated by dividing a cell's signal level by the maximum signal level found in all of the single cells within the entire dataset of 194 cells. These scaled values for all of the amacrine associated genes in each cell were summed, and then the sums were scaled, such that the maximum score was 10. This classification procedure was repeated with markers of other retinal cell types to generate scores for each cell type. For an RPC score, genes associated with *FGF15, Sfrp2,* and *μ-crystallin* were used; for retinal ganglion cells, those associated with *NF68* and *Ebf3*; for Müller glia, those associated with *Apoe*; and for bipolar cells, those associated with *Og9x* (Trimarchi et al., 2008). In order to generate a photoreceptor score, the gene *Blimp1* was used to find associated genes. This gene has been shown to be expressed early in photoreceptor development and its expression tapers off as these cells

mature (Brzezinski et al., 2010; Katoh et al., 2010). This was considered a more appropriate marker for newly postmitotic cells that would likely achieve the rod fate, instead of a more typical rod photoreceptor marker, such as *rhodopsin*, whose expression is later in development.

Using this classification scheme, the majority of the N1-CKO cells scored highly as incipient rod photoreceptors (Figure 2.2, see N1-CKO cells 1-10). Three of the N1-CKO cells scored highly as amacrine precursor cells (Figure 2.2, see N1-CKO cells 11-13). Most of the WT cells were classified as RPCs (Figure 2.2, see WT cells 2-6, 8, 12), while some cells had high rod (Figure 2.2, see rod WT cells 9-11, 13) or amacrine scores (Figure 2.2, see amacrine WT cell 7). Some WT cells had intermediate scores for RPC, rod, and amacrine cell types (discussed below) (Figure 2.2, see WT cells 1, 2, 6). These outcomes support the idea that *Notch1* signaling was depleted in N1-CKO cells, as none of these cells scored as RPCs and the majority were classified as rod precursor cells. It is worth noting that none of these postnatal cells had a ganglion cell signature. This gives confidence in the classification scheme, and is in keeping with the idea that primarily mitotic or newly postmitotic cells adjacent to the subretinal space were electroporated. Ganglion cells would have already been produced and would have migrated away from this surface by P0 when the retina was electroporated. Overall, these molecular data support the observed cell fate changes, as well as provide a source of gene expression changes that are likely informative with regards to the network that is regulated by *Notch1*.

Figure 2.2. Classification of single profiled cells

Profiled cells were classified as RPCs, rod photoreceptors, bipolar cells, amacrine cells, ganglion cells, or Müller glia based on the expression levels of genes associated with a known marker of that particular cell type. Genes associated with one or several cell type-specific markers were determined by a Fisher's exact test and the relative expression level for each associated gene was calculated by dividing the cell's signal level by the maximum signal level found in a large collection of single cells (Trimarchi et al., 2007). These values were summed and normalized to generate a cell type score for each cell, with 10 being the maximum score for each cell type. Genes associated with *FGF15, Sfrp2,* and *μ-crystallin* were used to generate a RPC score, genes associated with *Blimp1* for rod photoreceptors, genes associated with *Ogx9* for bipolar cells, genes associated with *Tcfap-2β, Gad1,* and *Glyt1* for amacrine cells, genes associated with *NF68* and *Ebf3* for ganglion cells, and genes associated with *Apoe* for Müller glia. For comparison, previously profiled cells, which were classified as amacrine (Cherry et al., 2009) or rod precursors (unpublished), are shown. The highest score for each cell is boxed in red.

Figure 2.2 continued

	RPC	rod	bipolar	amacrine	ganglion	Muller
WT cell 1	1.9	2.4	0.5	2.0	1.3	0.3
WT cell 2	3.2	1.7	0.9	0.8	0.7	0.6
WT cell 3	3.8	3.1	0.5	0.9	0.7	0.6
WT cell 4	4.2	1.1	0.7	1.2	0.7	0.6
WT cell 5	3.2	2.4	0.5	0.8	0.5	0.5
WT cell 6	2.9	2.6	0.6	1.5	0.7	0.5
WT cell 7	0.9	1.8	0.5	2.6	1.9	0.2
WT cell 8	3.8	1.4	0.6	1.4	0.5	0.6
WT cell 9	5.6	9.9	0.9	2.1	1.5	0.3
WT cell 10	2.8	4.7	1.0	1.7	1.9	0.5
WT cell 11	1.8	8.4	0.9	0.9	1.1	0.5
WT cell 12	5.1	2.6	0.7	1.7	0.5	0.6
WT cell 13	1.8	6.6	0.6	1.1	0.7	0.4
N1-CKO cell 1	1.6	6.8	0.6	1.0	0.7	0.3
N1-CKO cell 2	1.9	3.3	0.6	2.7	1.3	0.3
N1-CKO cell 3	3.2	4.3	1.0	1.1	0.6	0.5
N1-CKO cell 4	1.9	5.8	0.7	1.2	0.7	0.5
N1-CKO cell 5	0.8	9.6	0.7	1.1	1.1	0.4
N1-CKO cell 6	1.4	10.0	1.4	1.3	0.3	0.3
N1-CKO cell 7	1.0	6.8	0.8	1.5	0.9	0.3
N1-CKO cell 8	1.7	8.6	1.7	1.4	1.0	0.3
N1-CKO cell 9	2.2	6.3	0.9	1.7	0.3	0.6
N1-CKO cell 10	2.2	8.9	0.9	1.9	0.7	0.5
N1-CKO cell 11	1.7	2.1	0.7	2.8	1.9	0.4
N1-CKO cell 12	1.0	2.7	1.2	4.2	1.7	0.2
N1-CKO cell 13	1.1	2.2	1.1	3.6	2.2	0.4
P0 cell E1	1.1	7.1	1.4	1.0	0.9	0.4
P5 cell C4	1.1	7.8	0.9	1.5	0.7	0.2
P5 cell D2	1.9	5.0	1.2	1.3	1.2	0.3
P5 cell C2	1.8	4.1	1.0	1.1	1.0	0.3
P0 cell A4	1.7	1.9	1.3	6.8	1.8	0.3
P0 cell B1	1.9	1.4	1.1	3.8	2.9	0.6
P0 cell D1	1.6	0.9	1.7	8.9	2.6	0.4
P0 cell G3	1.1	1.4	0.8	5.6	3.2	0.4

Figure 2.2

Changes in RPC and cell cycle gene expression in single cells that have lost *Notch1*

At P3, the majority of RPCs divide symmetrically to produce two neurons, as proliferation is nearly over at this time in the center of the retina, and it is waning in the periphery (Young, 1985a). These newborn neurons will differentiate into mature cell types over the course of the next few weeks. With this time frame in mind, we profiled single cells on microarrays three days after the introduction of Cre recombinase into the *Notch1*$^{fl/fl}$ background. It was anticipated that the downstream changes in gene expression would represent relatively early gene expression changes. Some of these genes were predicted to be those that regulate or drive cell cycle, as loss of *Notch1* has been reported to lead to cell cycle exit (Yaron et al., 2006; Jadhav et al., 2006b). The levels of cell cycle genes, *Geminin, Ccna2, CyclinB1, Cdc20,* and *CyclinB2* (Trimarchi et al., 2008), were thus assessed in N1-CKO and WT cells (Figure 2.3). Indeed, the N1-CKO cells showed a reduction in the expression levels of these cell cycle genes (Figure 2.3, see N1-CKO cells 4-13). Moreover, the cells with the most comprehensive reduction in cell cycle genes were the same cells that showed the most robust loss of Notch target genes (Figure 2.3, see N1-CKO cells 4-13). The WT cells with low levels of Notch signaling targets, also had reduced levels of these same cell cycle genes (Figure 2.3, see WT cells 7-13). In contrast, WT and N1-CKO cells that expressed Notch target genes had high levels of cell cycle genes (Figure 2.3, see WT cells 1-6 and N1-CKO cells 1-3).

In addition to cell cycle genes, expression of other previously identified RPC genes was assessed. Some of these genes are in all or most RPCs, but are also expressed in subsets of neurons (e.g. *Pax6*). We chose to analyze expression of genes that are expressed in most RPCs, but are not expressed in many neurons. These included *Lhx2,*

Mik67, Cdca8, Cdc2a, Fgf15, Ttyh1, and *μ-crystallin* (Figure 2.3) (Blackshaw et al., 2004; Trimarchi et al., 2008). Most N1-CKO cells had low levels of these genes and were the same cells that had scored highly as neurons in the classification scheme described above (Figure 2.2 and 2.3, see N1-CKO cells 4-13). Interestingly, the WT cells that showed low levels of Notch target genes and cell cycle genes retained expression of some RPC genes (Figure 2.3, see WT cells 7-13), even though they were classified as neurons when the wider range of marker genes was scored in the classification scheme (Figure 2.2, see WT cells 7-13). This observation may indicate that these WT cells had a slower pace of exiting the RPC state and executing their differentiation process. In contrast, a number of WT cells that expressed high levels of Notch target genes and cell cycle genes, also expressed high levels of most RPC genes (Figure 2.3, see WT cells 1-6). This group of cells was classified as RPCs, with the exception of WT cell 1, which had an intermediate RPC and rod score (Figure 2.2). As a point of reference, rod and amacrine precursor cells that have been analyzed in the past by our lab are shown in Figure 2 and 3 (Trimarchi et al., 2007, 2008; Cherry et al., 2009). These cells also had low levels of Notch target, cell cycle, and RPC genes (Figure 2.3, see cells P0 cell E1, P5 cell C4, P5 cell D2, P5 cell C2, P0 cell A4, P0 cell B1, P0 cell D1, P0 cell G3). These data show that Notch signaling was indeed depleted from most N1-CKO cells, as well as from some WT cells that were presumably exiting the cell cycle at these stages. Additionally, these data reveal which genes are sensitive to Notch1 signaling and provide examples of single cells at various stages in the transition between RPC and determined states.

Figure 2.3. Gene expression of selected Notch target, cell cycle, and progenitor genes in WT and N1-CKO single cells

The microarrays performed on single cells from WT and N1-CKO cells (described in Figure 2.1) were analyzed for the expression of selected genes. The signals for different types of genes are shown as a heatmap that was generated using Treeview software. The expression levels of Notch target genes, progenitor genes, and cell cycle genes are shown. For comparison, expression levels of selected genes in previously profiled cells, which were classified as amacrine (Cherry et al., 2009) or rod precursors (unpublished), are shown. The signal intensity from Affymetrix microarray chips has been scaled and is represented by a gradation in color, from bright red to black. Signals below 3,000 are black and signals from 3,000 to 10,000 are the appropriate shade of red. For Affymetrix identifier, Unigene number, and full gene name, see Appendix.

Figure 2.3 continued

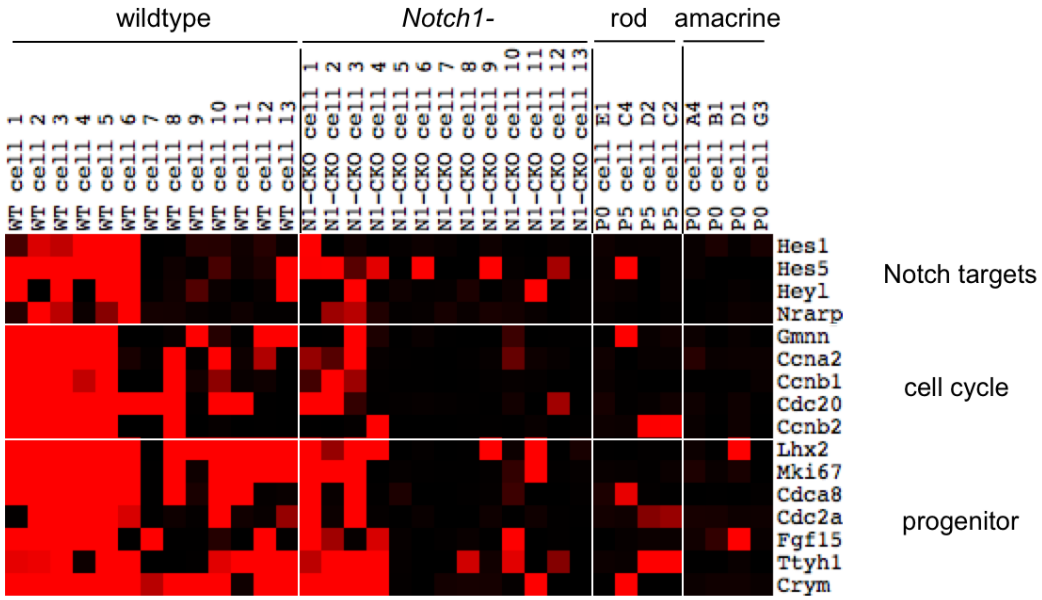

Figure 2.3

Unbiased search for genes with expression changes following loss of *Notch1*

An unbiased search for significantly downregulated genes was conducted by comparing gene expression levels in cells classified as RPCs (WT cells 2-6, 8, 12) to those in cells classified as rod precursor cells (N1-CKO cells 1-10). These particular cells were selected, since it was anticipated that RPCs express different sets of genes than rod precursor cells. T-test analysis with a cutoff p-value of <0.05 was performed to find significantly downregulated genes (Table A1, Appendix). We observed that Notch target genes such as *Hes1* and *Hes5* were found to be significantly downregulated, as predicted from visual inspection (Figure 2.1).

As loss of Notch signaling leads to the overproduction of rod photoreceptors at this stage of retinal development, it was anticipated that genes involved in photoreceptor development would be upregulated in *Notch1* deficient cells. Again, gene expression levels were compared between WT RPC cells and N1-CKO rod precursor cells. T-test analysis with a cutoff p-value of <0.05 was performed to find significantly upregulated genes (Table A2, Appendix). *NeuroD1*, *Math3,* and *Blimp1* are three such genes that were upregulated in N1-CKO cells (Figure 2.4 and Appendix). *NeuroD1* and *Math3* encode pro-neurogenic bHLH transcription factors that can lead to overproduction of rods when misexpressed (Inoue et al., 2002). Interestingly, *Math3* was upregulated in the N1-CKO cells that were classified as incipient rods, but not in the cells classified as amacrine precursor cells (Figure 2.2, 2.4, see rod N1-CKO cells 1-10 and amacrine N1-CKO cells 11-13), while *NeuroD1* was upregulated in N1-CKO cells classified as amacrine cells, as well as in those classified as rods (Figure 2.2 and 2.4, see N1-CKO cells 1-13). This is in keeping with the expression of *NeuroD1* in amacrine cells and the induction of amacrine

cells, along with rods, following *NeuroD1* misexpression (Morrow et al., 1999; Inoue et al., 2002). *Blimp1*, a gene that has been demonstrated to positively regulate the production of photoreceptor cells through repression of the bipolar cell fate (Brzezinski et al., 2010; Katoh et al., 2010), also was upregulated in N1-CKO cells (Figure 2.4, 2.5, discussed below). Because its expression is transient in retinal development, *Blimp1* is thought to demarcate the early period of photoreceptor formation. The robust upregulation of these key photoreceptor genes provides additional support for the validity of the single cell microarray approach in defining the genes responding to the loss of *Notch1* and inducing the rod fate.

In order to independently validate that the expression of these genes changes after the removal of *Notch1*, we performed a qPCR assay on populations of N1-CKO and WT cells. Retinas of *Notch1*$^{fl/fl}$ P0 pups were electroporated *in vitro* with plasmids encoding CAG:Cre, along with a Cre-responsive GFP reporter, (CALNL-GFP). For controls, the retinas of sibling *Notch1*$^{fl/fl}$ pups were electroporated with CAG:GFP. Electroporated retinas were cultured for three days, then dissociated to single cells. GFP+ cells (pooled from two retinas for each sample) were sorted by flow cytometry and collected. RNA was extracted from each sample and cDNA was generated. Samples were subjected to quantitative real time PCR in order to detect expression of *actin* (as a control), *Hes1*, *Nrarp*, *Math3*, *NeuroD1*, and *Blimp1* (Figure 2.4, B). In concordance with the changes observed by microarray analysis, *Hes1* and *Nrarp* were downregulated in N1-CKO cells, as compared to WT cells (Figure 2.4, B). Additionally, *Math3*, *NeuroD1*, and *Blimp1* were all upregulated in N1-CKO cells as compared to WT cells (Figure 2.4, B).

Figure 2.4. Analysis of genetic changes in NI-CKO and WT cells

The microarrays performed on single cells from WT and N1-CKO cells (described in Figure 2.1) were analyzed for the expression of genes that were up- and downregulated following removal of *Notch1*. A histogram depicting a subset of these genes is shown (A). *NeuroD1*, *Math3*, and *Blimp1* were all strongly upregulated in N1-CKO cells, as well as, in several WT cells. See also Tables in Appendix. qPCR analysis of gene expression in N1-CKO and WT cells. *Hes1* and *Nrarp* are known Notch target genes that were downregulated in N1-CKO cells as compared to WT cells. *NeuroD1*, *Math3*, and *Blimp1* were upregulated in N1-CKO cells as compared to WT cells (B). p-value < 0.05.

Figure 2.4 continued

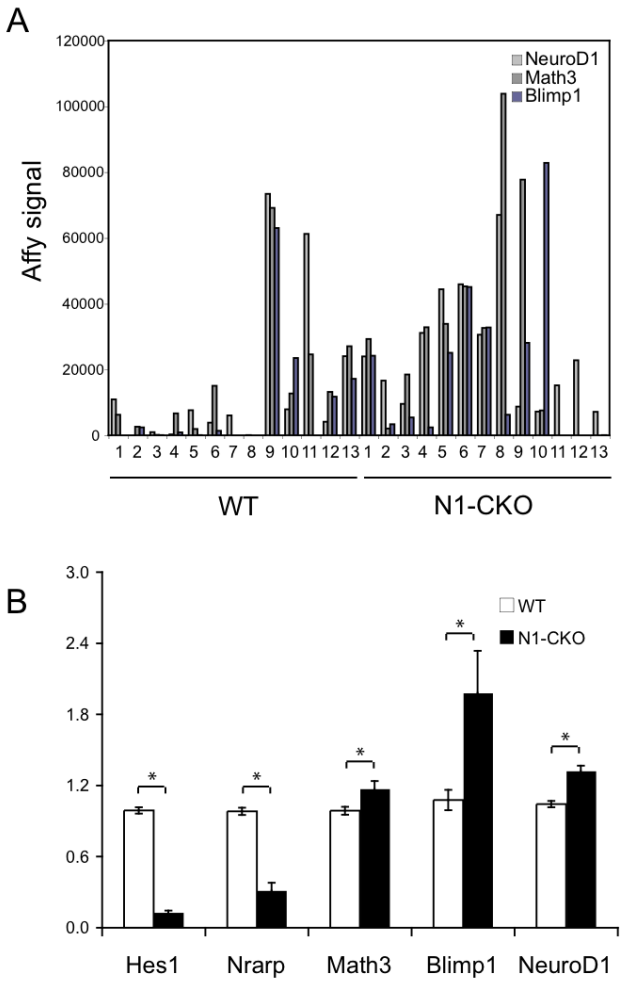

Figure 2.4.

Identification of genes associated with *Blimp1*

Blimp1 is expressed from embryonic time points to early postnatal stages in the developing retina in a temporal and spatial pattern highly correlated with incipient photoreceptors (Chang et al., 2002; Brzezinski et al., 2010; Katoh et al., 2010). Double immunohistochemistry experiments showed that *Blimp1*+ cells do not express RPC markers, but do coexpress *NeuroD1* (Brzezinski et al., 2010). Since cells expressing *Blimp1* have the molecular characteristics of early rods, the genes that are co-regulated with *Blimp1* are candidates for genes involved in photoreceptor differentiation. Using the pairwise comparison described above to find co-regulated genes, genes with expression patterns similar to *Blimp1* with p-values of $<10^{-3}$ were identified (Figure 2.5, A). Some known factors that closely tracked with *Blimp1* included *Rax*, *Math3*, and *Rbp3*. These genes are either markers of developing rods (*Rbp3*) or have been shown to play a role during photoreceptor genesis (*Rax*, *Math3*) (Chen and Cepko, 2002; Inoue et al., 2002; Jin et al., 2009) (Figure 2.5, A). In addition, *Epha8*, a gene not previously identified as associated with rod development, was identified. This may be a novel marker of rod photoreceptors, perhaps playing a functional role during rod specification and/or differentiation (Figure 2.5, A).

In order to validate if *Epha8* has a similar expression pattern to *Blimp1*, *in situ* hybridization (ISH) was performed on retinal sections at E16, P3, P9 and adult stages. Detection of *Blimp1* expression by ISH matched previous reports of Blimp1 expression by ISH, immunohistochemistry, and transgene expression (Chang et al., 2002; Brzezinski et al., 2010; Katoh et al., 2010). At E16, *Blimp1* expression was faintly expressed in the scleral outer neuroblastic layer (ONBL), where incipient photoreceptors are located. A

Figure 2.5. Analysis of Blimp1 associated genes

The microarrays performed on single cells from WT and N1-CKO cells (described in Figure 2.1) were analyzed to identify genes whose expression patterns correlated with *Blimp1*. A heatmap was generated using Treeview software to visualize expression levels of *Blimp1* and its associated genes in NI-CKO and WT cells (A). Signals below 3,000 are black and signals from 3,000 to 10,000 are a corresponding shade of red. For Affymetrix identifier, Unigene number, and full gene name, see Appendix. ISH for a novel gene correlated with *Blimp1* expression was performed at E16 (B, F), P3 (C, G), P9 (D, H), and adult (E, I) stages. Probes used were *Blimp1* (B-E) and *Epha8* (F-I). Cellular laminae are denoted: ONBL = outer neuroblastic layer, INBL = inner neuroblastic layer, ONL = outer nuclear layer, INL = inner nuclear layer.

Figure 2.5 continued

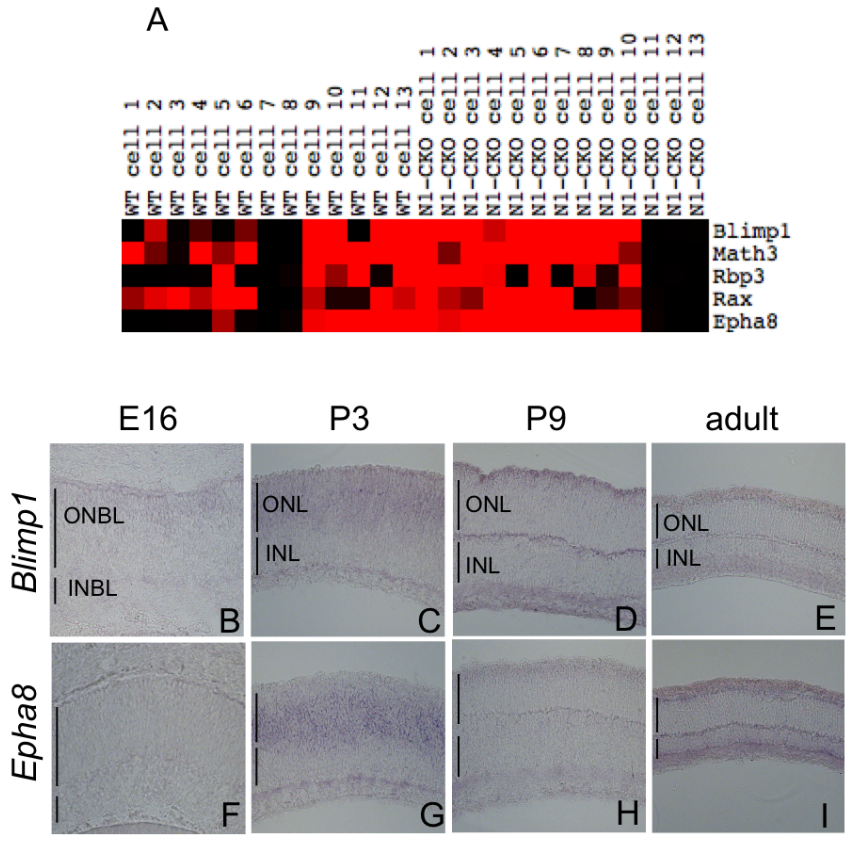

Figure 2.5

similar expression pattern was observed at P3 and P9 (Figure 2.5, C, D). Very faint staining was detected at adult stages (Figure 2.5, E). Next, the expression pattern of *Epha8* was investigated at the same stages. *Epha8* expression was not detected at E16 (Figure 2.5, F). At P3, staining in the ONBL was observed, similar to the pattern of *Blimp1* expression (Figure 2.5, C, G). *Epha8* expression was at a very low level throughout the retinal layers at P9 and adult stages (Figure 2.5, H, I). These results corroborated the microarray analysis, as *Epha8* expression was very similar to *Blimp1* expression (Figure 2.5). Further study is necessary to identify a functional role for *Epha8* during retinal development.

Markers of cell types expressed by profiled single cells

In addition to learning about genes involved in rod development, it was of interest to probe the microarray data from WT and N1-CKO cells for the expression of genes that are markers of amacrine cells, bipolar cells, and Müller glia. These fates are the ones normally taken by approximately 30% of the postnatally generated cells, and which are greatly reduced in the N1-CKO population. The expression patterns of known amacrine markers were compared to rod marker expression in WT and N1-CKO cells. They were also compared to the values in cells previously analyzed by our lab, which had been classified as either rod or amacrine precursor cells (Figure 2.6). P3 N1-CKO cells, which had been classified as rod precursor cells, expressed rod marker genes robustly, but did not express amacrine marker genes (Figure 2.2 and 2.6, see N1-CKO cells 1-10). The transcriptional profiles of these cells resembled those of previously profiled rod precursor cells (Figure 2.6, see P0 cell E1, P5 cell C4, P5 cell D2, P5 cell C2) (Trimarchi et al.,

2007). Conversely, N1-CKO cells classified as developing amacrine cells expressed amacrine marker genes and not rod marker genes (Figure 2.2, 2.6, see N1-CKO cells 11-13). The expression profiles of these cells were similar to cells classified as amacrine precursor cells in our previous studies (Trimarchi et al., 2007; Cherry et al., 2009) (Figure 2.6, see P0 cell A4, P0 cell B1, P0 cell D1, P0 cell G3).

Interestingly, some WT cells expressed marker genes specific to mature amacrine cells, as well as other genes specific to rod photoreceptors. This is in keeping with the scores on the classification scheme, as some of these WT cells did not exhibit scores indicating clear cell type identities. Only three WT cells scored highly as rod precursor cells (Figure 2.2, see WT cells 9-11). Examples of cells that expressed several amacrine marker genes (such as *Tcfap-2β*, *Fgf13*, *Nhlh2*) and rod marker genes (such as *Crx*, *Otx2*, *Nrl*) include WT cells 1, 2, and 6 (Figure 2.6). These cells did not score highly in the classification scheme for any of the potential cell types (Figure 2.2, see WT cells 1, 2, and 2.6) and retained expression of cell cycle and RPC marker genes (Figure 2.3, see WT cells 1, 2, and 6).

The profiled cells also were examined for expression of Müller glial and bipolar cell marker genes. Previous studies have shown that a number of genes expressed by mature Müller glial cells, such as *Sox2*, *μ-crystallin*, and *Dkk3,* were also expressed in WT late RPCs (Blackshaw et al., 2004; Trimarchi et al., 2007, 2008; Roesch et al., 2008; Cherry et al., 2009). Some of these shared genes were downregulated in N1-CKO cells (Figure 2.3 and Appendix). Additionally, marker genes thought to be specific for Müller glial cells, such as *Apoe* and *clusterin* (Blackshaw et al., 2004; Roesch et al., 2008), were not expressed above detectable levels in almost any of the profiled cells (Figure 2.7). For

Figure 2.6. Expression of selected rod and amacrine marker genes in N1-CKO and WT cells

The microarrays performed on single cells from WT and N1-CKO cells (described in Figure 2.1) were analyzed for the expression of genes that are expressed in rod photoreceptors and amacrine cells. A heatmap was generated using Treeview software to visualize the expression of these genes. For comparison, expression levels of selected genes in previously profiled cells, which were classified as amacrine (Cherry et al., 2009) or rod precursors (unpublished), are shown. The signal intensity from Affymetrix microarray chips has been scaled and is represented by a gradation in color, from bright red to black. Signals below 3,000 are black and signals from 3,000 to 10,000 are the appropriate shade of red. For Affymetrix identifier, Unigene number, and full gene name, see Appendix.

Figure 2.6 continued

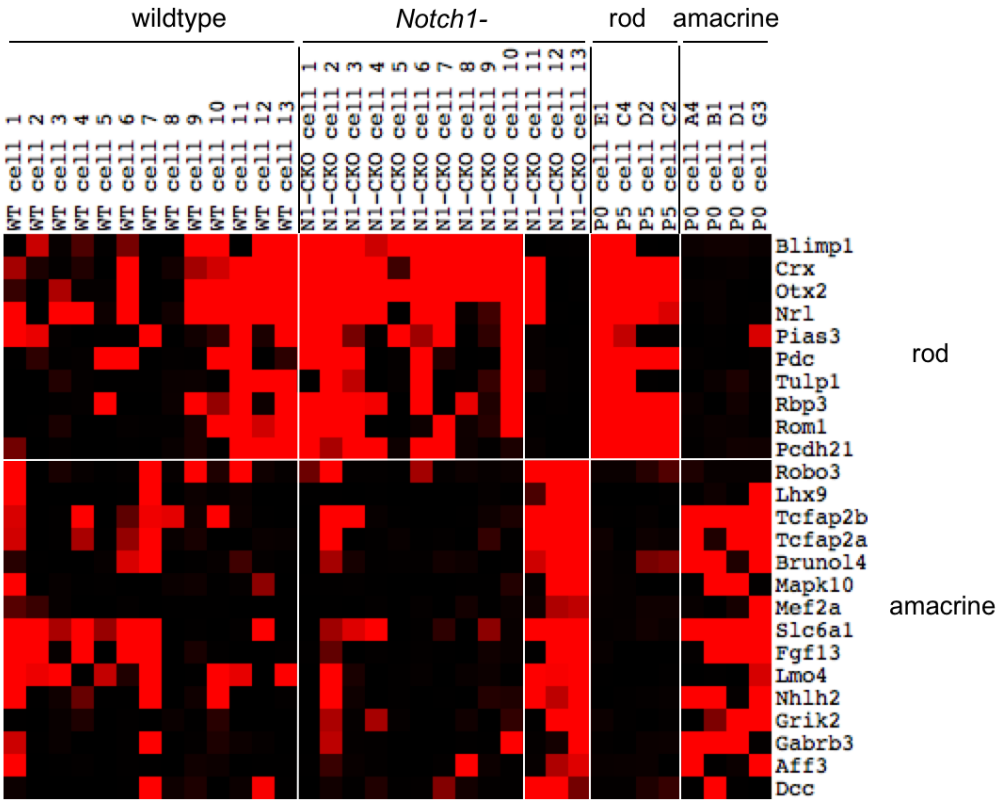

Figure 2.6

these reasons, it was difficult to determine by direct inspection of the heatmaps if cells were becoming Müller glia. In addition, using the classification scheme, which relies on a large number of Müller glial genes, none of the P3 cells were classified as Müller glial cells (Figure 2.2). Inspection of the profiled cells for expression of bipolar genes did not yield many positives, which may not be surprising, as known bipolar marker genes are not robustly expressed at P3 *(e.g. Lhx3*, *Car8*, *Car10*, and *Nfasc)* (Kim et al., 2008b) (Figure 2.7). The absence of these marker genes does not preclude the possibility that some of these cells may later express bipolar genes or be on the path to becoming bipolar cells.

Discussion

In this study, we profiled single N1-CKO and WT retinal cells on Affymetrix microarrays. Using this unbiased method, we identified a large number of genes that were either up or downregulated in the absence of *Notch1*. The cohort of downregulated genes included cell cycle regulators or progenitor markers, some of which were not yet appreciated to be *Notch1* sensitive (e.g. *Fgf15*, *Cdc20*, *Crym*). Upregulated genes included known regulators or markers of rod photoreceptor development, such as *NeuroD1*, *Math3*, *Rbp3* and *Blimp1*. Future experiments need to be performed to test the novel Notch responsive genes identified by this study for their roles in retinal development.

Figure 2.7. Expression of selected Müller glial and bipolar marker genes in WT and N1-CKO cells

The microarrays performed on single cells from WT and N1-CKO cells (described in Figure 2.1) were analyzed for the expression of genes that are expressed in Müller glial cells (A) or bipolar cells (B). A heatmap was generated using Treeview software to visualize expression levels of these genes in WT and N1-CKO cells. The signal intensity from Affymetrix microarray chips has been scaled and is represented by a gradation in color, from bright red to black. Signals below 3,000 are black and signals from 3,000 to 10,000 are the appropriate shade of red. For Affymetrix identifier, Unigene number, and full gene name, see Appendix.

Figure 2.7 continued

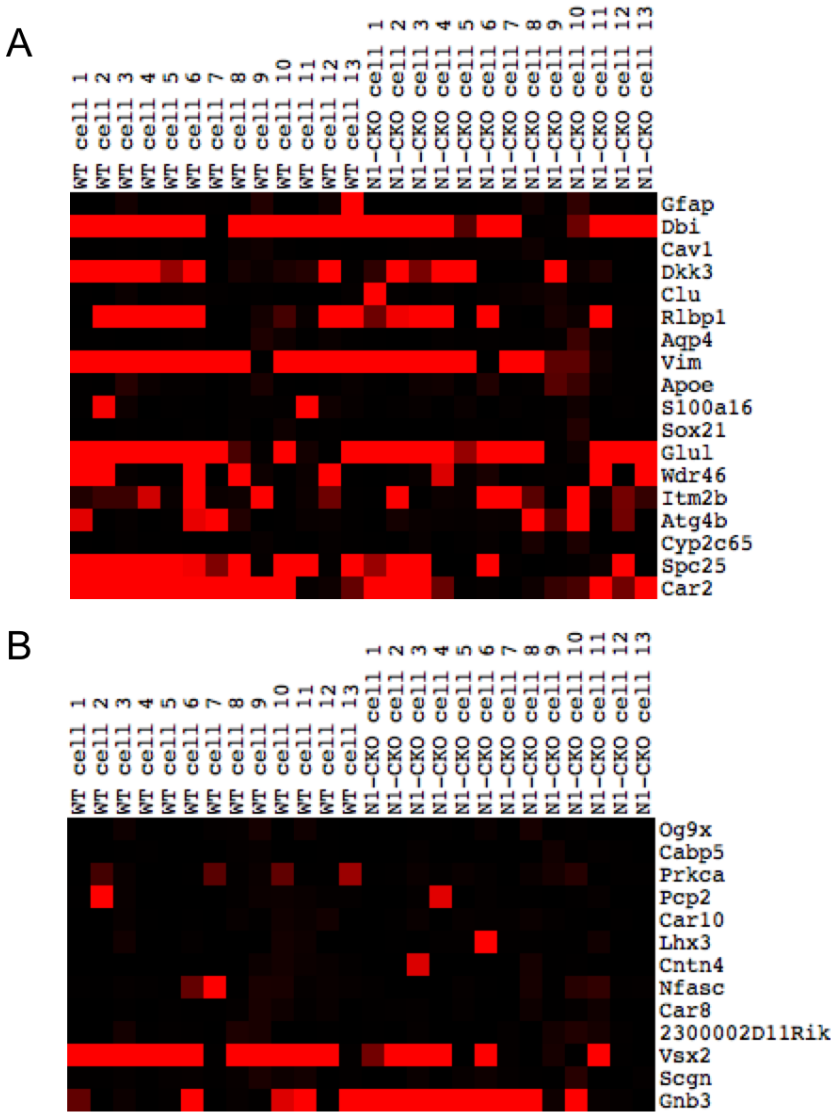

Figure 2.7

The majority of the profiled N1-CKO cells were classified as incipient photoreceptors using *Blimp1* as a marker. As described above, *Blimp1* is expressed in rod precursor cells. Genes whose expression patterns were highly correlated with *Blimp1* included known genes known to be expressed in rods, such as *Math3*, *Rbp3*, and *Rax*, in addition to the newly identified gene, *Epha8*. The expression pattern of *Epha8* at P3 suggests that this gene is a good marker of early rod photoreceptors, similar to *Blimp1*. Due to its lack of expression embryonically, *Epha8* could potentially be specifically expressed in early rod photoreceptors and not in cone photoreceptors, which are produced only during embryogenesis. Future experiments will determine this specificity, as well as elucidate whether *Epha8* plays a functional role in retinal development.

Single cell analysis also revealed that newly postmitotic retinal cells co-expressed amacrine and rod marker genes. This result is consistent with the idea that cells go through a plastic phase shortly after exiting the cell cycle, during which they can express marker genes of different cell types. Alternatively, the coexpression of markers of two cell types does not indicate plasticity, but indicates that certain loci are derepressed, independently of whether a cell is still plastic enough to choose more than one cell fate. The co-expression of rod and amacrine markers does not appear to be an artifact of the single cell profiling method. Only certain genes were coexpressed, and the same ones were seen in multiple cells. If, for example, coexpression was the result of contamination of a single cell's RNA preparation with RNAs from another cell, one might predict random patterns, as opposed to consistent genes in the profiles. In addition, many cells that appeared more mature, as assessed by height levels of specific genes and

classification scores that indicated a more definitive fate, did not coexpress genes of two cell types (Figure 2.2).

It is unclear what population of cells is represented by the cells that coexpress these markers. If the majority of RPCs are determined to give rise to stereotyped progeny, and coexpression of amacrine and rod genes occurs in the RPCs that will give rise to a rod and an amacrine, then only a few single cells should coexpress amacrine and rod marker genes. This prediction is based upon Young's birthdating data, as amacrine cells are only a small percentage (1-2%) of the progeny of P0 RPC (Young, 1985a). However, most of the profiled WT cells in this study coexpressed amacrine and rod marker genes. If there are determined subsets of RPCs that produce a rod and an amacrine, a rod and a bipolar, or a rod and Müller glial cell, then single cells coexpressing rod and bipolar genes, as well as single cells coexpressing rod and Müller genes would have been predicted. In fact, Müller glial genes are expressed in the majority of P0 RPCs, though only a small percentage of the progeny of postnatal RPCs (<10%) will be Müller glial cells (Young, 1985a; Blackshaw et al., 2004; Roesch et al., 2008; Trimarchi et al., 2008). Single WT cells did coexpress marker genes shared by late RPCs and Müller glial cells, but not marker genes exclusive to Müller glial cells. In addition, the single cells did not express known markers of bipolar cells. However, since none of the known marker genes for bipolar cells are expressed as early as P3, this is not surprising. There may be active repression of bipolar genes by *Blimp1*, which is expressed in these cells, and has been shown to inhibit bipolar fate (Brzezinski et al., 2010; Katoh et al., 2010). This repression may be transient, as *Blimp1* expression wanes late in the first postnatal week, when many bipolar cells are born and/or begin to differentiate (Young, 1985a; Kim et al., 2008b).

Further analysis of all of these genetic relationships will be required to understand how these cells sort out their fates, and to understand the meaning of the coexpression of amacrine and rod genes in such a large percentage of these cells.

Transcriptional profiling of individual N1-CKO and WT cells revealed the genetic changes that occur when cells transition from the progenitor state to that of a newly postmitotic cell. The absence of *Notch1* signaling resulted in the downregulation of a number of cell cycle and progenitor markers in N1-CKO cells. Interestingly, we observed the same genetic changes in WT cells that scored highly as incipient neurons as well, suggesting that turning down Notch signaling and the identified genes is part of the normal cell cycle exit process. If *Notch1* is absent during the fate specification process, the majority of newly postmitotic cells will turn on markers of rod photoreceptors and take on this fate, while a few will become amacrine cells. The role of *Notch1* in the developing retina may be to maintain cells in an uncommitted state long enough for some of them to respond to intrinsic programs and/or extrinsic cues to then eventually take on a non-photoreceptor fate.

Methods

Animals

Notch1$^{fl/fl}$ were maintained as homozygotes (Radtke et al., 1999). WT CD-1 mice were obtained from Charles River Laboratories. All experiments were approved by the Institutional Animal Care and Use Committee at Harvard University.

In vivo and *in vitro* Electroporation

In vivo electroporation were performed as previously described (Turner and Cepko, 1987; Matsuda and Cepko, 2004, 2007). DNA constructs and retroviruses used include CAG:GFP, CAG:Cre, CALNL-GFP (Matsuda and Cepko, 2004).

Single Cell Probe Preparation and Affymetrix Array Hybridization

Single cells were isolated and profiled as described previously (Trimarchi et al., 2007, 2008). Cells were chosen based on GFP expression. Probe reactions were performed as described previously, and Affymetrix microarrays were hybridized and processed using standard Affymetrix protocols (Trimarchi et al., 2007, 2008; Roesch et al., 2008; Cherry et al., 2009). Global scaling was performed using the Affymetrix Microarray Software (MAS 5.0) and the target intensity was set to 500. The signal data for each probe set was exported for further analyses in Microsoft Excel. To eliminate probesets called marginal or absent and to reduce the false-positive rate, only probesets with a RS > 1000, as determined by MAS 5.0 were considered in this analysis. Previous reports suggest that this threshold corresponds to transcripts that are present at between 10 and 100 copies per cell (Tietjen et al., 2003). Treeview software was utilized to view the microarray signal data. The raw and processed Affymetrix data files have been deposited in the NCBI Gene Expression Omnibus (GEO). GEO submission: GSE35682.

FACS purification and quantitative PCR

FACS was performed on a BD Aria II sorter, gated for GFP detection. 3-5 x 10^5 GFP+ cells were collected from two dissociated retinas for each sample. After sorting, GFP+ cells were lysed in Trizol (Invitrogen) and stored at -80°C. Phenol-chloroform extractions

were performed to isolate total RNA. cDNA was generated using Accuscript High Fidelity (Agilent Technologies) according to manufacturer's guidelines. Quantitative real time PCR was performed and gene expression was normalized according to *actin* expression in each sample. Primers used included: *actin* – accaactgggacgacatggagaa, tacgaccagaggcatacagggac; *Nrarp* - agggccagacagcactacac, cttggccttggtgatgagat; *Hes1* - acaccggacaaaccaaagac, atgccgggagctatctttct; *Blimp1* - cacacaggagagaagccaca, ttgtgacactgggcacactt; *Math3* – attcagggctcgaagagtca, gttccttgccagtcgaagag; *NeuroD1* – gtgtcccgaggctccagggt, gggaccttggggctgaggct.

Section *in situ* hybridization

Retinas were collected at various developmental time points. ISH on retinal sections was performed as previously described (Trimarchi et al., 2008).

REFERENCES

Blackshaw, S., Harpavat, S., Trimarchi, J., Cai, L., Huang, H., Kuo, W.P., Weber, G., Lee, K., Fraioli, R.E., Cho, S.-H., et al. (2004). Genomic analysis of mouse retinal development. PLoS Biol *2*, E247.

Brady, G., and Iscove, N.N. (1993). Construction of cDNA libraries from single cells. Meth. Enzymol *225*, 611–623.

Brzezinski, J.A., Lamba, D.A., and Reh, T.A. (2010). Blimp1 controls photoreceptor versus bipolar cell fate choice during retinal development. Development *137*, 619–629.

Chang, D.H., Cattoretti, G., and Calame, K.L. (2002). The dynamic expression pattern of B lymphocyte induced maturation protein-1 (Blimp-1) during mouse embryonic development. Mech. Dev *117*, 305–309.

Chen, C.-M.A., and Cepko, C.L. (2002). The chicken RaxL gene plays a role in the initiation of photoreceptor differentiation. Development *129*, 5363–5375.

Cherry, T.J., Trimarchi, J.M., Stadler, M.B., and Cepko, C.L. (2009). Development and diversification of retinal amacrine interneurons at single cell resolution. Proc. Natl. Acad. Sci. U.S.A *106*, 9495–9500.

Dulac, C., and Axel, R. (1995). A novel family of genes encoding putative pheromone receptors in mammals. Cell *83*, 195–206.

Inoue, T., Hojo, M., Bessho, Y., Tano, Y., Lee, J.E., and Kageyama, R. (2002). Math3 and NeuroD regulate amacrine cell fate specification in the retina. Development *129*, 831–842.

Iscove, N.N., Barbara, M., Gu, M., Gibson, M., Modi, C., and Winegarden, N. (2002). Representation is faithfully preserved in global cDNA amplified exponentially from sub-picogram quantities of mRNA. Nat. Biotechnol *20*, 940–943.

Iso, T., Sartorelli, V., Chung, G., Shichinohe, T., Kedes, L., and Hamamori, Y. (2001). HERP, a new primary target of Notch regulated by ligand binding. Mol. Cell. Biol *21*, 6071–6079.

Jadhav, A.P., Mason, H.A., and Cepko, C.L. (2006). Notch 1 inhibits photoreceptor production in the developing mammalian retina. Development *133*, 913–923.

Jin, M., Li, S., Nusinowitz, S., Lloyd, M., Hu, J., Radu, R.A., Bok, D., and Travis, G.H. (2009). The role of interphotoreceptor retinoid-binding protein on the translocation of visual retinoids and function of cone photoreceptors. J. Neurosci *29*, 1486–1495.

Katoh, K., Omori, Y., Onishi, A., Sato, S., Kondo, M., and Furukawa, T. (2010). Blimp1 suppresses Chx10 expression in differentiating retinal photoreceptor precursors to ensure proper photoreceptor development. J. Neurosci *30*, 6515–6526.

Kim, D.S., Ross, S.E., Trimarchi, J.M., Aach, J., Greenberg, M.E., and Cepko, C.L. (2008). Identification of molecular markers of bipolar cells in the murine retina. J. Comp. Neurol *507*, 1795–1810.

Krebs, L.T., Deftos, M.L., Bevan, M.J., and Gridley, T. (2001). The Nrarp gene encodes an ankyrin-repeat protein that is transcriptionally regulated by the notch signaling pathway. Dev. Biol *238*, 110–119.

Livesey, F.J., and Cepko, C.L. (2001). Vertebrate neural cell-fate determination: lessons from the retina. Nat. Rev. Neurosci *2*, 109–118.

Matsuda, T., and Cepko, C.L. (2004). Electroporation and RNA interference in the rodent retina in vivo and in vitro. Proc. Natl. Acad. Sci. U.S.A *101*, 16–22.

Matsuda, T., and Cepko, C.L. (2007). Controlled expression of transgenes introduced by in vivo electroporation. Proc. Natl. Acad. Sci. U.S.A *104*, 1027–1032.

Morrow, E.M., Furukawa, T., Lee, J.E., and Cepko, C.L. (1999). NeuroD regulates multiple functions in the developing neural retina in rodent. Development *126*, 23–36.

Ohtsuka, T., Ishibashi, M., Gradwohl, G., Nakanishi, S., Guillemot, F., and Kageyama, R. (1999). Hes1 and Hes5 as notch effectors in mammalian neuronal differentiation. Embo J *18*, 2196–2207.

Radtke, F., Wilson, A., Stark, G., Bauer, M., van Meerwijk, J., MacDonald, H.R., and Aguet, M. (1999). Deficient T cell fate specification in mice with an induced inactivation of Notch1. Immunity *10*, 547–558.

Roesch, K., Jadhav, A.P., Trimarchi, J.M., Stadler, M.B., Roska, B., Sun, B.B., and Cepko, C.L. (2008). The transcriptome of retinal Müller glial cells. J. Comp. Neurol *509*, 225–238.

Tietjen, I., Rihel, J.M., Cao, Y., Koentges, G., Zakhary, L., and Dulac, C. (2003). Single-cell transcriptional analysis of neuronal progenitors. Neuron *38*, 161–175.

Trimarchi, J.M., Stadler, M.B., and Cepko, C.L. (2008). Individual retinal progenitor cells display extensive heterogeneity of gene expression. PLoS ONE *3*, e1588.

Trimarchi, J.M., Stadler, M.B., Roska, B., Billings, N., Sun, B., Bartch, B., and Cepko, C.L. (2007). Molecular heterogeneity of developing retinal ganglion and amacrine cells revealed through single cell gene expression profiling. J. Comp. Neurol *502*, 1047–1065.

Turner, D.L., and Cepko, C.L. (1987). A common progenitor for neurons and glia persists in rat retina late in development. Nature *328*, 131–136.

Wong, L.L., and Rapaport, D.H. (2009). Defining retinal progenitor cell competence in Xenopus laevis by clonal analysis. Development *136*, 1707–1715.

Yaron, O., Farhy, C., Marquardt, T., Applebury, M., and Ashery-Padan, R. (2006). Notch1 functions to suppress cone-photoreceptor fate specification in the developing mouse retina. Development *133*, 1367–1378.

Young, R.W. (1985a). Cell differentiation in the retina of the mouse. Anat. Rec *212*, 199–205.

Young, R.W. (1985b). Cell proliferation during postnatal development of the retina in the mouse. Brain Res *353*, 229–239.

Chapter 3

Notch1 and downstream factors are required in newly postmitotic cells to inhibit the rod photoreceptor fate

Karolina Mizeracka, Jeffrey M. Trimarchi, Michael B. Stadler, and Constance L. Cepko

Contributions: J.M.T and M.B.S assisted in performing analysis of microarray data

Summary

Several models of cell fate determination can be invoked to explain how single retinal progenitor cells produce different cell types in a terminal division. To gain insight into this process, *Notch1*, a regulator of cell fate, was specifically removed from newly postmitotic cells using a conditional allele of *Notch1* (N1-CKO) in mice. Almost all newly postmitotic N1-CKO cells became rod photoreceptors, whereas wildtype (WT) cells achieved a variety of fates. Single cell profiling of wildtype (WT) and *Notch1* deficient (N1-CKO) retinal cells transitioning from progenitor to postmitotic states has revealed differential expression of *Inhibitor of differentiation 1* and *3* genes. Misexpression of these genes is sufficient to drive production of Müller glial or progenitor-like cells. Moreover, *Id1* and *3* can rescue the production of Müller glial cells in the absence of *Notch1*.

Introduction

The retina is an area of the central nervous system that offers excellent accessibility and a well-characterized anatomy and physiology. These attributes have allowed investigation of its development, including lineage analyses (Turner and Cepko, 1987; Holt et al., 1988; Wetts and Fraser, 1988; Turner et al., 1990) and birthdating studies (Young, 1985a; Rapaport et al., 2004). The types of neurons found in the retina represent the types of neurons found throughout the nervous system, including neurons which receive information (rod and cone photoreceptors), local neurons which process information (the interneurons, including amacrine cells, horizontal cells, and bipolar cells), output neurons (retinal ganglion cells), and one type of glial cell (Müller glia). During development, retinal neurons arise in a conserved, temporal sequence from multipotent, cycling retinal progenitor cells (RPCs) (Livesey and Cepko, 2001). Retinal ganglion cells are born first, followed by horizontal cells, cone photoreceptors, rod photoreceptors, amacrine cells, bipolar cells, and Müller glia (Young, 1985a; Wong and Rapaport, 2009).

Previous studies have not definitively established how a retinal cell makes a cell fate decision. One possibility is that a RPC might decide the fate of daughter cells and then pass on this decision to its daughter cells via determinants and/or chromatin state. For example, heterochronic mixing experiments using retinal cells have provided an example wherein embryonic mitotic cells appeared to determine the fate of their amacrine cell daughters (Belliveau and Cepko, 1999). Furthermore, recent studies on chick and zebrafish retinas revealed that some horizontal cells were produced by RPCs that made horizontal cells exclusively, suggesting the inheritance of the horizontal fate from a

committed RPC (Godinho et al., 2007; Rompani and Cepko, 2008). In another well studied CNS tissue, the cerebral cortex, the laminar fate of cortical cells was shown to be determined in the late S or G2 stage of a terminal cell cycle, and thus in the progenitor cell (McConnell and Kaznowski, 1991). Alternatively, newly postmitotic daughter cells might remain plastic, and use other mechanisms to ultimately determine their fates, likely in combination with information inherited from their progenitor cell. A result that was consistent with this possibility was observed when newly postmitotic cells fated to be rod photoreceptor cells were treated with ciliary neurotrophic factor. The treated cells did not express rod markers, but did express some markers of bipolar cells, even though they would not normally do so (Ezzeddine et al., 1997). These observations are consistent with the idea that some retinal cells are plastic, or at least can change fate under some conditions after exiting cell cycle. It is possible that cell fate determination can occur at different stages in the continuum from RPC to postmitotic daughter, perhaps with different cell types choosing their fates at different time points. In order to gain further insights into this process, we removed *Notch1*, a gene known to influence cell fate choice, from newly postmitotic cells, to see if it played a role in cell fate determination after cell cycle exit.

As cells exit the cell cycle, genes that regulate cell cycle turn off, and a cohort of genes indicative of different fates are turned on. During retinal development, the Notch signaling pathway regulates both cell cycle exit and cell fate specification (Yaron et al., 2006; Jadhav et al., 2006b). Genetic removal of *Notch1*, or Notch downstream effectors such as *Hes1* and *RBP-J*, during early stages of retinal development resulted in precocious cell cycle exit and neurogenesis (Tomita et al., 1996; Yaron et al., 2006;

Jadhav et al., 2006b; Riesenberg et al., 2009; Zheng et al., 2009). Loss of *Notch1* embryonically resulted in the overproduction of cone photoreceptors, whereas depletion of *Notch1* during postnatal retinal development led to the overproduction of rod photoreceptors (Jadhav et al., 2006b), in keeping with the birth order of rod and cone photoreceptor cells. Therefore, Notch signaling is not only crucial for maintenance of the retinal progenitor pool, but also for the repression of photoreceptor fate.

One interpretation of the previous *Notch1* knockout experiments is that *Notch1* carried out both of its functions, cell cycle regulation and cell fate determination, in a cycling RPC. If this were the case, *Notch1* would establish fate decisions in RPCs, and this decision would be inherited by postmitotic daughter cells. Alternatively, *Notch1* activity may be essential for cell fate determination in cells that have recently exited the cell cycle. In order to investigate if cell fate determination was dependent on *Notch1* after cell cycle exit, a *Notch1* conditional allele was deleted specifically in newly postmitotic cells. Genetic removal of *Notch1* from these cells resulted in the overproduction of rod photoreceptors at the expense of the other cell types normally produced at this time. *Notch1* is thus required in postmitotic cells to regulate the cell fate decision, and this role is distinct from its role in regulating cell cycle exit.

Results

Viral mediated loss of *Notch1* reveals activity in newly postmitotic cells

In order to determine if Notch1 signaling plays a role in cell fate specification in newly postmitotic cells, two independent strategies were undertaken to genetically remove *Notch1* from these cells. The first approach took advantage of the manner in which some

types of retroviruses infect and mark cells (Figure 3.1 A, B). Upon entering a host cell, viral reverse transcriptase creates only a single copy of the viral genome in the cytoplasm. The pre-integration complex of a Type-C retrovirus, which is the type used for lineage tracing, cannot penetrate the nuclear envelope. Thus, the integration of the viral DNA into the host genome, which allows for stable marking of a clone, can only occur after the breakdown of the nuclear envelope during M phase (Turner and Cepko, 1987; Roe et al., 1997). Since the host genome will be 4N at this time, and there is a single copy of the viral genome, only one of the daughter cells of the initially infected cell will inherit the viral genome. In all subsequent cell cycles, the integrated viral genome will be replicated along with that of the host, and thus all of the progeny of the cell with the integrated viral genome will be marked. Clones can consist of one to thousands of cells following infection of the retina at various times (Turner and Cepko, 1987; Turner et al., 1990; Fields-Berry et al., 1992; Fekete et al., 1994; Rompani and Cepko, 2008). A one cell clone results from an initially infected progenitor cell that divides to produce a virally marked daughter cell that does not further divide (Figure 3.1, B). These aspects of the viral life cycle provide a means by which to assess changes in gene expression in newly postmitotic cells. Any transgene carried by the virus (GFP, Cre, etc) will be expressed only after integration, and if the clone consists of one cell, then the expression will be initiated only in a postmitotic cell.

We wanted to remove *Notch1* at a time point when the majority of clones produced normally would be one cell clones. Studies of proliferation in the rat and mouse retina showed that mitotic activity decreases in the postnatal period, and ends in the second postnatal week (Young, 1985a; Rapaport et al., 2004). Consequently, many small

Figure 3.1. Clonal inactivation of *Notch1* in newly postmitotic cells

Almost all clones derived from a P3 infection consist of one or two cells, as progenitor cells only divide once or twice at these late developmental stages. The replication incompetent retroviruses used in this study can only integrate into the genome of a host cell after the break down of the nuclear envelope during mitosis. Additionally, once a progenitor cell is infected with a retrovirus, only one of its daughter cells will inherit the single copy of the viral genome. Hence, two cell clones are derived from daughter cells that are mitotic, whereas one cell clones are derived from daughter cells that are postmitotic (A, B). *Notch1*$^{fl/fl}$ retinas were infected with BAG virus which encodes β-galactosidase (to mark wildtype clones) and Lia-Cre virus which encodes Cre-ires-AP expressing (to mark *Notch1*- clones) viruses at P3 and the fate of single cell clones was assessed after P21 (C). Percentage of wildtype or *Notch1*- single cell clones after P3 infection (D). Quantification of cell types found in wildtype or *Notch1*- single cell clones (E). n=3 retinas per condition. p-value < 0.01.

Figure 3.1 continued

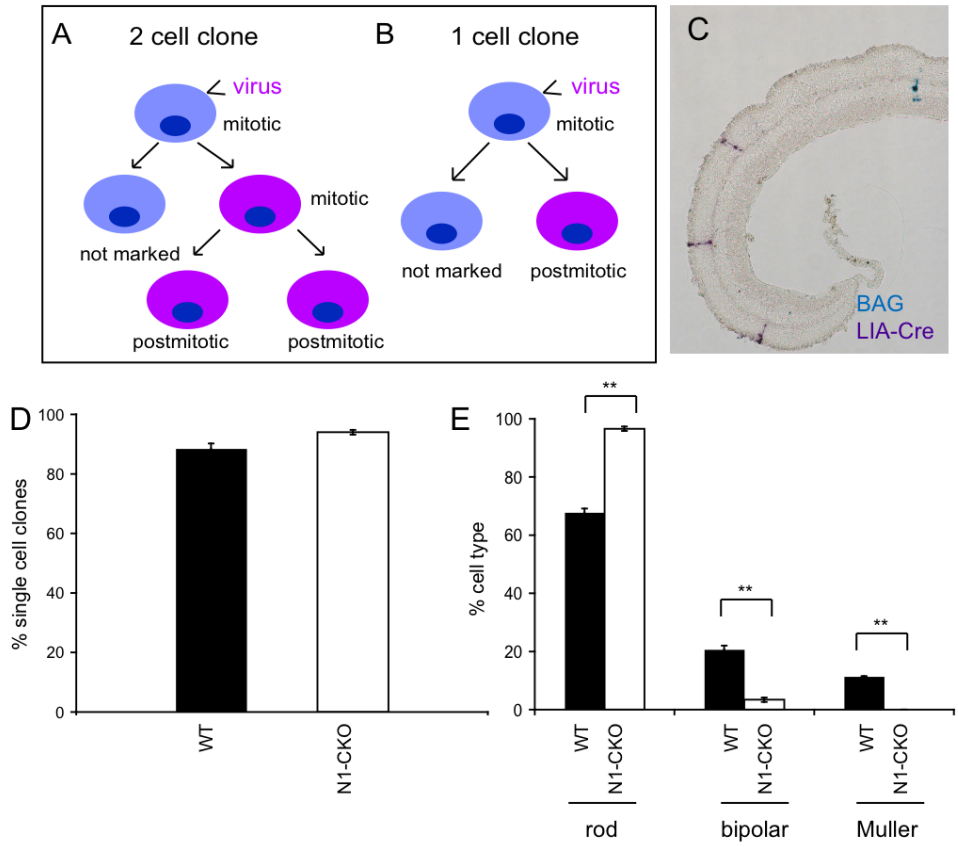

Figure 3.1

and single cell clones have been observed following viral infection in the postnatal period (Turner and Cepko, 1987; Turner et al., 1990; Fields-Berry et al., 1992). Therefore, in order to deplete postmitotic cells of *Notch1*, postnatal day 3 (P3) was chosen as a time point for infection of *Notch1*$^{fl/fl}$ mice with a retrovirus encoding Cre (LIA-Cre, described below). As a control, BAG, a virus encoding *lacZ*, but not *Cre*, was delivered at the same time to the same retinas. This allowed an assessment of the clone size and the types of cells normally produced by P3 RPCs. The titer and dose of the viruses were low, such that no cell would be co-infected by both BAG and LIA-Cre.

BAG and LIA-Cre retroviruses were co-injected *in vivo* into the subretinal space of P3 *Notch1*$^{fl/fl}$ retinas. After the completion of retinal development (P21 or later), three retinas were processed via histochemical staining to detect BAG clones and LIA-Cre clones. BAG-infected cells were identified by histochemical staining for X-gal, which rendered the cells blue. The LIA-Cre virus encodes *Cre-IRES-human placental alkaline phosphatase* (AP), allowing for detection of infected cells histochemically with BCIP plus NBT, which creates a purple precipitate (Figure 3.1, C). As predicted by previous birthdating experiments (Young, 1985a), 88.6+/-1.7% of BAG clones comprised only one cell. These data demonstrate that 88.6+/-1.7% of cells that integrated the viral genome did not re-enter the cell cycle, i.e. were postmitotic (Figure 3.1, D). Among the single cell BAG clones, 67.9+/-1.4% of cells were rods, 20.7+/-1.3% were bipolars, and 11.4+/-0.1% were Müller glial cells (Figure 3.1, C, E). In contrast, the single cell clones derived from infection with LIA-Cre resulted in 96.6+/-0.8% rods, 3.4+/-0.8% bipolar, and 0+/-0% Müller glial cells (Figure 3.1, C, E). There also was an increase in the frequency of single cell clones, to an average of 94.3+/-0.8% as compared to 88.6+/-1.7%

in three retinas (Figure 3.1, D). This is likely due to the loss of *Notch1* in cells that would normally re-enter the cell cycle to produce two cell clones. The overproduction of rods at the expense of other cell types is consistent with *Notch1* being required to inhibit non-rod fates in newly postmitotic cells.

Loss of *Notch1* function in newly postmitotic, electroporated N1-CKO cells

A second, independent approach was undertaken to assess the role of *Notch1* signaling in newly postmitotic cells. Newly postmitotic cells were identified among cells that had been electroporated with a plasmid encoding GFP, but which had not undergone an S-phase. This was accomplished by labeling with EdU, a thymidine analog that is incorporated during S phase (Salic and Mitchison, 2008). A plasmid encoding CAG:Cre, which uses the broadly active CAG promoter to drive Cre expression, and a plasmid, CALNL-GFP, which uses CAG to drive expression of a Cre-responsive GFP reporter (Matsuda and Cepko, 2007) were co-electroporated *in vivo* into WT and *Notch1*$^{fl/fl}$ retinas at P1. Mitotic cells were labeled with three injections of EdU: immediately after electroporation, 8 hours after electroporation, and 24 hours after electroporation. These EdU injections were timed according to the lengths of the cell cycle phases (16 hrs for S, minimum of 2.6 hrs for G2, 8.5 hrs for G1, and 2.5 hr for M) and the overall cell cycle length at P1 (approximately 30 hrs) (Young, 1985b) to ensure that all cycling cells were labeled (Figure 3.2, A). As previous work suggested that mitotic cells were preferentially electroporated (Matsuda and Cepko, 2004), GFP+ EdU- cells were interpreted as cells that were electroporated as they were exiting the cell cycle, or had recently exited, but

Figure 3.2. Depletion of Notch signaling in newly postmitotic cells

Plasmids encoding CAG:Cre along with a Cre-responsive GFP reporter were electroporated into wildtype and *Notch1*$^{fl/fl}$ retinas at P1 (green cells). In order to assess the fate of electroporated, newly postmitotic cells, the entire mitotic cell population was labeled at the time of electroporation. Based on the length of the cell cycle (around 30 hrs) and S-phase (around 16 hours), three EdU injections were performed to ensure that all cycling cells were labeled (Alexiades and Cepko, 1996) (A). First, immediately after electroporation, mice were injected with EdU to label cells in S-phase (magenta nuclei). 8 hours after electroporation, mice were injected with EdU a second time to label any electroporated cells that had reentered the cell cycle and progressed into S-phase (green cells with magenta nuclei). 24 hours after electroporation, mice were injected with EdU for a third time to label any cells that had been in G2 at the time of electroporation and had reentered the cell cycle (non-green cells with magenta nuclei). Cells that had exited the cell cycle after electroporation were identified as GFP+ and EdU- (green cells with non-labeled nuclei) (A). Retinas were harvested after P14, sectioned, and stained for GFP (B, C), EdU (B',C'), and DAPI (B",C"). The fate of GFP+ EdU- cells was assessed by location either in the outer nuclear layer (rod photoreceptors) vs. the inner nuclear layer (interneurons) (B, B', B", C, C', C"). Scale bar, 50 μm. Quantification of GFP+ EdU- rod photoreceptors (D). n=3 retinas per condition. p-value < 0.01.

Figure 3.2 continued

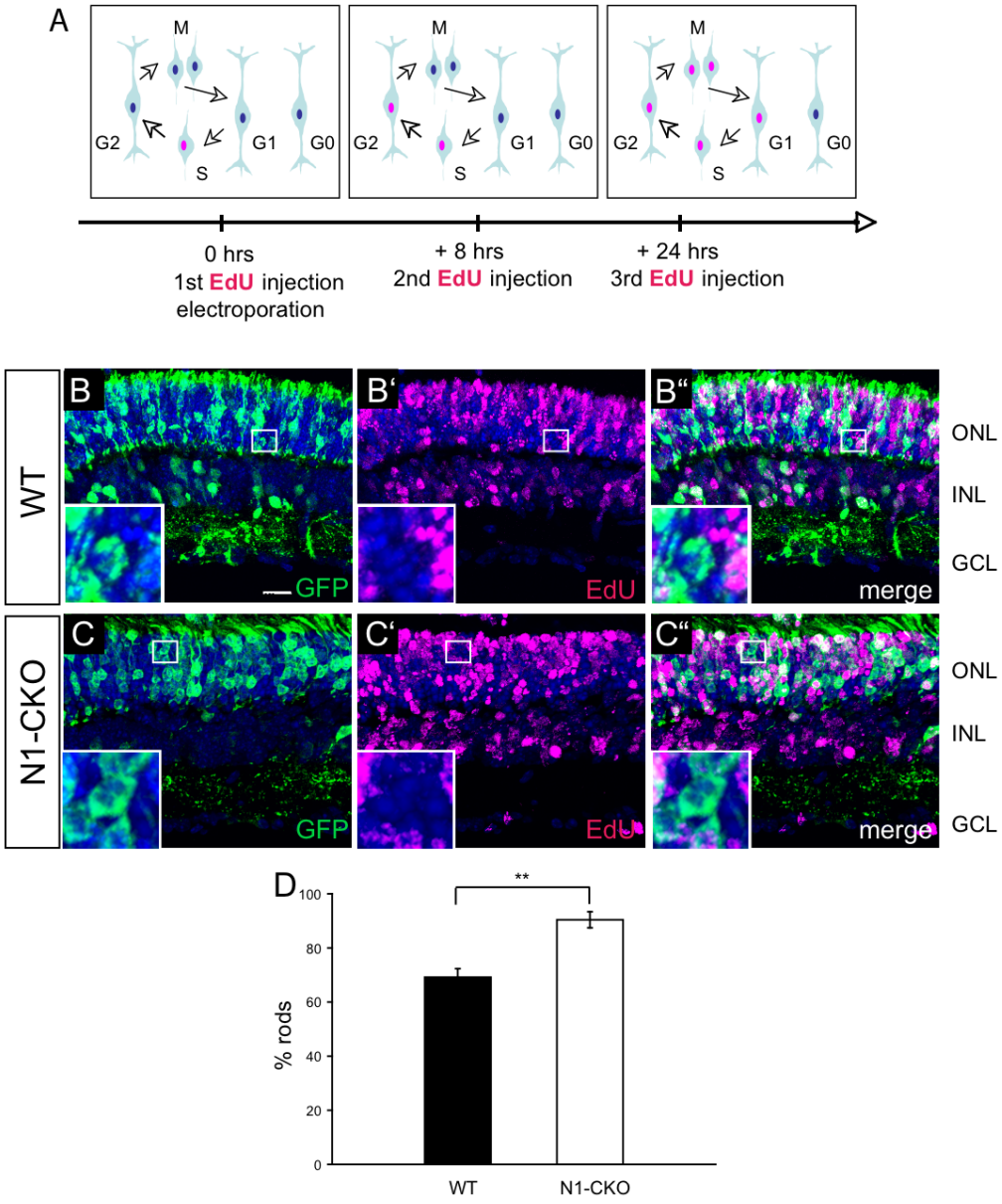

Figure 3.2

might still be at the scleral surface where the DNA was delivered in the subretinal injection. Retinas were harvested after P14 and the fate of GFP+ EdU- cells was assessed by location in the outer nuclear layer (presumed photoreceptors) vs. inner nuclear layer (presumed interneurons and Müller glia). 90+/-3.2% of GFP+ EdU- cells became photoreceptors in *Notch1*$^{fl/fl}$ retinas as compared to 69+/-3.0% in WT retinas, providing evidence that postmitotic precursors that lost *Notch1* became rod photoreceptors at the expense of other cell types (Figure 3.2, D). These results are in accord with the viral Cre experiments described above.

Id1 and *Id3* expression is downregulated in the absence of *Notch1*

Microarray analysis of single N1-CKO and WT cells described in Chapter 2 provided novel candidate genes that may mediate Notch signaling. We found that *Inhibitor of DNA binding* (*Id*) factors *1* and *3* were almost completely absent in N1-CKO cells, but robustly expressed in a number of WT control cells (Figure 3.3, A).

In order to independently validate that the expression of these genes changes after the removal of *Notch1*, we performed a qPCR assay on populations of N1-CKO and WT cells. Retinas of *Notch1*$^{fl/fl}$ P0 pups were electroporated *in vitro* with plasmids encoding CAG:Cre, along with a Cre-responsive GFP reporter, CALNL-GFP. For controls, the retinas of sibling *Notch1*$^{fl/fl}$ pups were electroporated with CAG:GFP. Electroporated retinas were cultured for three days, and dissociated to single cells. GFP+ cells (pooled from two retinas for each sample) were sorted by flow cytometry and collected. RNA was extracted from each sample and cDNA was generated. Samples were subjected to quantitative real time PCR in order to detect expression of *actin* (as a control), *Id1,* and

Figure 3.3. Analysis of Id1 and Id3 expression in NI-CKO and WT cells

The microarrays performed on single cells from WT and N1-CKO cells (described in Figure 2.1) were analyzed for the expression of *Id1* and *Id3*. Signal levels of these genes are shown in a histogram (A). See also Table 1 in Appendix. qPCR analysis of Id1 and Id3 expression in N1-CKO and WT cells (B). p-value < 0.05.

Figure 3.3 continued

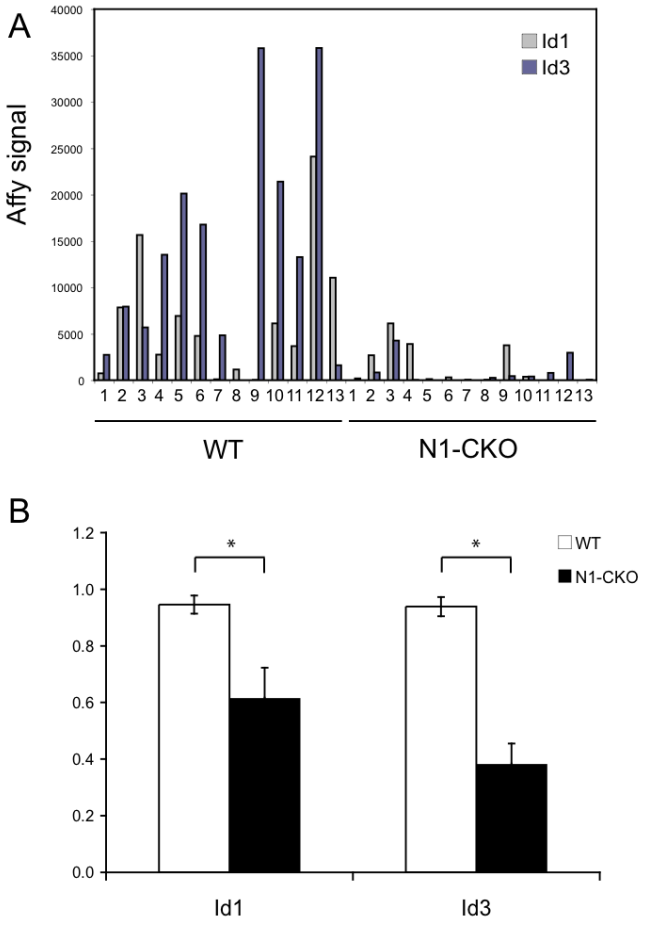

Figure 3.3.

Id3. In concordance with the changes observed by microarray analysis, *Id1* and *Id3* were downregulated in N1-CKO cells as compared to WT cells (Figure 3.3, B).

Id factors are of particular interest as they have been shown to prevent differentiation during neurogenesis in the central nervous system, similar to the outcomes of Notch activation (Lyden et al., 1999; Cai et al., 2000). Additionally, a previous study in *Xenopus* suggested that *Id3* may be a direct target of Notch signaling (Reynaud-Deonauth et al., 2002). For these reasons, we tested the function of *Id1* and *Id3* in the developing retina.

Functional analysis of Id1 and Id3 in the developing wild type retina

In order to better understand Id function, retinas of WT P0 pups were electroporated *in vivo* with plasmids encoding CAG:Id1, CAG:Id3, or both, along with CAG:GFP (Matsuda and Cepko, 2007). Retinas were harvested after P14, and the fate of the electroporated cells was assessed by morphology and molecular markers. Misexpression of CAG:Id1 and CAG:Id3 led to the overproduction of cells that exhibited features of both RPCs and Müller glial cells as compared to WT control retinas. First, the morphology of the induced cells resembled that of RPCs or Müller glial cells, in that their cell bodies were located in the INL, with long processes that extended both into the photoreceptor layer and the GCL (Figure 3.4, B). Furthermore, these cells were positive for a marker of both RPCs and Müller glial cells, p27, by immunofluorescence (Figure 3.4, B). Misexpression of CAG:Id1 or CAG:Id3 alone also resulted in induction of extra RPC/Müller-like cells, but not to the extent observed when CAG:Id1 and CAG:Id3 were expressed together (data not shown).

We wanted to quantify the amounts of RPC/Müller glial cells induced by CAG:Id1 and CAG:Id3. A FACS-based assay was employed in order to objectively count large populations of cells in a high-throughput manner. Wild type retinas were electroporated *in vitro* with combinations of CAG:GFP, CAG:Id1, CAG:Id3, and a cell type specific reporter at P0. Cell type specific reporters included regulatory sequences upstream of *Cralbp* (to mark Müller glial cells) and *Hes1* (to mark progenitor cells) driving dsRed and tdTomato expression, respectively (Matsuda and Cepko, 2007). Plasmids that did not express any genes were added to DNA mixtures such that the molar ratio of all plasmids was equal among electroporations. After electroporation, retinas were cultured *in vitro* as explants for 11-12 days and dissociated to single cells. Flow cytometry was used to analyze samples and count single (GFP+) and double positive cells (GFP+dsRed+ or GFP+tdTomato+). Double positive (GFP+dsRed+ or GFP+tdTomato+) cells were identified as electroporated cells that also expressed a particular cell type specific promoter construct, a proxy for the fate of that cell. In wild type retinas, 2.5+/-0.55% of GFP+ cells were also Cralbp:dsRed+ (Figure 3.4, C). Coexpression of CAG:Id1 or CAG:Id3 alone, along with CAG:GFP, and Cralbp:dsRed did not change the amount of double positive cells (data not shown). However, coexpression of both CAG:Id1 and CAG:Id3, along with CAG:GFP, and Cralbp:dsRed resulted in an increase of double positive cells, to 5.0+/-1.6% (Figure 3.4, C).

Figure 3.4. Functional analysis of *Id1* and *Id3* in the wild type postnatal retina

Ectopic expression of Id factors in the developing retina. Plasmids encoding CAG:GFP with or without CAG:Id1 and CAG:Id3 were electroporated *in vivo* into wild type P0 mouse retinas. The fates of electroporated cells were analyzed in the mature retina after P14 (A, B). Electroporation of CAG:GFP alone or CAG:GFP with CAG:Id1 and CAG:Id3 labeled photoreceptors, interneurons, and Müller glial cells. P27 staining labeled Müller glial cells (A, B). Scale bar, 50 μm. Combinations of plasmids encoding CAG:GFP, cell type specific promoters, and Id factors were electroporated *in vitro* into P0 wild type retinas. Retinas were cultured for 11-12 days and dissociated to single cells. Fluorescently activated cell sorting was utilized to count GFP+ and GFP+Red+ cells. Plasmids encoding Cralbp:dsRed marked Müller glial cells. Percentage of CAG:GFP+Cralbp:dsRed+ (WT) or CAG:GFP+Cralbp:dsRed+CAG:Id1+CAG:Id3 (Id1+Id3) cells out of total GFP+ cells per retina (C). n=5 retinas per condition. Plasmids encoding Hes1:tdTomato marked retinal progenitor cells. Percentage of CAG:GFP+Hes1:tdTomato+ (WT) or CAG:GFP+ Hes1:tdTomato+CAG:Id1+CAG:Id3 (Id1+Id3) cells out of total GFP+ cells (D). n=5 retinas per condition. p-value < 0.05. Knockdown of Id factors in the developing retina. Percentage of CAG:GFP+Hes1:tdTomato+GAPDH RNAi (WT), or CAG:GFP+Hes1:tdTomato+Id1 RNAi+Id3 RNAi (Id1+3 RNAi) out of total GFP+ cells (E). n=2 retinas per condition

Figure 3.4 continued

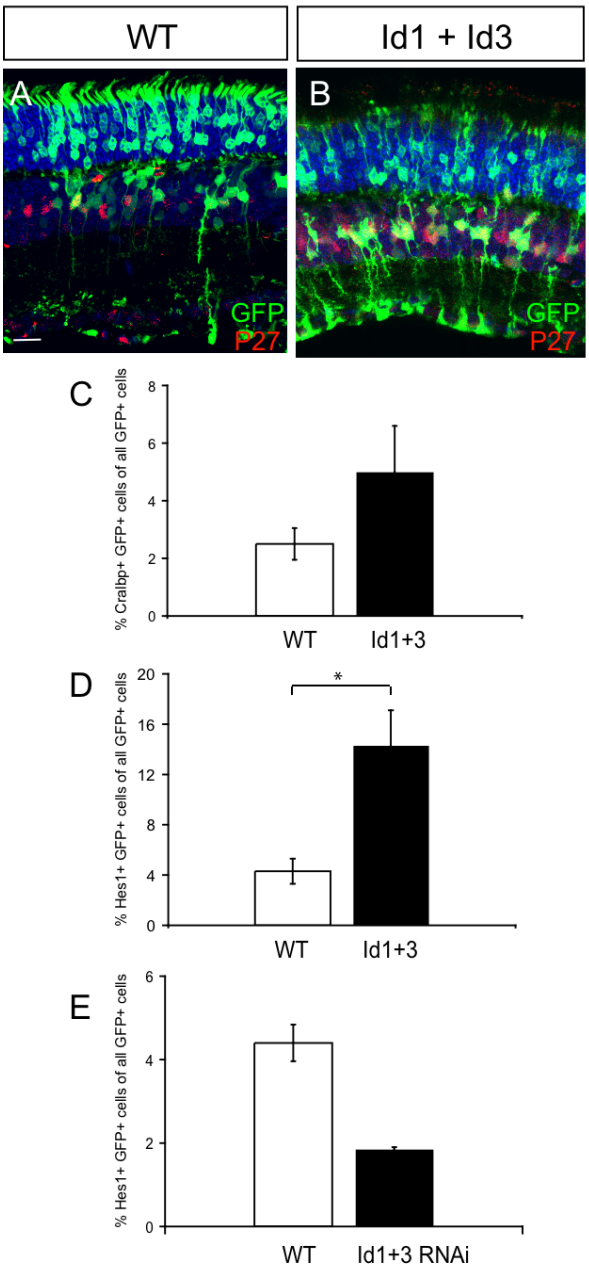

Figure 3.4.

Next, *Hes1* reporter expression was utilized as a proxy for progenitor status. In wild type retinas, 4.3+/-1.0% of GFP+ cells were also *Hes1*:tdTomato+ (Figure 3.4, D). Coexpression of CAG:Id1 or CAG:Id3 alone, along with CAG:GFP, and Hes1:tdTomato resulted in an increase of double positive cells (data not shown). Coexpression of both CAG:Id1 and CAG:Id3, along with CAG:GFP, and Hes1:tdTomato resulted in a robust increase of double positive cells, 14.3+/-2.8% (Figure 3.4, D).

We wanted to test the effect of *Id1* and *Id3* knockdown on postnatal retinal development. Two individual RNAi constructs targeting either *Id1* or *Id3*, respectively, were electroporated together with CAG:GFP and Hes1:tdTomato at P0. For controls, GAPDH RNAi, which does not have an effect on retinal development, was coelectroporated with CAG:GFP and Hes1:tdTomato. Under these conditions, 4.4+/-0.44% of cells were positive for GFP and tdTomato. In contrast, coexpression of *Id1* and *Id3* RNAi resulted in a decreased amount of double positive cells, 1.9+/-0.05% (Figure 3.4, E).

Rescue of *Notch1* loss of function phenotype by *Id1* and *Id3*

Because *Id1* and *Id3* were robustly downregulated in the absence of *Notch1*, we hypothesized that under wild type conditions expression of these genes is activated or maintained by Notch1 signaling. Moreover, ectopic expression of *Id1* and *Id3* in WT retinas resulted in an induction of RPC/Müller-like cells, which is also observed when NICD is transduced into the developing retina. These results led us to believe that *Id1* and *Id3* could be mediating Notch1 signaling, and we wanted to determine if these factors could rescue the production of non-rod cell fates in the absence of *Notch1*.

In order to test this idea, retinas of *Notch1*$^{fl/fl}$ animals were electroporated *in vivo* at P0 with combinations of CAG:Cre, CALNL-GFP, CAG:Id1 and CAG:Id3. Retinas were harvested after P14, sectioned, and stained for GFP and cell type specific markers. Because it was observed that Müller glial cells and bipolars were the predominate cell types lost in the absence of *Notch1* (Jadhav et al. 2006, and discussed above), the production of these cell types was used as a means to assess the extent of rescue by *Id1* and *Id3*. The fate of electroporated cells was assessed by morphology and immunofluorescence. Detection of Chx10 expression was used as marker of bipolar cells, whereas p27 was used as a marker of Müller glial cells, as described above. As a control, P0 CAG:GFP electroporation into wild type retinas resulted in GFP+ cells that were identified as rod photoreceptors, amacrine cells, bipolar cells, and Müller glial cells by morphology in the mature retina. Furthermore, p27 marked Müller glial cells (Figure 3.5, A) and Chx10 expression marked bipolar cells as expected (Figure 3.5, D). When CAG:Cre and CALNL-GFP were coexpressed in *Notch1*$^{fl/fl}$ retinas, none of the resultant GFP+ cells resembled Müller glial cells or bipolar cells. Additionally, none of these marked cells expressed p27 (Figure 3.5, B) or Chx10 (Figure 3.5, E). Next, retinas were electroporated with CAG:Cre, CALNL-GFP, CAG:Id1, and CAG:Id3 (Figure 3.5, C, F). Under these conditions, both bipolar and Müller glial cells were observed, although fewer than in wild type retinas. These cells could be positively identified by morphology and expression of p27 or Chx10, respectively (Figure 3.5, C, F). Ectopic expression of CAG:Id1 or CAG:Id3 individually in the absence of *Notch1* also resulted in partial rescue of the phenotype, but not to the same extent as *Id1* and *Id3* together (data not shown).

Figure 3.5. *Id1* and *Id3* expression in *Notch1* deficient cells

Ectopic expression of Id factors in *Notch1* deficient cells during retinal development. Plasmids encoding CAG:GFP or CAG:Cre with CALNL-GFP with or without CAG:Id1 and CAG:Id3 were electroporated *in vivo* into *Notch1*$^{fl/fl}$ P0 mouse retinas. The fates of electroporated cells were analyzed in the mature retina after P14. P27 immunofluorescence marked Müller glial cells, and Chx10 marked bipolars cells. Electroporation of CAG:GFP alone labeled GFP+ photoreceptors, interneurons, and Müller glial cells, some of which were positive for p27 or Chx10 (A, D). Electroporation of CAG:Cre and CALNL-GFP into *Notch1*$^{fl/fl}$ retinas labeled GFP+ photoreceptors and some amacrine cells, none of which were positive for p27 or Chx10 (B, E). Electroporation of CAG:Cre, CALNL-GFP, CAG:Id1, and CAG:Id3 labeled photoreceptors, interneurons, and Müller glial cells, some of which were positive for p27 and Chx10 (C, F). Arrowheads demarcate double positive cells. Scale bar, 50 μm. Combinations of plasmids encoding CAG:GFP or CAG:Cre and CALNL-GFP, cell type specific promoters, and Id factors were electroporated *in vitro* into P0 *Notch1*$^{fl/fl}$ retinas. Retinas were cultured for 11-12 days and dissociated to single cells. Fluorescently activated cell sorting was utilized to count GFP+ and GFP+Red+ cells. Plasmids encoding Rhodopsin:dsRed marked rod photoreceptors, Cralbp:dsRed marked Müller glial cells, Chx10:tdTomato marked bipolar cells, and Ndrg4:dsRed marked amacrine cells. Percentage of CAG:GFP+red+ (WT), or CAG:Cre+CALNL-GFP+red+ (N1-CKO), or CAG:Cre+CALNL-GFP+red+CAG:Id1+CAG:Id3 (N1-CKO+Id1+Id3) cells out of total GFP+ cells (G). n=5 retinas per condition. p-value < 0.05.

Figure 3.5 continued

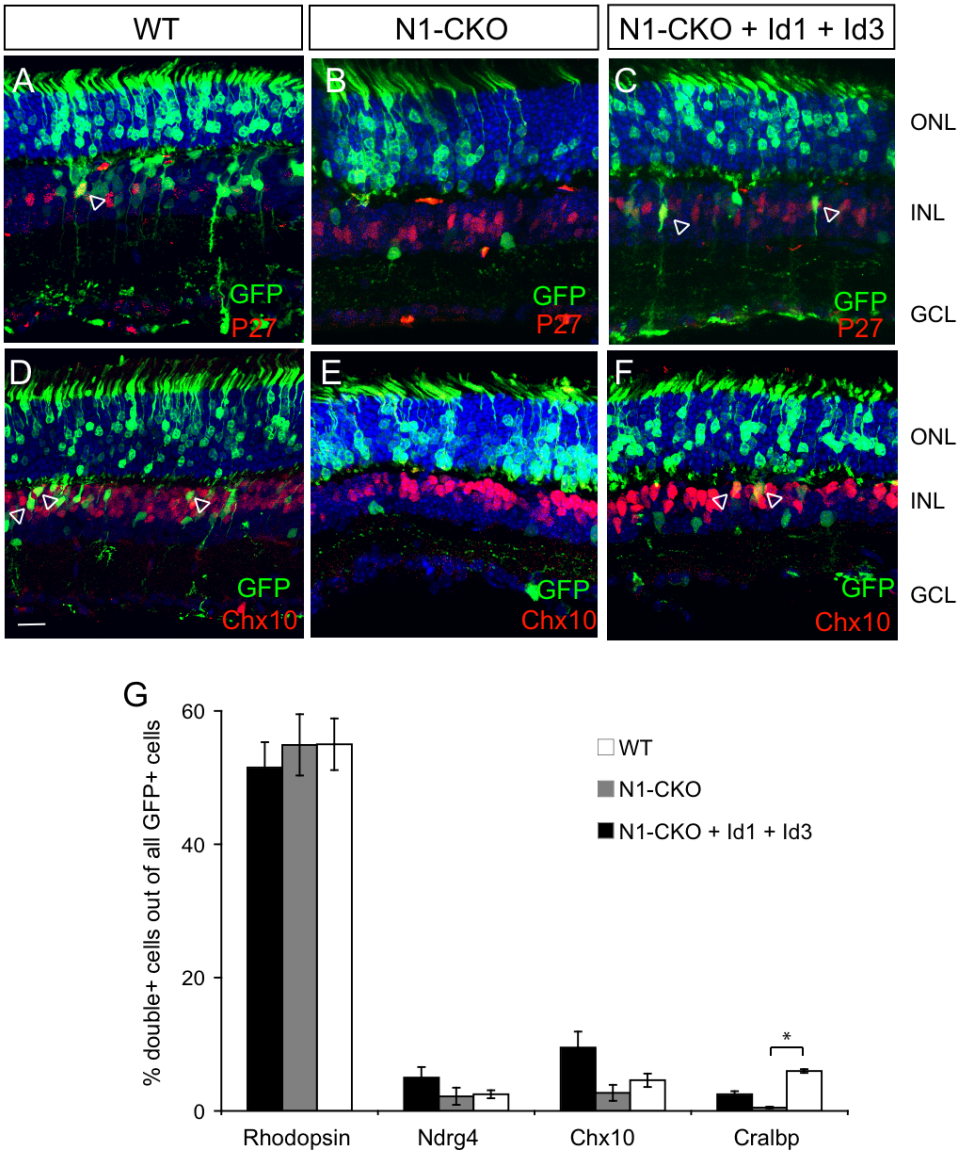

Figure 3.5.

Next, the FACS assay described above was used to quantify the extent of rescue by CAG:Id1 and CAG:Id3 in *Notch1* deficient cells. In this experiment, the expression of a particular cell type specific promoter was utilized as a proxy for the fate decision of the electroporated cell. Cell type specific reporters included regulatory sequences upstream of *Rhodopsin* (to mark rods), *Ndrg4* (to mark amacrine cells), *Chx10* (to mark bipolar cells) and *Cralbp* (to mark Müller glial cells) driving either dsRed or tdTomato expression (Matsuda and Cepko, 2007; Kim et al., 2008a). For controls, P0 wild type or *Notch1*$^{fl/fl}$ retinas were electroporated *in vitro* with combinations of CAG:GFP and a cell type specific reporter. For *Notch1* knockout conditions, plasmids encoding CAG:Cre, CALNL-GFP, and different cell type specific reporters were electroporated *in vitro* into P0 *Notch1*$^{fl/fl}$ retinas. In rescue experiments, *Notch1*$^{fl/fl}$ retinas were electroporated *in vitro* with combinations of CAG:Cre, CALNL-GFP, CAG:Id1, CAG:Id3, and a cell type specific reporter at P0. Each cell type specific promoter was analyzed separately and at least three retinas were assessed per condition. Conditions in which CAG:Id1 or CAG:Id3 were not added to the electroporation mixture, plasmids that did not express any genes were added to DNA mixtures such that the molar ratio of all plasmids was equal among electroporations. Retinas were cultured *in vitro* as explants for 11-12 days and dissociated to single cells. Flow cytometry was used to analyze samples and count single (GFP+) and double positive cells (GFP+dsRed+ or GFP+tdTomato+). In wild type conditions, 51.5+/-3.8% of GFP+ cells were double positive for Rhodopsin:dsRed, 5.0+/-1.6% of GFP+ cells were double positive for Ndrg4:dsRed, 9.5+/-2.4%, were double positive for Chx10:tdTomato, and 2.5+/-0.47% were double positive for Cralbp:dsRed out of the total GFP+ population (Figure 3.5, G). Expression of CAG:Cre, CALNL-GFP,

and the different cell type specific promoters in *Notch1*$^{fl/fl}$ retinas resulted in 54.9+/-4.6% GFP+Rhodopsin:dsRed+ cells, 2.2+/-1.3% GFP+Ndrg4:dsRed+ cells, 2.7+/-1.2% GFP+Chx10:dsRed+ cells, and 0.82+/-0.13% of GFP+Cralbp:dsRed+ cells out of total GFP+ cells in that condition (Figure 3.5, G). Coexpression of CAG:Id1 and CAG:Id3, along with CAG:Cre, CALNL-GFP, and the different cell type specific promoters resulted in 55+/-3.9% GFP+ cells that were Rhodopsin:dsRed+, 2.5+/-0.6% GFP+ cells that were Ndrg4:dsRed+, 4.6+/-1.0% of GFP+ cells that were Chx10+, and an increased percentage of GFP+Cralbp:dsRed+ to 6.0+/-0.28 out of total GFP+ cells for each condition (Figure 3.5, G). The results of these experiments supported that *Id1* and *Id3* misexpression in the absence of *Notch1* could partially rescue the production of bipolar cells and result in the overproduction of Müller glial cells, at least at the level of turning on a cell type specific reporter.

Finally, we undertook a viral approach to address the ability of Id factors to rescue *Notch1* loss of function in newly postmitotic cells. A viral vector that expresses three genes, *Id1*, *Cre*, and *AP* (Id1-2A-Cre-IRES-AP) in the LIA backbone was constructed (Figure 3.6, A). This virus was injected *in vivo* into the subretinal space of P3 *Notch1*$^{fl/fl}$ pups and retinas were harvested after retinal maturation (P21 or later). LIA-Id1-2A-Cre-IRES-AP infected cells were detected by histochemical staining for AP activity. As described previously, we focused our analysis on single cell clones, because these cells represent expression of viral transgenes after cell cycle exit (Figure 3.1, A). Single cell clones derived from these infections comprised 89.6+/-0.54% rod photoreceptors, 7.7+/-0.50% bipolar cells, and 2.77+/-0.11% Müller glial cells (Figure 3.6, B).

Figure 3.6. Clonal expression of *Id1* in *Notch1* deficient newly postmitotic cells

Almost all clones derived from a P3 infection consist of one or two cells, as progenitor cells only divide once or twice at these late developmental stages. As depicted in Figure 3.1, one cell clones are derived from daughter cells that are postmitotic. The LIA retrovirus was engineered to express Id1, Cre, and AP (A). *Notch1*$^{fl/fl}$ retinas were infected with LIA-Id1-2A-Cre-IRES-AP at P3 and the fate of single cell clones was assessed after P21 by histochemical staining. Quantification of cell types found in BAG (WT), LIA-Cre (N1-CKO) (described in Figure 3.1), and LIA-Id1-2A-Cre (N1-CKO+Id1) single cell clones (B). n=3 retinas per condition. p-value < 0.01.

Figure 3.6 continued

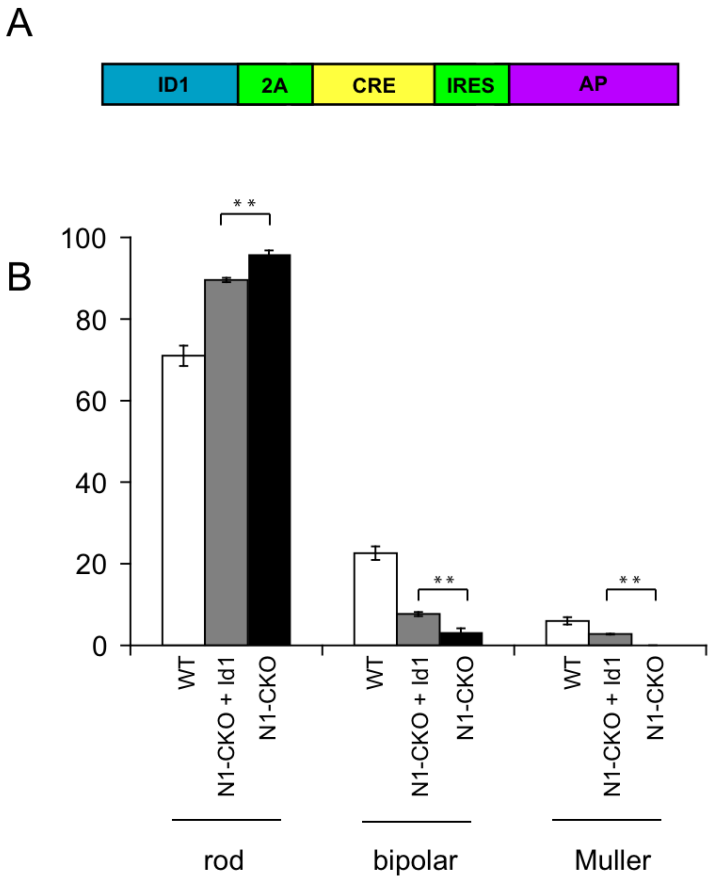

Figure 3.6

In comparison, LIA-Cre infection into *Notch1*$^{fl/fl}$ resulted in 96.6+/-0.8% rods, 3.4+/-0.8% bipolar, and 0+/-0% Müller glial cells. Wild type control clones consisted of 67.9+/-1.4% rods, 20.7+/-1.3% bipolars, and 11.4+/-0.1% Müller glial cells (Figure 3.1, E and 3.6, B). These results indicated that *Id1* alone was sufficient to partially rescue the *Notch1* loss of function phenotype, even in newly postmitotic cells.

Discussion

Notch signaling plays diverse roles during embryogenesis. In this study, *Notch1* was specifically removed from newly postmitotic cells in order to determine the role of this signaling pathway in retinal cells after cell cycle exit. Almost all newly postmitotic cells that lost *Notch1* became photoreceptors at the expense of other cell types produced concurrently. These results provided evidence that newly postmitotic cells require *Notch1* to achieve a non-rod fate, such as the bipolar or Müller glial fate. An interpretation of these results is that *Notch1* signaling maintains cells in an undetermined state, allowing them time to choose a non-rod fate. Alternatively, or additionally, it may retain rod-inducing genes at sub-threshold levels in cells that are already biased to become non-rods. There are some data in support of the latter scenario. First, lineage analysis has revealed many stereotyped two cell clones that consist of a rod and a bipolar cell, a rod and an amacrine cell, or a rod and Müller glial cell (Turner and Cepko, 1987; Fields-Berry et al., 1992). These data are consistent with the existence of predetermined RPCs that make a combination of a rod and a non-rod in a terminal division. If this is the case, there must be asymmetric inheritance of determinants by the two types of daughter cells.

Notch1 must then keep rod-inducing factors off in cells fated to become bipolar or Müller glial cells, at least for a period of time until the fate is set.

Another possibility is that newly postmitotic cells do not inherit determinants that bias them towards a specific non-rod cell fate. The default state of every newly postmitotic cell might be to become a photoreceptor cell, perhaps as a result of the way the eye evolved. Early photoreceptive organs likely had only photoreceptor cells. In order to generate cells that were available to take on non-photoreceptor fates, inhibition of the photoreceptor fate would have been necessary. As *Notch* is a highly conserved regulator, it is possible that it was recruited in these early eyes for this role. Additionally, inducers of other fates would have been required. A network of transcription factors could have evolved to allow the development of non-photoreceptor fates. This network might be inherited by newly postmitotic cells, along with their propensity to take on a photoreceptor fate. The level of *Notch1* signaling in a newly postmitotic cell would then allow a cell to escape a photoreceptor fate and choose another fate promoted by its inherited network.

In order to understand the network that regulates cell fate determination in the developing retina, microarray analysis of single retinal cells was performed from WT or N1-CKO conditions (Chapter 2). From these studies, we identified *Id1* and *Id3* as genes that were downregulated in the absence of *Notch1*. Id factors play an important role in maintaining the progenitor state, as *Id1* and *3* double knockout mice exhibit precocious neurogenesis and premature depletion of the progenitor pool (Lyden et al., 1999). The ability of the Id factors to maintain cells in an undifferentiated state is attributed to their function of binding pro-neurogenic bHLH transcription factors. Id factors contain a HLH

binding domain through which they interact with other bHLH transcription factors. However, these proteins lack the basic DNA binding domain and do not directly bind DNA (Benezra et al., 1990). Thus, they are thought to function in a dominant negative manner, rendering bHLH transcription factors inactive and thereby prevent differentiation.

We found that ectopic expression of these factors in the postnatal wild type retina resulted in the overproduction of cells that resemble RPC/Müller glial cells. This observation is in keeping with Id factors being potential downstream mediators of Notch signaling. Expression of the activated form of the Notch receptor, the NICD, in the postnatal retina resulted in cells that also had characteristics of RPCs and Müller glial cells (Furukawa et al., 2000). However, unlike in the case of NICD overexpression, only a portion of cells ectopically expressing *Id1* and *Id3* became RPC/Müller glial cells. This is likely due to NICD being a more potent regulator of gene expression.

Next, we found that Id factors could rescue the Notch loss of function phenotype. Depending on the assay, Id factors either completely or partially rescued Müller glial production, and partially rescued bipolar cell production in the absence of *Notch1*. Overproduction of Müllers in the FACS-based assay was likely due to the fact that the readout for this assay was only contingent on the activation of the Cralbp:dsRed reporter construct. It is more likely that Id factors only partially rescue the production of mature Müller glial cells, as observed in the *in vivo* electroporation and infection assays. Taken together, these results suggested that Id genes are not just general progenitor genes, but are directly involved in cell fate specification. In addition, they are sufficient for induction of the Müller glial fate, even in the absence of Notch regulated genes, which

are thought to be necessary for the production of this cell type. Using a viral approach, we showed that expression of Id1 was able to partially rescue the production of bipolar cells and Müller glial cells in newly postmitotic cells.

It is known that Notch signaling activates expression of Hes family members, which can transcriptionally repress pro-neurogenic factors. Potentially, in a postmitotic cell, Notch signal transduction leads to the expression of Hes and Id factors, which then prevent the activity of rod-inducing factors, at the level of RNA expression and protein function. High levels of expression of Notch downstream target genes, such as Hes and Id factors, have been shown to direct Müller glial fate. However, it is unclear how Notch signaling can specifically inhibit rod-inducing factors, while permitting activity of pro-neurogenic factors that lead to bipolar fate. One possibility is that, in this particular context, Id factors only inactivate bHLH transcription factors, or even non-bHLH transcription factors, that are specific to rod induction.

Our findings demonstrate a novel role for *Notch1* in specifying cell fate in newly postmitotic cells. This function can be separated from RPC state maintenance, which is the more canonical role of this signaling pathway. Specifically, *Notch1* is essential for the diversification of neuronal cell types in the postnatal retina, so that not all of the cells become rod photoreceptors. The maintenance of rod-inducing genes at low levels by Notch signaling allows newly postmitotic cells to stay in a plastic state or execute the fate specification program endowed by their progenitor cell. These results provide a more in depth view of a genetic network that regulates cell fate determination during retinal development.

Methods

Animals

Notch1$^{fl/fl}$ were maintained as homozygotes (Radtke et al., 1999). CD-1 mice were obtained from Charles River Laboratories. All experiments were approved by the Institutional Animal Care and Use Committee at Harvard University.

Misexpression constructs

The plasmids CAG:Id1 and CAG:Id3 were constructed by PCR amplification from a full-length mouse cDNA clone using primer sets and cloning into the CAG vector (Matsuda and Cepko, 2004), using EcoRI and NotI restriction sites. Each construct was verified by sequencing.

Electroporation and Infection

In vivo injections of DNA constructs and viruses were performed as previously described with the exception that an oocyte microinjector (Drummond) and pulled glass pipettes (Dumont/Drummond) were used to deliver 0.2 μl of 1 μg/μl DNA solution or 10^7 viral titer into the subretinal space of the postnatal mouse eye. Viruses used include LIA-Cre (Bao and Cepko, 1997; Jadhav et al., 2006b), LIA-Id1-2A-Cre, and BAG (Price et al., 1987). DNA constructs used include CAG:GFP, CAG:Cre, CALNL-GFP (Matsuda and Cepko, 2004). CAG:Id1, and CAG:Id3. Intraperitoneal injections into newborn pups were performed to deliver EdU.

In vitro electroporation were performed as previously described (Matsuda and Cepko, 2004). DNA constructs used include CAG:GFP, CAG:Cre, CALNL-GFP (Matsuda and

Cepko, 2004), CAG:Id1, CAG:Id3, Rhodopsin:dsRed, Cralbp:dsRed, Hes1:tdTomato, Ndrg4:dsRed (Matsuda and Cepko, 2007), and Chx10:tdTomato (Kim et al., 2008a).

Histology

Retinas were fixed either as wholemounts for 30 minutes at room temperature or as eyeballs for 2 hours in 4% PFA in PBS, pH 7.4, at room temperature. Retinas were dissected away from the rest of the eyeball in PBS. After dissection, retinas were stained for X-gal, AP, GFP, and/or EdU. Retinas were equilibrated in sucrose/PBS solutions of increasing sucrose concentrations (5, 20, 30%). Retinas were equilibrated for >1 hour in a 1:1 solution of OCT (Tissue-Tek), and 30% sucrose/PBS, and frozen on dry ice. 20 μm cryosections were cut using a disposable blade on a Leica CM3050S cryostat.

Immunofluorescence

Retinal cryosections were blocked for 1 hour in 0.1% Triton, 0.02% SDS, 1% BSA in 1X PBS. Sections were then incubated in a humidified chamber at 4°C overnight with primary antibodies diluted in blocking solution. Primary antibodies used in this study included the following: chicken anti-GFP (1:2000; Abcam), rabbit anti-Chx10 (1:500; C. L. Cepko Laboratory), mouse anti-$p27^{Kip1}$ (1:50; BD Biosciences Transduction Laboratories), Slides were then washed three times in 1X PBS and incubated for 2 hours with fluorescently coupled secondary antibodies (Jackson ImmunoResearch) and DAPI (Sigma-Aldrich). EdU detection was performed according to manufacturer's instruction (Invitrogen). Slides were washed three times with 1X PBS and mounted using Fluoromount-G (Southern Biotechnology Associates).

Microscopy and image analysis

Images were acquired using a Leica TCS SP5 confocal microscope. Images were analyzed, quantified, and uniformly adjusted for brightness and contrast using Imaris 5.7 software (Bitplane). Colocalization of molecular markers in individual cells was assessed by analysis of three-dimensional *Z*-series with Imaris 5.7 software.

FACS assay

Electroporated retinas were dissociated to single cells via papain treatment (Trimarchi et al., 2007). FACS was performed on a BD Aria II sorter, gated for GFP and dsRed/tdTomato detection.

REFERENCES

Alexiades, M.R., and Cepko, C. (1996). Quantitative analysis of proliferation and cell cycle length during development of the rat retina. Dev. Dyn *205*, 293–307.

Bao, Z.Z., and Cepko, C.L. (1997). The expression and function of Notch pathway genes in the developing rat eye. J. Neurosci *17*, 1425–1434.

Belliveau, M.J., and Cepko, C.L. (1999). Extrinsic and intrinsic factors control the genesis of amacrine and cone cells in the rat retina. Development *126*, 555–566.

Benezra, R., Davis, R.L., Lockshon, D., Turner, D.L., and Weintraub, H. (1990). The protein Id: a negative regulator of helix-loop-helix DNA binding proteins. Cell *61*, 49–59.

Cai, L., Morrow, E.M., and Cepko, C.L. (2000). Misexpression of basic helix-loop-helix genes in the murine cerebral cortex affects cell fate choices and neuronal survival. Development *127*, 3021–3030.

Ezzeddine, Z.D., Yang, X., DeChiara, T., Yancopoulos, G., and Cepko, C.L. (1997). Postmitotic cells fated to become rod photoreceptors can be respecified by CNTF treatment of the retina. Development *124*, 1055–1067.

Fekete, D.M., Perez-Miguelsanz, J., Ryder, E.F., and Cepko, C.L. (1994). Clonal analysis in the chicken retina reveals tangential dispersion of clonally related cells. Dev. Biol *166*, 666–682.

Fields-Berry, S.C., Halliday, A.L., and Cepko, C.L. (1992). A recombinant retrovirus encoding alkaline phosphatase confirms clonal boundary assignment in lineage analysis of murine retina. Proc. Natl. Acad. Sci. U.S.A *89*, 693–697.

Furukawa, T., Mukherjee, S., Bao, Z.Z., Morrow, E.M., and Cepko, C.L. (2000). rax, Hes1, and notch1 promote the formation of Müller glia by postnatal retinal progenitor cells. Neuron *26*, 383–394.

Godinho, L., Williams, P.R., Claassen, Y., Provost, E., Leach, S.D., Kamermans, M., and Wong, R.O.L. (2007). Nonapical symmetric divisions underlie horizontal cell layer formation in the developing retina in vivo. Neuron *56*, 597–603.

Holt, C.E., Bertsch, T.W., Ellis, H.M., and Harris, W.A. (1988). Cellular determination in the Xenopus retina is independent of lineage and birth date. Neuron *1*, 15–26.

Jadhav, A.P., Mason, H.A., and Cepko, C.L. (2006). Notch 1 inhibits photoreceptor production in the developing mammalian retina. Development *133*, 913–923.

Kim, D.S., Matsuda, T., and Cepko, C.L. (2008). A core paired-type and POU homeodomain-containing transcription factor program drives retinal bipolar cell gene expression. J. Neurosci. *28*, 7748–7764.

Livesey, F.J., and Cepko, C.L. (2001). Vertebrate neural cell-fate determination: lessons from the retina. Nat. Rev. Neurosci *2*, 109–118.

Lyden, D., Young, A.Z., Zagzag, D., Yan, W., Gerald, W., O'Reilly, R., Bader, B.L., Hynes, R.O., Zhuang, Y., Manova, K., et al. (1999). Id1 and Id3 are required for neurogenesis, angiogenesis and vascularization of tumour xenografts. Nature *401*, 670–677.

Matsuda, T., and Cepko, C.L. (2004). Electroporation and RNA interference in the rodent retina in vivo and in vitro. Proc. Natl. Acad. Sci. U.S.A *101*, 16–22.

Matsuda, T., and Cepko, C.L. (2007). Controlled expression of transgenes introduced by in vivo electroporation. Proc. Natl. Acad. Sci. U.S.A *104*, 1027–1032.

McConnell, S.K., and Kaznowski, C.E. (1991). Cell cycle dependence of laminar determination in developing neocortex. Science *254*, 282–285.

Price, J., Turner, D., and Cepko, C. (1987). Lineage analysis in the vertebrate nervous system by retrovirus-mediated gene transfer. Proc. Natl. Acad. Sci. U.S.A *84*, 156–160.

Radtke, F., Wilson, A., Stark, G., Bauer, M., van Meerwijk, J., MacDonald, H.R., and Aguet, M. (1999). Deficient T cell fate specification in mice with an induced inactivation of Notch1. Immunity *10*, 547–558.

Rapaport, D.H., Wong, L.L., Wood, E.D., Yasumura, D., and LaVail, M.M. (2004). Timing and topography of cell genesis in the rat retina. J. Comp. Neurol *474*, 304–324.

Reynaud-Deonauth, S., Zhang, H., Afouda, A., Taillefert, S., Beatus, P., Kloc, M., Etkin, L.D., Fischer-Lougheed, J., and Spohr, G. (2002). Notch signaling is involved in the regulation of Id3 gene transcription during Xenopus embryogenesis. Differentiation *69*, 198–208.

Riesenberg, A.N., Liu, Z., Kopan, R., and Brown, N.L. (2009). Rbpj cell autonomous regulation of retinal ganglion cell and cone photoreceptor fates in the mouse retina. J. Neurosci *29*, 12865–12877.

Roe, T., Chow, S.A., and Brown, P.O. (1997). 3'-end processing and kinetics of 5'-end joining during retroviral integration in vivo. J. Virol *71*, 1334–1340.

Rompani, S.B., and Cepko, C.L. (2008). Retinal progenitor cells can produce restricted subsets of horizontal cells. Proc. Natl. Acad. Sci. U.S.A *105*, 192–197.

Salic, A., and Mitchison, T.J. (2008). A chemical method for fast and sensitive detection of DNA synthesis in vivo. Proc. Natl. Acad. Sci. U.S.A *105*, 2415–2420.

Tomita, K., Ishibashi, M., Nakahara, K., Ang, S.L., Nakanishi, S., Guillemot, F., and Kageyama, R. (1996). Mammalian hairy and Enhancer of split homolog 1 regulates

differentiation of retinal neurons and is essential for eye morphogenesis. Neuron *16*, 723–734.

Trimarchi, J.M., Stadler, M.B., Roska, B., Billings, N., Sun, B., Bartch, B., and Cepko, C.L. (2007). Molecular heterogeneity of developing retinal ganglion and amacrine cells revealed through single cell gene expression profiling. J. Comp. Neurol *502*, 1047–1065.

Turner, D.L., and Cepko, C.L. (1987). A common progenitor for neurons and glia persists in rat retina late in development. Nature *328*, 131–136.

Turner, D.L., Snyder, E.Y., and Cepko, C.L. (1990). Lineage-independent determination of cell type in the embryonic mouse retina. Neuron *4*, 833–845.

Wetts, R., and Fraser, S.E. (1988). Multipotent precursors can give rise to all major cell types of the frog retina. Science *239*, 1142–1145.

Wong, L.L., and Rapaport, D.H. (2009). Defining retinal progenitor cell competence in Xenopus laevis by clonal analysis. Development *136*, 1707–1715.

Yaron, O., Farhy, C., Marquardt, T., Applebury, M., and Ashery-Padan, R. (2006). Notch1 functions to suppress cone-photoreceptor fate specification in the developing mouse retina. Development *133*, 1367–1378.

Young, R.W. (1985a). Cell differentiation in the retina of the mouse. Anat. Rec *212*, 199–205.

Young, R.W. (1985b). Cell proliferation during postnatal development of the retina in the mouse. Brain Res *353*, 229–239.

Zheng, M.-H., Shi, M., Pei, Z., Gao, F., Han, H., and Ding, Y.-Q. (2009). The transcription factor RBP-J is essential for retinal cell differentiation and lamination. Mol Brain *2*, 38.

Chapter 4

Notch1 is required in embryonic newly postmitotic cells to inhibit the photoreceptor fate

Karolina Mizeracka and Constance L. Cepko

Summary

Notch signaling regulates proliferation and cell fate specification during retinal development. Genetic removal of *Notch1* from newly postmitotic cells during postnatal stages resulted in the overproduction of rod photoreceptors at the expense of bipolar and Müller glial cells. In order to test whether *Notch1* functions similarly during embryonic development, we tested whether the Math5:Cre driver line is active specifically in postmitotic cells. Previous experiments have determined that Cre expressed under the control of the Math5 promoter marks only a subset of embryonically produced retinal cell types. We found that Math5:Cre+ cells were not in S-phase when embryos were harvested a short while after an EdU pulse, suggesting that these cells were postmitotic. *Math5:Cre* mice were crossed to *Notch1*$^{fl/fl}$ mice and the resultant progeny were analyzed. Loss of *Notch1* in the Math5+ lineage resulted in the overproduction of photoreceptors at the expense of horizontal, amacrine, and ganglion cells. These results are in keeping with a role for *Notch1* in preventing newly postmitotic cells from taking on the photoreceptor fate.

Introduction

Our understanding of some of the major features of RPCs is derived from retroviral lineage tracing. Infection of single RPCs at early time points in the developing retina results in the production of large clones that can comprise all the cell types found in the adult retina (Turner et al., 1990). This observation, along with other experiments, led to the insight that single RPCs are multipotent and change competence over time to generate many different cell types. Even postnatal RPCs which almost exclusively divide symmetrically to give rise to two neurons, can give rise to two very different neurons, or even a neuron and a glial cell (Turner and Cepko, 1987). The retroviruses in these studies are thought to infect RPCs at random, and thus the emerging perspective has been based on the behavior of the most common RPC type. Recent studies have identified more restricted RPCs that produce only subsets of retinal cell types (Godinho et al., 2007; Rompani and Cepko, 2008, Hafler et al., in press). The development of knock-in and transgenic mouse lines, in which promoter regions of developmentally regulated genes are used to drive Cre, now provides genetic access to populations that were previously underappreciated by lineage tracing of randomly marked RPCs. One such useful knock-in is *Math5:Cre,* a mouse line in which Cre has replaced the coding sequence of *Math5*, a single exon gene.

Math5, a basic helix-loop-helix (bHLH) transcription factor, is an ortholog of the *Drosophila* gene, *atonal*. Onset of *Math5* expression occurs at E11 and coincides with ganglion cell genesis. It is expressed robustly until P0 after which it is faintly detected in a few ONL cells (Yang et al., 2003). In addition, HA tagged *Math5* is detected in cycling RPCs, as well as, newly postmitotic cells (Feng et al., 2010). Loss and gain-of-function

experiments have determined that this transcription factor plays an important role in the production of ganglion cells, the first cell type produced during retinal neurogenesis. Studies of *Math5* mutant retinas have determined that ganglion cells are not produced, with a concurrent increase in cones and horizontal cells (Brown et al., 2001; Wang et al., 2001; Feng et al., 2010). In addition, ectopic expression of *Math5* resulted in the overproduction of ganglion cells (Yao et al., 2007). However, despite its integral role in ganglion cell specification, fate mapping experiments performed by crossing the *Math5:Cre* line to a Cre sensitive reporter resulted in the labeling of cones, rods, horizontal cells, amacrine cells, and ganglion cells (Yang et al., 2003; Feng et al., 2010). These observations suggest that Math5+ cells are not just ganglion cells, but a subset of RPCs and postmitotic precursors that produce biased progeny, namely only the early-born cell types.

In the previous Chapter, I described a role for Notch signaling in newly postmitotic cells. Removal of *Notch1* in newly postmitotic cells led to the overproduction of rod photoreceptors at the expense of other cell types produced postnatally. We wanted to test whether *Math5:Cre* could be used as a driver to genetically remove *Notch1* in embryonic postmitotic cells and determine if *Notch1* regulates cell fate in Math5+ descendants.

Results

In order to determine whether Math5:Cre+ cells were mitotic, postmitotic, or transitioning cells, *Math5:Cre* mice were crossed to the conditional GFP reporter *Epe* line, in which cells constitutively express GFP after Cre-mediated recombination. In

order to determine if GFP+ cells were cycling RPCs or newly postmitotic cells, EdU, a thymidine analog that is incorporated during S-phase, was injected intraperitoneally at E13.5 into pregnant moms (Salic and Mitchison, 2008). Following the EdU pulse, embryos were harvested either 3 or 15 hours later. Retinas were sectioned and stained for EdU and GFP detection.

Harvest of retinas 3 hours after the EdU pulse resulted in almost no overlap between GFP+ and EdU+ populations (Figure 4.1, A). This suggested that cells with a history of *Math5:Cre* expression were not currently in S-phase, and further, would never be in S-phase. This conclusion could be drawn, because at the time of harvest, GFP+ cells represented a mixed population of cells, some of which had just recently turned on Cre expression, and some that had turned on Cre well before the EdU injection. Moreover, retinas harvested after 15 hours after the EdU pulse, did contain a population of GFP+EdU+ cells (Figure 4.1, B). These cells were likely ones that had incorporated EdU during their last division, exited the cell cycle, and turned on GFP. Based on these experiments, the onset of *Math5:Cre* expression likely occurs in mitotic RPCs, but the lag time of Cre activity and GFP expression results in the marking of postmitotic progeny cells.

In order to manipulate Notch signaling in newly postmitotic cells, *Math5:Cre* mice were crossed to *Notch1*$^{fl/fl}$ mice, along with a reporter line, *PFwe,* which constitutively expresses nuclear *lacZ* after Cre-mediated recombination (Radtke et al., 1999; Farago et al., 2006). *Math5:Cre; Notch1*$^{fl/fl}$; *PFwe* and *Math5Cre; PFwe* littermate control retinas were stained for nuclear β-galactosidase activity at adult stages. The fate

Figure 4.1. EdU labeling of E13.5 *Math5:Cre; Epe* retinas

Math5:Cre mice were crossed to a Cre-sensitive GFP reporter line, *Epe* (Yang et al., 2003, Dymecki lab, unpublished). EdU, a thymidine analog that is incorporated during S-phase was delivered to E13.5 *Math5:Cre; Epe* embryos by intraperitoneal injections into the pregnant mom. Embryos were harvested three hours later, sectioned, and retinas were stained for EdU and GFP detection (A). Another set of embryos was harvested fifteen hours later, sectioned, and retinas were stained for EdU and GFP detection (B).

Figure 4.1 continued

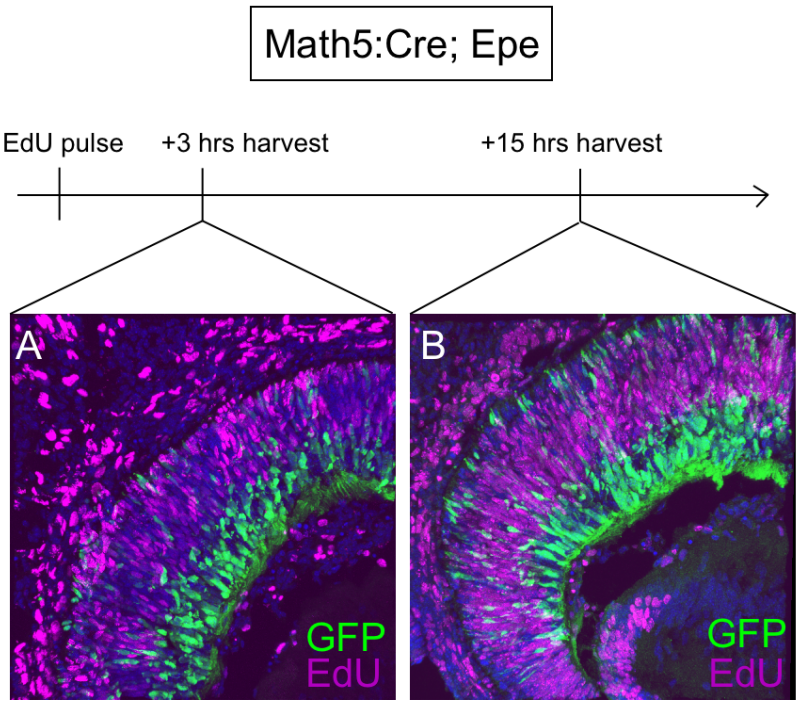

Figure 4.1

of *Notch1* conditional knockout (CKO) β-gal+ cells and wildtype (WT) β-gal+ cells was assessed by their location in the retinal layers (Figure 4.2, A, B).

In the *Math5:Cre; PFwe* retina, β-gal+ cells consisted of 41% photoreceptors, 22.5% amacrine cells, 8% horizontal cells, and 28% ganglion cells. Conversely, 63% of β-gal+ cells were photoreceptors, 16.5% were amacrine cells, 4.5% were horizontal cells, and 15% were ganglion cells in the *Math5:Cre; Notch1$^{fl/fl}$; PFwe* retina (Figure 4.2, C).

Discussion

Previous studies have determined that Notch signaling regulates proliferation and cell fate determination during retinal neurogenesis. Removal of *Notch1* from mitotic RPCs during early retinal development resulted in precocious cell cycle exit and the overproduction of cone photoreceptors at the expense of other early born cell types (Jadhav et al., 2006b). RPCs in which *Notch1* was clonally inactivated during postnatal development preferentially became rod photoreceptors and a few amacrines, but not Müller glial or bipolar cells. We wanted to examine the role of Notch signaling in cell fate specification separate from its role in regulating proliferation. To do this, we utilized a viral approach to express Cre in the *Notch1$^{fl/fl}$* background in retinal cells that had exited the cell cycle (Chapter 3). In this experiment, the majority of *Notch1* deficient cells also took on the rod photoreceptor fate, suggesting that newly postmitotic cells require *Notch1* to take on non-rod fates during postnatal development.

Figure 4.2. Conditional removal of *Notch1* from Math5:Cre+ descendants

Math5:Cre; Notch1$^{fl/fl}$; PFwe triple and *Math5:Cre; PFwe* double transgenic mice were generated. The reporter line *PFwe*, which encodes a Cre-sensitive nuclear *LacZ* allele, was used to mark cells with *Math5:Cre* expression history. Retinas from these crosses were harvested after P14, sectioned, and stained for nuclear β-galactosidase activity (A, B). Percentage of β-gal+ photoreceptors, horizontal cells, amacrine cells, and ganglion cells produced in *Math:Cre; PFwe* (WT) or *Math5:Cre; Notch1$^{fl/fl}$; PFwe* (CKO) retinas (C). Pr-photoreceptor, Hz-horizontal cell, Ac-amacrine cell, Ga-ganglion cell.

Figure 4.2 continued

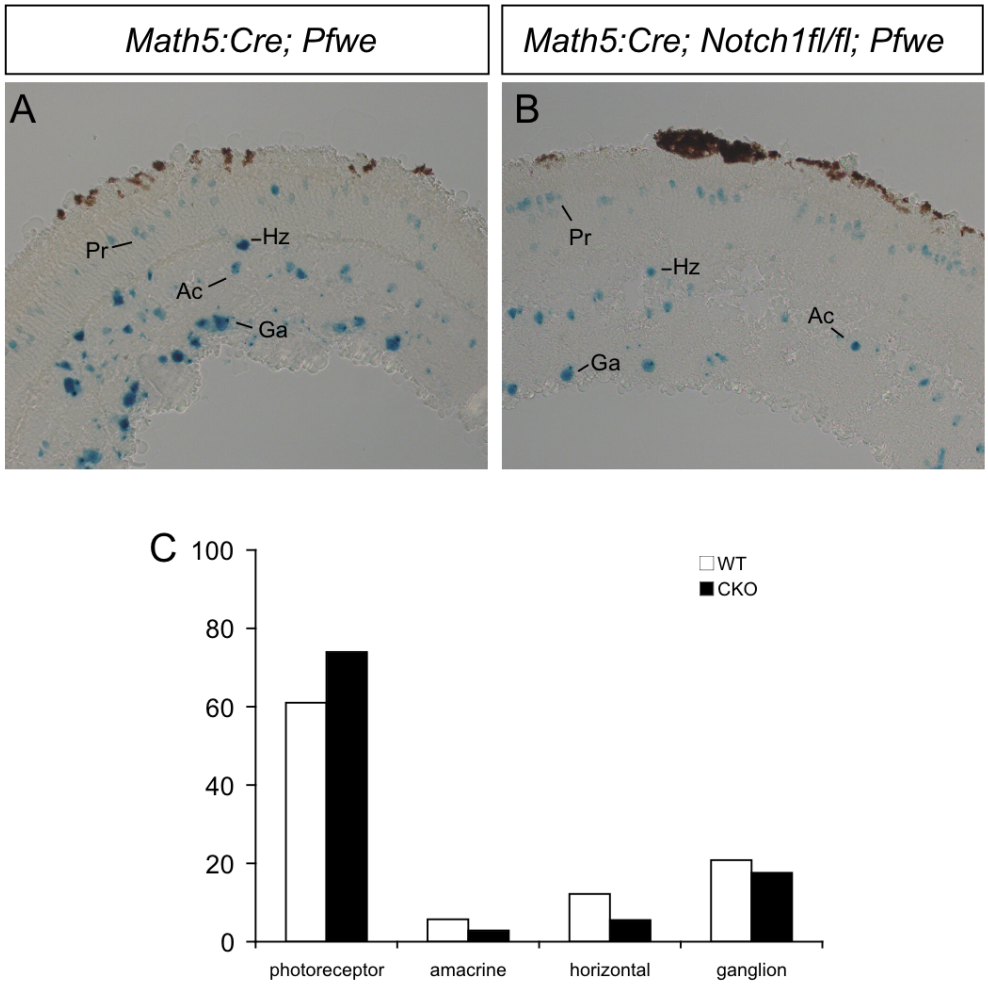

Figure 4.2

We wanted to test whether embryonically produced postmitotic cells require *Notch1* for cell fate determination. *Math5:Cre* is expressed early in retinal development, and based on fate mapping experiments, only marks early-born cell types. Moreover, we determined that Math5:Cre+ cells are not EdU+, suggesting that they are likely to be cells that are exiting the cell cycle. Subsequently, Math5:Cre was utilized to conditionally remove *Notch1* during embryonic development and the resultant mutant cells were tracked in a cell-autonomous manner. In the absence of *Notch1*, a larger percentage of Math5+ descendants acquired the photoreceptor fate (as assessed by where nuclear β-galactosidase staining was located in the retinal layers) as compared to WT cells with Math5 history. In this assay, it was unclear whether the generated photoreceptors were cone or rod photoreceptors. These results suggest that *Notch1* is required in newly postmitotic cells during embryonic stages to inhibit the photoreceptor fate, which is consistent with the role of this signaling pathway during postnatal retinal development.

Methods

Animals

Notch1$^{fl/fl}$ were maintained as homozygotes (Radtke et al., 1999). *Math5:Cre* mice were obtained from Dr. Lin Gan. *Epe* and *PFwe* reporter mice were a kind gift from Dr. Susan Dymecki. All experiments were approved by the Institutional Animal Care and Use Committee at Harvard University.

Histology

Embryos were fixed overnight at 4% PFA in PBS, pH 7.4, at 4°C. Adult retinas were dissected from the rest of the eyeball and fixed as wholemounts for 30 minutes in 0.5% glutaraldehyde in PBS, pH 7.4 at room temperature. Wholemount retinas were stained for X-gal activity. Embryos and retinas were equilibrated in sucrose/PBS solutions of increasing sucrose concentrations (5, 20, 30%). Embryos and retinas were equilibrated for >1 hour in a 1:1 solution of OCT (Tissue-Tek), and 30% sucrose/PBS, and frozen on dry ice. 20 μm cryosections were cut using a disposable blade on a Leica CM3050S cryostat.

Immunofluorescence

Retinal cryosections were blocked for 1 hour in 0.1% Triton, 0.02% SDS, 1% BSA in 1X PBS. Sections were then incubated in a humidified chamber at 4°C overnight with primary antibodies diluted in blocking solution. The primary antibody used in this study was chicken anti-GFP. Slides were then washed three times in 1X PBS and incubated for 2 hours with fluorescently coupled secondary antibodies (Jackson ImmunoResearch) and DAPI (Sigma-Aldrich). EdU detection was performed according to manufacturer's instruction (Invitrogen). Slides were washed three times with 1X PBS and mounted using Fluoromount-G (Southern Biotechnology Associates).

Microscopy and image analysis

Images were acquired using a Leica TCS SP5 confocal microscope. Images were analyzed and uniformly adjusted for brightness and contrast using Imaris 5.7 software (Bitplane). Colocalization of molecular markers in individual cells was assessed by analysis of three-dimensional *Z*-series with Imaris 5.7 software.

REFERENCES

Brown, N.L., Patel, S., Brzezinski, J., and Glaser, T. (2001). Math5 is required for retinal ganglion cell and optic nerve formation. Development *128*, 2497–2508.

Farago, A.F., Awatramani, R.B., and Dymecki, S.M. (2006). Assembly of the brainstem cochlear nuclear complex is revealed by intersectional and subtractive genetic fate maps. Neuron *50*, 205–218.

Feng, L., Xie, Z., Ding, Q., Xie, X., Libby, R.T., and Gan, L. (2010). MATH5 controls the acquisition of multiple retinal cell fates. Mol Brain *3*, 36.

Godinho, L., Williams, P.R., Claassen, Y., Provost, E., Leach, S.D., Kamermans, M., and Wong, R.O.L. (2007). Nonapical symmetric divisions underlie horizontal cell layer formation in the developing retina in vivo. Neuron *56*, 597–603.

Jadhav, A.P., Mason, H.A., and Cepko, C.L. (2006). Notch 1 inhibits photoreceptor production in the developing mammalian retina. Development *133*, 913–923.

Radtke, F., Wilson, A., Stark, G., Bauer, M., van Meerwijk, J., MacDonald, H.R., and Aguet, M. (1999). Deficient T cell fate specification in mice with an induced inactivation of Notch1. Immunity *10*, 547–558.

Rompani, S.B., and Cepko, C.L. (2008). Retinal progenitor cells can produce restricted subsets of horizontal cells. Proc. Natl. Acad. Sci. U.S.A *105*, 192–197.

Salic, A., and Mitchison, T.J. (2008). A chemical method for fast and sensitive detection of DNA synthesis in vivo. Proc. Natl. Acad. Sci. U.S.A *105*, 2415–2420.

Turner, D.L., and Cepko, C.L. (1987). A common progenitor for neurons and glia persists in rat retina late in development. Nature *328*, 131–136.

Turner, D.L., Snyder, E.Y., and Cepko, C.L. (1990). Lineage-independent determination of cell type in the embryonic mouse retina. Neuron *4*, 833–845.

Wang, S.W., Kim, B.S., Ding, K., Wang, H., Sun, D., Johnson, R.L., Klein, W.H., and Gan, L. (2001). Requirement for math5 in the development of retinal ganglion cells. Genes Dev. *15*, 24–29.

Yang, Z., Ding, K., Pan, L., Deng, M., and Gan, L. (2003). Math5 determines the competence state of retinal ganglion cell progenitors. Dev. Biol. *264*, 240–254.

Yao, J., Sun, X., Wang, Y., Xu, G., and Qian, J. (2007). Math5 promotes retinal ganglion cell expression patterns in retinal progenitor cells. Mol. Vis. *13*, 1066–1072.

Chapter 5

Discussion

Notch signaling and downstream mediators are necessary for cell fate determination during retinal development

A number of studies have demonstrated that Notch signaling regulates multiple aspects of retinal development (Jadhav et al., 2006b; Yaron et al., 2006; Riesenberg et al., 2009). Removal of *Notch1* from mitotic retinal progenitor cells (RPCs) resulted in precocious neurogenesis and overproduction of photoreceptors (Jadhav et al., 2006b). Microarray experiments performed on *Notch1* conditional knockout retinas revealed upregulation of genes involved in photoreceptor genesis. In these previous analyses, however, individual *Notch1*$^{-/-}$ cells were not easily traceable, and the general morphology of the mutant retinas was disrupted. Because Notch is a transmembrane receptor that receives extrinsic signals from the environment, it was important to ascertain whether the effects of *Notch1* removal on retinal development were manifested in a cell autonomous manner or were the product of an abnormal environment. The aim of the experiments described in Chapter 2 was to "look inside" individual *Notch1* conditional knockout (N1-CKO) cells just a few days after removal of *Notch1* to examine the resultant changes in gene expression. Single wild type (WT) P3 cells were profiled as controls.

Single cell profiling of wild type and Notch1 conditional knockout cells

In this study, 13 single N1-CKO and 13 WT P3 retinal cells were profiled on Affymetrix microarrays. These cells were harvested on the basis of GFP expression, which was introduced at P0 by electroporation. For reasons that are not well understood, electroporation into the developing retina results in preferential expression of DNA plasmids by mitotic RPCs (Matsuda and Cepko, 2004, 2007). Several days later, at P3, the P0 electroporated cells are likely to be progenitor cells that are in the process of, or have already undergone their final division to produce either two neurons or a neuron and

a glial cell. In order to discern which cells were still RPCs versus newly born neurons, all 26 cells were classified post hoc based on their transcriptional profiles using a previously described scheme (Trimarchi et al., 2007, 2008). The control cohort consisted of WT cells that were classified as RPCs, transitional cells (expressing some RPC marker genes and some neuronal marker genes), and cells that had neuronal identities. Consistent with its role in the retina, the majority of N1-CKO cells were classified as newly born rod photoreceptor cells. Three of these cells were classified as amacrine cells. Importantly, none of these cells were classified as RPCs, suggesting that the loss of *Notch1* resulted in a loss of RPC identity.

Next, we examined what happened to known marker genes of RPCs and different retinal cell types in N1-CKO cells. A number of RPC genes were downregulated in these cells, revealing novel cell cycle or progenitor genes that are sensitive to Notch1 activity (e.g. *Fgf15*, *Cdc20*, *Crym*) (Chapter 2). Genes that were robustly upregulated in N1-CKO cells included factors that are important for rod genesis, such as *NeuroD1*, *Math3*, and *Blimp1*. Previous studies have determined that ectopic expression of these genes results in overproduction of rod photoreceptors (Inoue et al., 2002; Brzezinski et al., 2010; Katoh et al., 2010). The robust upregulation of these genes in the absence of *Notch1* suggests that under wild type conditions, Notch signaling represses rod-inducing genes in RPCs and newly postmitotic cells. A major target of Notch signaling is the Hes family of transcription factors, which are known to be potent inhibitors of the expression of pro-neurogenic factors. It is possible that in cells fated to become non-rods, Hes factors specifically prevent the transcription of rod-inducing factors. However, the specificity of

how Notch signaling inhibits the rod photoreceptor fate, while permitting the expression of pro-neurogenic factors that drive bipolar fate is not yet understood.

Coexpression of different cell type marker genes in WT cells

As mentioned above, WT cells profiled at P3, which served as controls for N1-CKO cells, were classified based on their transcriptional profiles. According to their classification scores, this group of cells could be divided into cells that scored highly as RPCs, cells that were transitioning and had intermediate scores for RPC and neuronal genes, and cells that scored highly as neurons. Known marker genes of RPCs and the postnatal retinal cell types were examined in these different types of WT cells. Intriguingly, cells that had intermediate scores for RPC and neurons, coexpressed marker genes specific to newly born amacrine cells and rod photoreceptors (Chapter 2).

It is not clear what the coexpression of two different cell type markers means biologically. One possibility is that it represents a plastic period following cell cycle exit, during which cells are "testing" different fates. Alternatively, cells are already biased to become a certain fate, but are not fully committed. Control cells that had a high score for a particular cell type did not coexpress genes of two different cell types (Chapter 2).

The other surprising aspect of this finding was that these cells coexpressed amacrine and rod marker genes, but Müller glial and bipolar cell specific genes were not detected at robust levels. Not many cells at P3 will become amacrine cells, so the broad expression of these marker genes in many WT cells was not anticipated (Young, 1985).

Role of Notch1 in postmitotic cells

In Chapters 3 and 4, *Notch1* was specifically removed from newly postmitotic retinal cells in order to determine the role of this signaling pathway after cell cycle exit. Almost all newly postmitotic cells that lost *Notch1* became photoreceptors at the expense of other cell types produced concurrently. These results provided evidence that newly postmitotic cells require *Notch1* to acquire a non-rod fate, such as bipolar cells or Müller glial cells.

In the context of these results, it is possible that the single WT cells that coexpress marker genes of two different cell types represent cells transitioning through a period, maintained by Notch signaling, in which they are not fully committed. N1-CKO cells did not coexpress marker genes of two different cell types, rather these cells either expressed rod markers or amacrine cell markers. This observation suggested that the cell fates of N1-CKO cells are more "locked in" than their WT counterparts at this time.

The function of Notch signaling in specifying non-rod fates in postmitotic cells may be either instructive or permissive. If the signal were permissive, then newly postmitotic cells would be endowed with determinants that specify non-rod fates, but would require *Notch1* to maintain rod-inducing factors at low levels. Conversely, if Notch were instructive, newly postmitotic cells would require Notch input to express factors that specify bipolar and Müller glial cells. In either case, expression of rod-inducing genes may be the default state of newly postmitotic cells.

Ectopic expression of NICD in the cortex and retina provided evidence that Notch signaling plays an instructive role in glial cell development (Furukawa et al., 2000; Gaiano et al., 2000). Expression of NICD in RPCs resulted in the production of Müller

glia-like cells that also retained some progenitor cell characteristics (Furukawa et al., 2000; Jadhav et al., 2006a). Moreover, expression of NICD in postmitotic cells was sufficient to induce neurons to take on the Müller glia fate (Jadhav et al., 2006a). It is likely that in order for a cell to exit the cell cycle, Notch signaling must either be turned off or dialed down to very low levels. After cell cycle exit, relatively high levels of Notch instruct postmitotic cells to acquire the Müller glial fate.

Less is known about early factors that determine bipolar fate. One possibility is that intermediate levels of Notch instruct cells to take on the bipolar fate. Alternatively, an intrinsic program that specifies bipolar fate is endowed to newly born cells, but requires a permissive Notch signal to be enacted. A set of experiments determined that exogenous addition of CNTF to postmitotic rod precursor cells resulted in the induction of bipolar fate (Ezzeddine et al., 1997). CNTF could induce this cell fate change up until these incipient rods started to express opsin proteins, suggesting that at a certain stage retinal neurons become fully committed to their fate choice. Potentially, Notch signaling maintains a subset of postmitotic cells in an uncommitted state, during which extrinsic cues like CNTF or intrinsic determinants can influence fate decisions.

As mentioned in the Introduction, some RPCs may be intrinsically programmed to produce restricted cell types. For example, Olig2 is a transcription factor whose expression appears to mark RPCs that divide once to produce a biased set of progeny (Hafler et al., in press). Interestingly, postnatal Olig2+ RPCs produce rod photoreceptors and amacrine cells, the same cell types that are generated when *Notch1* is removed during postnatal development. Could Olig2+ cells represent wild type retinal cells that "act" like *Notch1*$^{-/-}$ cells? It is certainly possible that Olig2 marks committed RPCs that are either

insensitive to Notch signaling or permanently stop expressing the Notch receptor after cell cycle exit. Future experiments will elucidate whether Notch sensitive and insensitive cell fate decisions occur during retinal development.

Id1 and Id3 mediate Notch signaling in the developing retina

Examination of genes that were significantly downregulated in the absence of *Notch1* resulted in the identification of *Id1* and *Id3* as potential downstream mediators of Notch signaling. *Inhibitor of differentiation* (or *DNA binding*) proteins contain a helix-loop-helix binding domain, but lack the basic DNA binding domain found in the bHLH family of transcription factor (Benezra et al., 1990). Similar to Notch function, Id factors have been shown to play an important role in progenitor state maintenance. $Id1^{-/-}Id3^{-/-}$ double knockout mice exhibit precocious neurogenesis and premature depletion of the progenitor pool (Lyden et al., 1999). Biochemical analyses have determined that these factors function by directly binding pro-neurogenic bHLH transcription factors, and subsequently inhibit their ability to activate downstream target genes (Jen et al., 1992).

Ectopic expression of *Id1* and *Id3* in the wild type retina at postnatal stages resulted in the overproduction of cells that resembled RPCs or Müller glial cells (Chapter 3). This phenotype is similar to, but not as robust as the misexpression of the activated form of the Notch receptor, NICD. All NICD transduced cells in the postnatal retina overproliferate and express RPC/Müller glial markers, whereas, *Id1* and *Id3* induced the overproduction of RPC/Müller glial cells only in a proportion of cells (Furukawa et al., 2000, Chapter 3). Knockdown of *Id1* and *Id3* by RNAi resulted in fewer progenitor cells (as marked by *Hes1* expression) (Chapter 3). Misexpression of *Id1* and *Id3*, either alone

or together, was sufficient to partially rescue production of bipolar and Müller glial cells, the major cell types that are lost in the absence of *Notch1*. Moreover, viral expression of *Id1* in *Notch1*$^{-/-}$ newly postmitotic cells also resulted in a partial rescue of bipolar and Müller glial cell production. These findings suggest that Id genes are not just general progenitor genes, but are directly involved in cell fate specification under the regulation of Notch signal transduction.

Source of ligand and the lateral inhibition model

The studies in this dissertation assessed the role of the Notch1 receptor in a cell autonomous manner during retinal development. However, when and where the various ligands expressed in the retina activate the receptor remains a mystery. Delta and Jagged ligands are expressed during retinal development, in both mitotic and postmitotic cells (Henrique et al., 1995; Bao and Cepko, 1997; Nelson and Reh, 2008; Trimarchi et al., 2008; Rocha et al., 2009). In the chicken retina, a study determined that *Delta1* was expressed in newly postmitotic cells (Henrique et al., 1995). In keeping with the lateral inhibition model based on work in *Drosophila* and *C. elegans*, this outcome suggested that the two major populations in the retina, RPCs and newly postmitotic cells, signal to each other to further delineate their disparate identities. RPCs express the Notch receptor and are activated by Delta-expressing postmitotic cells. Feedback via Notch signal from newly postmitotic cells onto RPCs would maintain these cells in a proliferative state, while Delta expressing cells would take on various neuronal fates. This model is an attractive one for the developing retina, however it cannot be reconciled with the changing proportions of RPCs to postmitotic cells, and thus changing potential for Notch

signal transduction in the developing retina. Early in retinal development, the majority of cells in the neuroepithelium are RPCs, with only a small population of newly born neurons. If only postmitotic cells could activate the Notch receptor, then there should be very few RPCs maintained in a proliferative state. Towards the end of neurogenesis, at postnatal stages, RPCs produce postmitotic cells almost exclusively. Lateral inhibition from all these postmitotic cells would presumably maintain a large population of RPCs. In actuality, the RPC pool becomes extinguished, suggesting that either these cells become insensitive to Notch or a more complex Notch-Delta signaling mechanism is at play.

Recently, the roles and expression patterns of *Delta1* and *Delta4* were analyzed in the developing mouse retina (Rocha et al., 2009). *In situ* hybridization experiments demonstrated that a larger proportion of cells express *Delta1* than *Delta4*. Unlike in the chicken retina, *Delta1* was found to be expressed in mitotic cells, whereas, *Delta4* was likely expressed in differentiating cells. The authors concluded that both ligands were expressed in the same population of cells, but in a temporal sequence, such that *Delta1* was expressed before *Delta4*. Conditional knockout of *Delta1* resulted in a phenotype that was milder, but similar to Notch loss of function. These retinas exhibited disrupted laminar morphology, precocious neurogenesis, and potentially, an overproduction of ganglion cells (Rocha et al., 2009). Taken together, these results point to mechanism in which there are either Delta+ RPCs or Notch+ RPCs that signal to each other, or RPCs that express both receptor and ligand, or a combination of those two possibilities. Single cell analysis by microarray profiling performed by our lab determined that individual RPCs can express both Notch and Delta (Trimarchi et al., 2007, 2008). These findings

point to a potential mechanism of RPCs signaling amongst each other, resulting in maintenance of a large pool early in development, and a smaller one in late development. Input from postmitotic cells, which express *Delta4* and *Jagged*, could potentially be a neurogenic signal, rather than a proliferative signal. Further experimentation is needed to elucidate how the lateral inhibition model fits into retinal development and how different sources of various ligands affect Notch signaling.

A model for Notch signaling

Two-cell clones, which are frequently observed after postnatal infections, represent a simplified view of a cell fate decision. These clones arise from a retrovirally marked RPC that divided once to make two postmitotic daughter cells. The most common two cell clones observed in the retina are two rods, a rod and a bipolar, a rod and a Müller, and a rod and amacrine (Turner and Cepko, 1987). Clones consisting of two bipolars or amacrines are very rare and a two Müller clone has never been observed. These findings suggest that postnatal RPCs have a tendency to make highly stereotyped progeny, and that this division is some times an asymmetric one in terms of the fate of the two daughter cells. Based on our studies, Notch signaling is essential for the production of non-rod cell fates. Therefore, it is likely that Notch plays a role in the division that gives rise to a rod-bipolar clone and a rod-Müller clone, since in the absence of this signal the majority of cells become rod photoreceptors (Figure 5.1). Rod-rod and rod-amacrine clones may not be dependent on Notch signal, and these may be the cells that express Olig2.

Figure 5.1. A model for the role of Notch signaling during cell fate decisions in the postnatal retina

A mitotic progenitor divides to give rise to two postmitotic cells. Postmitotic precursors that will become rod photoreceptors or certain amacrine cells do not require Notch1 activation. Postmitotic precursors that will become bipolar or Müller glial cells require either a permissive or instructive Notch1 signal to take on their respective fates.

Figure 5.1 continued

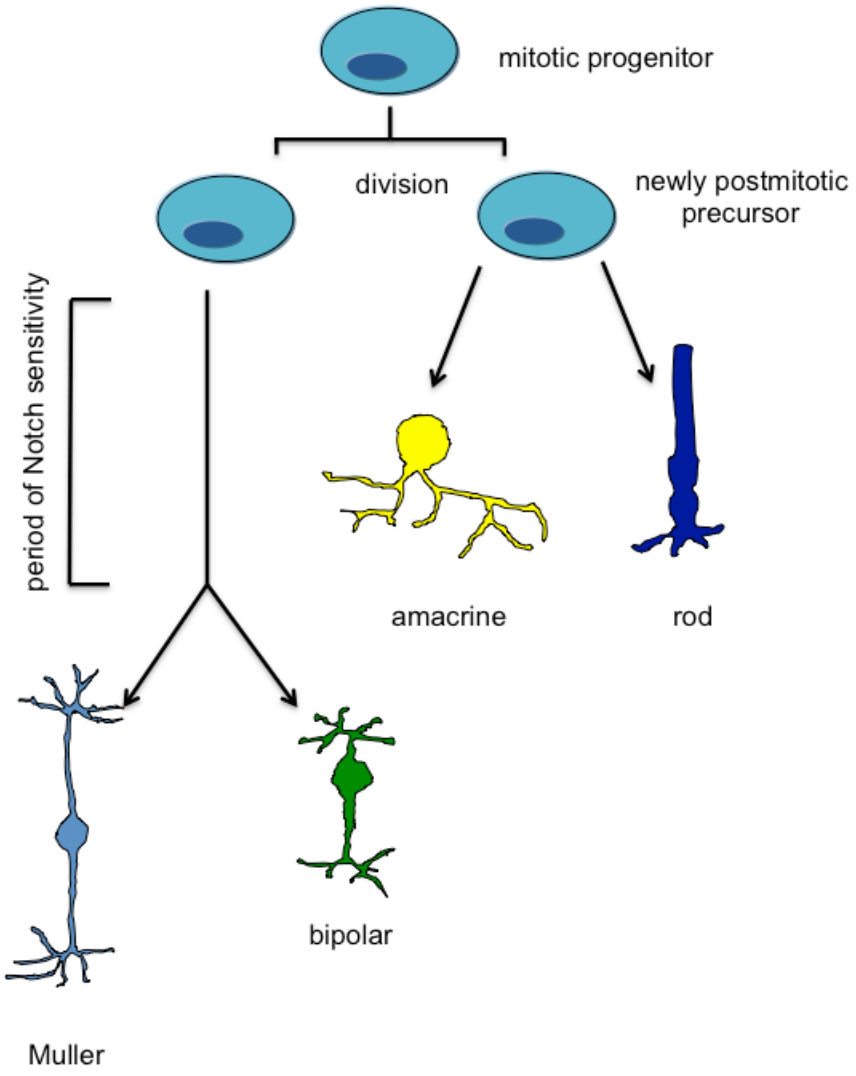

Figure 5.1

The Notch dependent asymmetric division which gives rise to a rod and a bipolar or a rod and a Muller is likely to be a binary switch similar to those described in the *Drosophila* nervous system (Chapter 1). Potentially, as the RPC divides to produce two daughter cells, one cell inherits the potential for Notch activation while the other cell does not. The cell that is capable of receiving Notch input will become either a Müller glial cell or a bipolar cell, perhaps by reading out Notch levels. High Notch levels would promote the Müller glial fate, while intermediate levels would result in the bipolar cell fate (Figure 5.1). The daughter cell that is insensitive to Notch (by inheriting Numb, for example) during this division will become a rod photoreceptor. Intriguingly, ectopic expression of Numb results in the overproduction of photoreceptors, which is consistent with this model (Cayouette and Raff, 2003).

Directed differentiation of ES cells to become photoreceptors

A thorough understanding of the mechanisms that govern embryogenesis is key for advances in treatment of human diseases. A major application of understanding how cell fate is determined during development is the ability to directly differentiate embryonic stem cells to become various retinal cell types. In particular, generation of photoreceptors *in vitro* is of great clinical relevance, as a number of human diseases, such as retinitis pigmentosa, cone dystrophy, and macular degeneration result in a loss of these cells. Transplantation of functional photoreceptors into the eye of a patient who is suffering vision loss is a major goal of stem cell therapy. Until recently, embryonic stem (ES) cells could be induced to become photoreceptors at a low efficiency, only in the presence of developing retinal tissues. A study found that adding the γ-secretase inhibitor,

DAPT, which blocks Notch signaling, resulted in an increased induction of photoreceptor precursor cells derived from mouse ES cells (Osakada et al., 2008). These cells could then be further induced to become cone or rod photoreceptors. Although this type of therapy is not yet ready for clinical application in humans, it exemplifies how an understanding of Notch signaling during development improves our ability to solve medical problems.

REFERENCES

Bao, Z.Z., and Cepko, C.L. (1997). The expression and function of Notch pathway genes in the developing rat eye. J. Neurosci *17*, 1425–1434.

Benezra, R., Davis, R.L., Lockshon, D., Turner, D.L., and Weintraub, H. (1990). The protein Id: a negative regulator of helix-loop-helix DNA binding proteins. Cell *61*, 49–59.

Brzezinski, J.A., Lamba, D.A., and Reh, T.A. (2010). Blimp1 controls photoreceptor versus bipolar cell fate choice during retinal development. Development *137*, 619–629.

Cayouette, M., and Raff, M. (2003). The orientation of cell division influences cell-fate choice in the developing mammalian retina. Development *130*, 2329–2339.

Ezzeddine, Z.D., Yang, X., DeChiara, T., Yancopoulos, G., and Cepko, C.L. (1997). Postmitotic cells fated to become rod photoreceptors can be respecified by CNTF treatment of the retina. Development *124*, 1055–1067.

Furukawa, T., Mukherjee, S., Bao, Z.Z., Morrow, E.M., and Cepko, C.L. (2000). rax, Hes1, and notch1 promote the formation of Müller glia by postnatal retinal progenitor cells. Neuron *26*, 383–394.

Gaiano, N., Nye, J.S., and Fishell, G. (2000). Radial glial identity is promoted by Notch1 signaling in the murine forebrain. Neuron *26*, 395–404.

Henrique, D., Adam, J., Myat, A., Chitnis, A., Lewis, J., and Ish-Horowicz, D. (1995). Expression of a Delta homologue in prospective neurons in the chick. Nature *375*, 787–790.

Inoue, T., Hojo, M., Bessho, Y., Tano, Y., Lee, J.E., and Kageyama, R. (2002). Math3 and NeuroD regulate amacrine cell fate specification in the retina. Development *129*, 831–842.

Jadhav, A.P., Cho, S.-H., and Cepko, C.L. (2006a). Notch activity permits retinal cells to progress through multiple progenitor states and acquire a stem cell property. Proc. Natl. Acad. Sci. U.S.A *103*, 18998–19003.

Jadhav, A.P., Mason, H.A., and Cepko, C.L. (2006b). Notch 1 inhibits photoreceptor production in the developing mammalian retina. Development *133*, 913–923.

Jen, Y., Weintraub, H., and Benezra, R. (1992). Overexpression of Id protein inhibits the muscle differentiation program: in vivo association of Id with E2A proteins. Genes Dev. *6*, 1466–1479.

Katoh, K., Omori, Y., Onishi, A., Sato, S., Kondo, M., and Furukawa, T. (2010). Blimp1 suppresses Chx10 expression in differentiating retinal photoreceptor precursors to ensure proper photoreceptor development. J. Neurosci *30*, 6515–6526.

Lyden, D., Young, A.Z., Zagzag, D., Yan, W., Gerald, W., O'Reilly, R., Bader, B.L., Hynes, R.O., Zhuang, Y., Manova, K., et al. (1999). Id1 and Id3 are required for neurogenesis, angiogenesis and vascularization of tumour xenografts. Nature *401*, 670–677.

Matsuda, T., and Cepko, C.L. (2004). Electroporation and RNA interference in the rodent retina in vivo and in vitro. Proc. Natl. Acad. Sci. U.S.A *101*, 16–22.

Matsuda, T., and Cepko, C.L. (2007). Controlled expression of transgenes introduced by in vivo electroporation. Proc. Natl. Acad. Sci. U.S.A *104*, 1027–1032.

Nelson, B.R., and Reh, T.A. (2008). Relationship between Delta-like and proneural bHLH genes during chick retinal development. Dev. Dyn. *237*, 1565–1580.

Osakada, F., Ikeda, H., Mandai, M., Wataya, T., Watanabe, K., Yoshimura, N., Akaike, A., Akaike, A., Sasai, Y., and Takahashi, M. (2008). Toward the generation of rod and cone photoreceptors from mouse, monkey and human embryonic stem cells. Nat. Biotechnol. *26*, 215–224.

Riesenberg, A.N., Liu, Z., Kopan, R., and Brown, N.L. (2009). Rbpj cell autonomous regulation of retinal ganglion cell and cone photoreceptor fates in the mouse retina. J. Neurosci *29*, 12865–12877.

Rocha, S.F., Lopes, S.S., Gossler, A., and Henrique, D. (2009). Dll1 and Dll4 function sequentially in the retina and pV2 domain of the spinal cord to regulate neurogenesis and create cell diversity. Dev. Biol. *328*, 54–65.

Trimarchi, J.M., Stadler, M.B., and Cepko, C.L. (2008). Individual retinal progenitor cells display extensive heterogeneity of gene expression. PLoS ONE *3*, e1588.

Trimarchi, J.M., Stadler, M.B., Roska, B., Billings, N., Sun, B., Bartch, B., and Cepko, C.L. (2007). Molecular heterogeneity of developing retinal ganglion and amacrine cells revealed through single cell gene expression profiling. J. Comp. Neurol *502*, 1047–1065.

Turner, D.L., and Cepko, C.L. (1987). A common progenitor for neurons and glia persists in rat retina late in development. Nature *328*, 131–136.

Yaron, O., Farhy, C., Marquardt, T., Applebury, M., and Ashery-Padan, R. (2006). Notch1 functions to suppress cone-photoreceptor fate specification in the developing mouse retina. Development *133*, 1367–1378.

Young, R.W. (1985). Cell differentiation in the retina of the mouse. Anat. Rec *212*, 199–205.

Appendix

Changes in gene expression in single Notch1 mutant cells versus single wild type progenitor cells

Karolina Mizeracka, Jeffery M. Trimarchi, Michael B. Stadler, and Constance L. Cepko

Table A.1. Downregulated genes in selected N1-CKO cells versus selected WT cells

An unbiased search for significantly downregulated genes was conducted by comparing gene expression levels in cells classified as RPCs (WT cells 2-6, 8, 12) to those in cells classified as rod precursors (N1-CKO cells 1-10). T-test analysis ($P<0.05$) was performed to find significantly downregulated genes.

Table A.1 continued

UniGene ID	Gene Symbol	P-value
Mm.284587	Ube2t	1.30349E-05
Mm.271711	Tagln2	3.79555E-05
Mm.25642	Lsm5	4.07614E-05
Mm.282242	Scarb1	6.30375E-05
Mm.282242	Scarb1	8.001E-05
Mm.235132	Zfp36l1	9.91957E-05
Mm.276362	Ttc5	0.000108651
Mm.313185	Cdca4	0.000118679
Mm.282242	Scarb1	0.000151393
Mm.181767	Ccdc34	0.00017166
Mm.42196	Uhrf1	0.000197122
Mm.271711	Tagln2	0.00024061
Mm.479578	Sorbs2	0.000301256
Mm.193099	Fn1	0.000336145
Mm.131150	Dek	0.000435084
Mm.436518	Nucks1	0.000465655
Mm.234832	Cadm1	0.000547321
Mm.309520	Nploc4	0.000595357
Mm.28265	Wdr5	0.000602419
Mm.255045	Rcc1	0.000783401
Mm.313185	Cdca4	0.000789719
Mm.313185	Cdca4	0.000865894
Mm.262059	Cbx5	0.00089899
Mm.426080	Add3	0.001052003
Mm.210676	Cd9	0.001077013
Mm.4974	Ncam1	0.001117479
Mm.19027	Mocs2	0.00121314
Mm.9621	Phospho2	0.001258904
Mm.42203	Kif11	0.001297078
Mm.1571	Cdh11	0.001369526
Mm.389499	Psrc1	0.001406391
Mm.216528	Vps29	0.001410766
Mm.279998	Hmgb2	0.001499837
Mm.290015	Nusap1	0.001533218
Mm.1904	Ttk	0.001544099
Mm.251779	2610036L11Rik	0.001619894
Mm.159684	Tmpo	0.0016733

Table A.1 continued

Mm.29760	Psmd13	0.001701699
Mm.3126	Fhl1	0.001754289
Mm.22701	Gas1	0.001756484
Mm.28222	Ddx39	0.001768598
Mm.45602	Brd8	0.001870101
Mm.4538	Lbr	0.00187971
Mm.426637	Tsn	0.001919021
Mm.227583	Atp2a2	0.002071524
Mm.110	**Id3**	0.002133723
Mm.28101	D030056L22Rik	0.00215273
Mm.288630	Calm3	0.002443836
Mm.27041	Map3k3	0.002453764
Mm.237941	Ypel1	0.002475242
Mm.22701	Gas1	0.002808995
Mm.227274	Prc1	0.002880058
Mm.24337	Pbk	0.002915075
Mm.479538	Tubb2c	0.002929926
Mm.261453	Ect2	0.002958134
Mm.257765	Clic4	0.003002032
Mm.227274	Prc1	0.003031258
Mm.204834	Slc1a3	0.003076251
Mm.478899	Pmepa1	0.003257114
Mm.285723	Cdca3	0.003320612
Mm.390674	Dusp13	0.003325332
Mm.180363	2610039C10Rik	0.003337215
Mm.45785	Ckap2l	0.0034958
Mm.212861	Cul4a	0.003500139
Mm.292470	Dbf4	0.003505434
Mm.371630	Rpl22l1	0.003545711
Mm.296158	Stt3b	0.003548872
Mm.24105	Nde1	0.003563451
Mm.158289	Myh14	0.003609778
Mm.1389	Nfatc2ip	0.003745131
Mm.259315	Abat	0.003792643
Mm.423000	Kpna2	0.003850371
Mm.259893	Topbp1	0.003863907
Mm.380027	Ccnb1	0.004001054
Mm.260714	Ttll4	0.00414153
Mm.251075	Tmem194	0.004146749
Mm.29133	Bub1b	0.004179003
Mm.473716	Rab11fip4	0.004201431

Table A.1 continued

Mm.7091	Ssr2	0.004314457
Mm.29133	Bub1b	0.004397399
Mm.180363	2610039C10Rik	0.004435559
Mm.1237	Pmp22	0.004461656
Mm.16769	Tmbim6	0.004610537
Mm.29133	Bub1b	0.004673031
Mm.77695	Ccnf	0.004717393
Mm.33903	Sema4d	0.004717621
Mm.2581	Epha2	0.004730674
Mm.273804	Racgap1	0.00475918
Mm.4189	Ccna2	0.00488955
Mm.41557	Scrn1	0.004960124
Mm.28873	Ppap2c	0.005003814
Mm.266627	Spred2	0.005168061
Mm.33831	Cdca2	0.005227701
Mm.440339	Trpm3	0.005277897
Mm.157322	Dkk4	0.005600776
Mm.330700	Zfp238	0.005756279
Mm.278758	Rrh	0.005763608
Mm.139695	Epn2	0.005781122
Mm.417427	Zfp191	0.005818954
Mm.379024	Tacc3	0.005854563
Mm.7598	Hr	0.005887116
Mm.273768	Klhl7	0.005962425
Mm.279998	Hmgb2	0.005976548
Mm.479533	Marcks	0.006057036
Mm.2952	Fen1	0.006107894
Mm.236401	Srgap3	0.006117463
Mm.206841	Smc4	0.006208622
Mm.261027	D19Bwg1357e	0.006290159
Mm.49884	Ube2d3	0.006349667
Mm.257590	Ncapd2	0.006375977
Mm.67949	Armcx3	0.006381302
Mm.371673	Ube2j2	0.006469942
Mm.10193	Grk6	0.006515202
Mm.455265	---	0.006524574
Mm.260114	Ccnb1	0.006705561
Mm.379733	Znhit3	0.006729835
Mm.10193	Grk6	0.006755111
Mm.8575	Sox13	0.006818704
Mm.213213	Hkdc1	0.006868367

Table A.1 continued

Mm.38910	Cep63	0.006888217
Mm.29524	Clic1	0.00690338
Mm.3794	Plk4	0.00697061
Mm.21762	Dnajc10	0.007045655
Mm.274884	4930422G04Rik	0.007105747
Mm.28101	D030056L22Rik	0.007181204
---	Shc4	0.007302052
Mm.23095	Chrac1	0.007312992
Mm.261006	Bcl2l12	0.007494116
Mm.219877	Gca	0.007558272
Mm.8552	Birc5	0.00765157
Mm.1258	Tnfrsf1a	0.007680875
Mm.234204	Pak2	0.007794422
Mm.136736	S1pr3	0.007799049
Mm.159684	Tmpo	0.007844706
Mm.479549	Grb10	0.00787939
Mm.273930	Vamp3	0.007966041
Mm.33118	Fam64a	0.007969722
Mm.306163	Prkar1b	0.007982248
Mm.478824	Sec14l1	0.007996708
Mm.170002	AI848100	0.008019135
Mm.235562	Ormdl2	0.008097433
Mm.261027	D19Bwg1357e	0.008117494
Mm.268027	2900064A13Rik	0.008161417
Mm.30173	F630043A04Rik	0.008188493
Mm.245890	Spred1	0.008257265
Mm.130607	Lypd6	0.008275076
Mm.281379	Casp6	0.008283989
Mm.24035	Ccdc52	0.008295087
Mm.447178	---	0.008313782
Mm.288324	Espl1	0.008392738
Mm.442452	Pi15	0.008396815
Mm.158700	Vcan	0.008496538
Mm.158361	Phactr4	0.008937349
Mm.285	Kdr	0.008969108
Mm.99	Rrm2	0.009183111
Mm.325800	Snn	0.009199409
Mm.25263	2700029M09Rik	0.009264278
Mm.472132	Rnf26	0.009396863
Mm.4405	Vsx2	0.009523515
Mm.4237	Top2a	0.009610931

Table A.1 continued

Mm.123714	Triobp	0.009690597
Mm.1886	Thoc4	0.009756624
Mm.22592	Ccnb2	0.009850902
Mm.430736	Elovl5	0.009938045
Mm.471813	Peg12	0.01003693
Mm.160088	Mbd3l1	0.010080601
Mm.200783	Ssx2ip	0.01011615
Mm.117541	Gm8203 /// H2afz	0.01015499
Mm.214514	Prelp	0.010155041
Mm.250438	Prss23	0.01019279
Mm.426637	Tsn	0.010361343
Mm.440259	2700099C18Rik	0.010487594
Mm.440156	Uck2	0.010495864
Mm.439690	Tuba1a /// Tuba1b /// Tuba1c	0.010649267
---	4932431P20Rik	0.010652671
Mm.259293	2700094K13Rik	0.010710634
Mm.380027	Ccnb1	0.010782108
Mm.241387	Tmem167	0.011125388
Mm.237095	Strbp	0.01113867
Mm.72173	Sgcg	0.011217505
Mm.5098	Gli3	0.011355456
Mm.16898	Phgdh	0.011391329
Mm.439701	Gnaq	0.01142074
Mm.21629	Abcf2	0.011442617
Mm.105331	Psip1	0.011443631
Mm.181860	Tubb6	0.011517408
Mm.478899	Pmepa1	0.011562717
Mm.241700	Gpm6a	0.011596695
Mm.24425	Naa16	0.011619516
Mm.478824	Sec14l1	0.011635042
Mm.158903	Hlf	0.011702266
Mm.478923	Nsun6	0.011709563
Mm.24219	1810037I17Rik	0.011808215
Mm.248212	Cenpl	0.011834433
Mm.440156	Uck2	0.01187451
Mm.29159	Pnrc2	0.011877837
Mm.99	Rrm2	0.011922892
Mm.379376	Syt11	0.01208688
Mm.5025	Etv4	0.012096573
Mm.172429	BC064078	0.012152164
Mm.9114	Crym	0.012237164

Table A.1 continued

Mm.440552	2610301B20Rik	0.012266505
Mm.2437	Wdr46	0.012266732
Mm.8846	Fgf9	0.012436572
Mm.102136	Tshz1	0.012569217
Mm.65396	Sox2	0.012617269
Mm.790	Tmem165	0.012804701
Mm.2000	Anapc13	0.012814057
Mm.331133	Iqgap3	0.012918767
Mm.46493	S1pr2	0.012967578
Mm.390021	Gm8096	0.013070992
Mm.283410	Suz12	0.013094275
Mm.390859	**Hes1**	0.013120504
Mm.42196	Uhrf1	0.013128198
Mm.347360	Exoc8	0.013140365
Mm.273405	2610029G23Rik	0.013195353
Mm.474662	Gm10401	0.013199382
Mm.281482	Parp2	0.013220412
Mm.115970	Adamts16	0.013256135
Mm.275036	Klf6	0.013354852
Mm.1886	Refbp2 /// Thoc4	0.013422617
Mm.45008	Fam33a	0.013427669
Mm.371601	Hn1l	0.013476257
Mm.252695	D2Ertd750e	0.013630463
Mm.295062	Btaf1	0.013632597
Mm.222228	Cks2	0.013647152
Mm.478276	Smu1	0.013678049
Mm.37199	Gstm1	0.013679314
Mm.17436	Trim37	0.013697086
Mm.25148	Atp6ap2	0.013738102
Mm.280544	Ddx52	0.013752012
Mm.347976	Ndufab1	0.013902994
Mm.133825	Crip2	0.013932082
Mm.290251	Cnbp	0.013945166
Mm.3616	Polg	0.014031482
---	5330409N07Rik	0.014117322
Mm.349493	Fanci	0.014332333
Mm.2313	Caml	0.014354159
Mm.222867	Dap	0.014399141
Mm.260105	Ipo8	0.01445691
Mm.370185	Gna12	0.014593726
Mm.46401	Son	0.014756972

Table A.1 continued

Mm.168478	Ckap5	0.014765492
Mm.33773	Nek2	0.014767974
Mm.216528	Vps29	0.01477997
Mm.460296	---	0.014905629
---	Acsl3	0.014921265
Mm.182574	Isoc1	0.014934208
Mm.27705	Prim2	0.014947065
Mm.422674	Rap2b	0.014989654
Mm.1912	Cdkn2c	0.015024134
Mm.3360	Ywhaz	0.015054718
Mm.209813	Efnb2	0.015175757
Mm.35788	Pold2	0.015304269
Mm.393532	---	0.015334274
Mm.281714	1700029F09Rik	0.015348303
Mm.64579	Hnrpll	0.015349378
Mm.254642	Ctso	0.015352851
Mm.473315	---	0.015393158
Mm.25559	Stk17b	0.01543301
Mm.250936	Golph3	0.01549248
Mm.444	**Id1**	0.015510273
Mm.250631	Tpst2	0.015518784
Mm.271578	Znrf1	0.015526909
Mm.272748	4921524J17Rik	0.015538203
Mm.29581	**Hey1**	0.015568694
Mm.27291	Ccnd3	0.015690827
Mm.291811	Rnf219	0.01570727
Mm.2437	Wdr46	0.015778994
Mm.20350	Mxd3	0.015780651
Mm.389191	Cdc73	0.015889972
Mm.29760	Psmd13	0.016000082
Mm.261226	B9d1	0.016012458
Mm.479140	Morf4l1	0.016032473
Mm.259320	AI646023	0.016163322
Mm.245394	Emx2	0.016229342
Mm.21094	Grinl1a	0.016272597
Mm.27308	Arf6	0.016288906
Mm.272969	Spc25	0.01633344
---	Acsl3	0.016386693
Mm.289747	Cdc20	0.016507
Mm.9394	Nfix	0.016732921
Mm.33773	Nek2	0.016870099

Table A.1 continued

Mm.1186	Car2	0.016937329
Mm.155708	Etv5	0.016940093
Mm.336898	Nab2	0.017062721
Mm.154093	Col23a1	0.017214877
Mm.4387	Bad	0.017263011
Mm.207709	Tox2	0.017284723
Mm.31204	Rpusd3	0.017297116
Mm.218889	Impad1	0.017364853
Mm.479641	Zfp617	0.017423813
---	4930513N20Rik	0.017495286
Mm.2185	Bub1	0.017520274
Mm.74887	---	0.017585663
Mm.426304	C030044B11Rik	0.017628978
Mm.218533	Rpl7l1	0.017648132
Mm.306482	Polr3k	0.017681098
Mm.260456	Vapb	0.017722354
Mm.22453	Tardbp	0.01782667
Mm.170002	AI848100	0.017914098
Mm.3941	Eif4e	0.017916271
---	2410042D21Rik	0.018024964
Mm.330986	LOC100046643 /// Spry1	0.018122308
Mm.279690	Ptn	0.018184516
Mm.316306	Hnrnpa3	0.018218277
Mm.389608	Speer4b	0.018289421
Mm.240566	E2f8	0.018326405
Mm.23503	6720463M24Rik	0.018417779
Mm.37199	Gstm1	0.018491787
Mm.139815	Tcf7l2	0.018532219
Mm.286602	Cdc25c	0.018532995
Mm.233843	Pkn3	0.018574067
Mm.12834	Lfng	0.018670033
Mm.21062	Nmd3	0.018730661
Mm.243962	Clspn	0.018744124
Mm.29680	Asf1b	0.018851931
Mm.379024	Tacc3	0.018862891
Mm.393162	---	0.018906173
Mm.3496	Fnta	0.018935474
Mm.447247	Hs3st4	0.018987906
Mm.24491	C330027C09Rik	0.019059034
Mm.209491	Fnbp1l	0.019123643
Mm.181860	Tubb6	0.019307178

Table A.1 continued

Mm.2805	Dclre1a	0.019496477
Mm.281367	Cdk1	0.019648067
Mm.17436	Trim37	0.019662224
Mm.87312	Gmfb	0.019691505
Mm.171186	Heatr1	0.01970205
Mm.440364	Agbl5	0.019826982
Mm.42015	Sema5b	0.019830636
Mm.216549	Ankle1	0.019927907
Mm.389499	Psrc1	0.019971498
Mm.306482	Polr3k	0.020116448
Mm.479549	Grb10	0.020289641
Mm.21848	Bzw1	0.020429827
Mm.41891	Yipf4	0.020487834
Mm.249437	Rad54b	0.020490885
Mm.1500	Mcm4	0.020574979
Mm.275003	Mcam	0.020687617
Mm.13787	Cp	0.020744278
Mm.27041	Map3k3	0.020906857
Mm.379024	Tacc3	0.02092518
Mm.16898	Phgdh	0.02093217
Mm.283410	Suz12	0.020942921
Mm.254494	Ptk2	0.020966334
Mm.289747	Cdc20	0.020979372
Mm.390835	Wdr67	0.021205968
Mm.104919	Bcas2	0.021315476
Mm.289456	Cdkn2aipnl	0.02135069
Mm.23834	Ythdf3	0.021384471
Mm.37533	Homer1	0.021501234
---	---	0.021539499
Mm.28217	Epb4.1l4b	0.02161008
Mm.2312	Tnfaip8l1	0.021653459
Mm.268582	Zfp213	0.021684293
Mm.275036	Klf6	0.021874271
Mm.46675	Kbtbd11	0.021969614
Mm.273295	Smoc1	0.02199923
Mm.27757	Bmp1	0.022028284
Mm.261664	Hist1h4a	0.022117898
Mm.143763	Parva	0.02224596
Mm.32012	Ncapg	0.022249301
Mm.264215	Espn	0.022273559
Mm.479533	Marcks	0.022438674

Table A.1 continued

Mm.358649	Banf1	0.022478042
Mm.41555	Rab28	0.022498326
Mm.251013	Kpnb1	0.022627665
Mm.202322	Appl1	0.022934255
Mm.549	Ifngr1	0.023054396
Mm.105331	Psip1	0.023342062
Mm.85388	---	0.023386682
Mm.244703	2310008H04Rik	0.023481308
Mm.30256	Ptcd3	0.023547853
Mm.247335	BC030867	0.023607387
Mm.297992	Fbln1	0.023631142
Mm.3496	Fnta	0.023679845
Mm.334918	Irf2bp2	0.023685691
Mm.88512	Gnl3	0.023759735
Mm.20818	Pef1	0.023772324
Mm.31259	Kdm1b	0.023802631
Mm.38529	Prpf18	0.023841542
Mm.371692	Usp1	0.023905653
Mm.316391	Plch1	0.024119676
Mm.130607	Lypd6	0.024165565
Mm.260256	Eif4g1	0.024318852
---	---	0.024434907
Mm.41933	Pitrm1	0.024482916
Mm.297440	Ran	0.024713523
Mm.391038	Strn	0.02494691
Mm.282158	Cct5	0.025000492
Mm.269088	Anp32a	0.025037627
Mm.273049	Ccnd1	0.025044954
Mm.244975	Brca1	0.025108013
Mm.196067	Ak3	0.025148033
Mm.52711	0610030E20Rik	0.02523863
Mm.170103	Vps54	0.025271942
Mm.109074	Rspry1	0.025306238
Mm.274160	Eri2	0.025312046
Mm.259547	1810008A18Rik	0.025327859
Mm.355614	Pde7a	0.025436154
Mm.332379	Gm447	0.025473168
Mm.16898	Phgdh	0.025495035
Mm.274086	Kif18a	0.025514275
Mm.301652	Cr1l	0.025517582
Mm.332607	Hnf1a	0.025626263

Table A.1 continued

Mm.286602	Cdc25c	0.025687327
Mm.257765	Clic4	0.025780549
Mm.274810	Pla2g16	0.025787847
Mm.291936	Map4k5	0.025976812
Mm.37801	Shcbp1	0.02603172
Mm.402215	Slc30a5	0.026073303
Mm.218657	Anp32e	0.026094467
Mm.189102	Dtl	0.026127417
---	2810455D13Rik	0.026130944
Mm.275974	Dpys	0.026173363
Mm.407737	Tpx2	0.026187242
Mm.41353	Wasf1	0.026351245
Mm.9593	Sh2d3c	0.026405553
Mm.247535	Fam118a	0.026517088
Mm.17709	Foxn4	0.026570061
Mm.479590	Notch2	0.026606122
Mm.37932	Frmd4a	0.026788173
Mm.289747	Cdc20	0.026842688
Mm.458006	Id4	0.026863856
---	---	0.026908212
Mm.193925	Gna13	0.026912735
Mm.102	Rfx2	0.026956068
Mm.479247	Nudcd1	0.026988294
Mm.291828	Eny2	0.027140601
Mm.257316	Chm	0.027173335
Mm.117365	Mesdc2	0.027303683
Mm.23095	Chrac1	0.027325377
Mm.5260	Slc6a1	0.027410578
Mm.29755	Incenp	0.027438703
Mm.297992	Fbln1	0.027502555
Mm.260114	Ccnb1	0.027524101
Mm.28366	Ide	0.027525669
Mm.290758	Pde12	0.027576353
Mm.103573	Hey2	0.027599738
Mm.371570	Pabpc1	0.027645373
Mm.39043	Trim68	0.027748219
Mm.197486	Rrm1	0.027950929
Mm.250717	Sbsn	0.028001097
Mm.440156	Uck2	0.028026941
Mm.466344	---	0.028182232
Mm.221758	Atad2	0.02818936

Table A.1 continued

Mm.196464	Gnai2	0.028210079
Mm.290563	Cenpa	0.028396644
Mm.168523	Aspm	0.028404373
Mm.430736	Elovl5	0.028444691
Mm.458189	Gstm7	0.028475781
Mm.28622	Txndc5	0.028538925
Mm.325643	Ptpn9	0.028791144
Mm.101153	Irx5	0.028793154
Mm.266515	Rfesd	0.028794273
Mm.359408	Hmgb1	0.028911683
Mm.29159	Pnrc2	0.029021764
Mm.41633	Dok5	0.029037317
Mm.477077	Ranbp1	0.029039111
Mm.2185	Bub1	0.02904041
Mm.218141	Per2	0.029079016
Mm.274810	Pla2g16	0.029163667
Mm.29685	Dnajc8	0.029239974
Mm.386950	Gm5617	0.02924341
Mm.16898	Phgdh	0.029322394
Mm.259879	Xiap	0.029352049
Mm.4189	Ccna2	0.029414062
Mm.77695	Ccnf	0.029495085
Mm.333881	Nav2	0.029691126
Mm.21281	Rnf4	0.029760157
---	4930539J05Rik	0.029834002
Mm.21144	C79407	0.02986699
Mm.237095	Strbp	0.029906442
Mm.458184	Eif3j	0.029966598
Mm.233083	Ids	0.029995543
Mm.255401	Mterfd3	0.030003561
---	Gm7072	0.030083881
Mm.479144	Ski	0.030098827
Mm.34261	Ubr7	0.030107519
Mm.29484	Mrps18b	0.030157213
Mm.200763	Lrch4 /// Lrch4-sap25 /// Sap25	0.030215851
Mm.153202	Sgol1	0.030250467
---	4930488N15Rik	0.030312462
Mm.479533	Marcks	0.030324617
---	1700129O19Rik	0.030381038
Mm.3014	Ndufab1	0.030444578

Table A.1 continued

---	Mtap4	0.030466937
Mm.41265	Rassf3	0.030848514
Mm.137268	**Hes5**	0.030851105
Mm.3360	Ywhaz	0.030903714
Mm.289456	Cdkn2aipnl	0.030972606
Mm.305925	Arih1	0.030976517
Mm.41449	Rdm1	0.030985096
Mm.441613	Mtmr9	0.031052525
Mm.282751	Anln	0.031070918
Mm.46529	Tmem101	0.031079749
Mm.182628	Rad21	0.031217766
Mm.46029	Gpatch4	0.031299435
Mm.22716	Slc43a1	0.031372013
---	Sco2	0.031414502
Mm.16898	Phgdh	0.0314182
Mm.211032	Pif1	0.031438878
Mm.10815	Zfp143	0.031459402
Mm.44683	Slc6a11	0.031498786
Mm.222228	Cks2	0.031550606
Mm.112824	Foxn2	0.031592148
Mm.246803	Smarca5	0.031656748
Mm.409670	Gpr37	0.031728669
Mm.258498	---	0.031739073
Mm.27560	Uba2	0.031778811
Mm.139314	Dppa5a	0.031795242
Mm.3741	Plekha7	0.032006537
Mm.140749	5730528L13Rik	0.032105071
Mm.27853	Exosc5	0.032174938
Mm.32646	Zfand2b	0.032281093
---	Gm4047	0.032387643
Mm.2238	Eif3a	0.032390898
Mm.440038	Znrd1	0.03240622
Mm.28038	Cdca8	0.032448693
Mm.20350	Mxd3	0.03251292
Mm.292208	Hdgf	0.032548013
Mm.322945	Cts	0.03263135
Mm.142856	Lhx2	0.032813974
Mm.247473	Sdcbp	0.032863272
Mm.24250	Spag5	0.032892198
Mm.130883	Mtdh	0.032941456
Mm.2952	Fen1	0.032964614

Table A.1 continued

Mm.268668	Melk	0.033032471
Mm.283893	Ngfr	0.033069219
Mm.440428	2900006K08Rik	0.033172435
Mm.2478	Sfrs4	0.033215511
Mm.272998	Mesdc1	0.033359157
Mm.440323	Cenpp	0.033440182
Mm.31672	Cdk6	0.033484168
Mm.248827	Canx	0.033590196
Mm.253264	G2e3	0.033980639
Mm.251779	2610036L11Rik	0.034004231
Mm.16898	Phgdh	0.034064387
Mm.271715	Phf5a	0.034194732
Mm.98200	Cyp2j6	0.034368326
Mm.30012	Hdlbp	0.034522462
Mm.41998	Ppp4c	0.034563829
Mm.140749	5730528L13Rik	0.034570167
Mm.196472	Twistnb	0.034767373
Mm.256342	Kif5c	0.034778978
Mm.335391	Ryk	0.034966367
Mm.85162	Fam83d	0.035063864
Mm.209419	Hspa9	0.035172727
Mm.22315	Ibtk	0.03520464
Mm.1400	Gcm1	0.035263536
Mm.279690	Ptn	0.035322773
Mm.272541	2410002O22Rik	0.035355121
Mm.277638	Ccdc43	0.03541652
Mm.272024	Mad2l1bp	0.035420191
Mm.356653	Ggnbp2	0.035421803
Mm.12309	D1Ertd622e	0.035476311
Mm.313345	Hmgb1	0.035828301
Mm.289516	Mlst8	0.035828947
Mm.252695	D2Ertd750e	0.035873064
Mm.321654	Pdzrn3	0.035929667
Mm.29729	Ttyh1	0.036067948
Mm.300814	Rragd	0.03624808
Mm.123211	Polb	0.036266669
Mm.20242	Cyb5b	0.036286655
Mm.39485	Rps19bp1	0.036308747
Mm.38951	Sucla2	0.036383115
Mm.274904	Lancl2	0.036411773
Mm.229322	Pter	0.036591548

Table A.1 continued

Mm.378921	Gja1	0.03670731
Mm.385194	---	0.036769846
Mm.478903	Paqr4	0.036949904
Mm.24397	Nudt4	0.036988779
Mm.143025	Tmem110	0.037021904
Mm.222867	Dap	0.037123613
Mm.387734	Srrt	0.037168038
Mm.458052	Ube2g1	0.03735748
Mm.197520	Fbxo5	0.037378835
Mm.320317	Cux1	0.037411361
Mm.250438	Prss23	0.037471872
Mm.176695	Trim59	0.037506426
Mm.227117	Slc30a10	0.037559274
Mm.13787	Cp	0.037593587
Mm.355686	Kif2a	0.037625906
Mm.21062	Nmd3	0.037686369
Mm.27705	Prim2	0.037732637
Mm.121361	Per3	0.037812098
Mm.38777	Fbxo41	0.037851249
Mm.138617	Zfp664	0.037903933
Mm.283410	Suz12	0.038025626
Mm.253564	Actn1	0.038048134
Mm.273379	Snx5	0.038155221
Mm.379292	Zzz3	0.03815537
Mm.196484	Csrp1	0.038196109
Mm.276133	Luc7l2	0.038196862
Mm.38474	Hmg20b	0.038215254
Mm.196484	Csrp1	0.038249224
Mm.154275	Rbbp8	0.038384549
Mm.3820	Cmas	0.038570903
Mm.276229	Fbxo30	0.038624575
Mm.286407	Sox9	0.038663155
Mm.3616	Polg	0.038708411
---	4930402H05Rik	0.03885078
Mm.32800	Sgol2	0.039077468
Mm.273147	Znhit1	0.039194961
Mm.292712	Kctd6	0.039210798
Mm.927	Bub3	0.039217681
Mm.150813	Fzd5	0.039374022
Mm.41423	Endod1	0.039444094
Mm.130504	Sdk2	0.039580928

Table A.1 continued

Mm.32084	Kif18b	0.039634053
Mm.464272	Cdkn2d /// Gm4694	0.039785027
Mm.320317	Cux1	0.039800755
Mm.129746	Cenpf	0.039816647
---	E130114P18Rik	0.039839435
Mm.101743	Ildr2	0.039864505
Mm.24250	Spag5	0.039868172
---	4933408M05Rik	0.039906454
Mm.9776	Lphn2	0.039965282
Mm.249280	Esco2	0.040106853
Mm.154796	Npy	0.040148026
Mm.301522	Taf5	0.040196824
Mm.277638	Ccdc43	0.04025122
Mm.35738	Ctnnd1	0.040447199
Mm.210188	Zcchc2	0.04045908
Mm.170905	Fyb	0.040509967
Mm.1457	Ddah2	0.040556659
Mm.245890	Spred1	0.040639724
Mm.440249	Gltscr1	0.040660584
Mm.371621	Tmx2	0.040731052
Mm.240473	Klf13	0.040733275
Mm.439824	---	0.040775966
Mm.22240	Sh3bgrl3	0.040868378
Mm.29729	Ttyh1	0.04086959
Mm.330160	Hspa5	0.040919546
Mm.479590	Notch2	0.040954354
Mm.143877	Mapre1	0.040980109
Mm.27917	Tanc1	0.040982589
Mm.434583	Sos1	0.041049269
Mm.385178	Phtf1	0.04105137
Mm.241700	Gpm6a	0.041166324
Mm.250414	Dpysl4	0.041293821
Mm.221440	Raly	0.04147062
Mm.29830	Rsph3a	0.041489188
Mm.171378	Ucp2	0.041497085
Mm.38445	Tmod3	0.041563315
Mm.2065	Ctps2	0.041723147
Mm.250256	Enpp2	0.04173852
Mm.116711	Exosc9	0.041800265
Mm.143771	Wdr4	0.041837985
---	---	0.041881699

Table A.1 continued

Mm.12775	Pdk3	0.04200848
Mm.358649	Banf1	0.042046736
Mm.25148	Atp6ap2	0.042071868
Mm.10815	Zfp143	0.042146433
Mm.312204	4930534B04Rik	0.04225252
Mm.286457	Bet1	0.042255662
Mm.27897	Dnaja1	0.042257914
Mm.22584	Strap	0.042303151
Mm.265384	2900052N01Rik	0.042313727
---	---	0.042344495
Mm.476905	Cul5	0.042461112
Mm.103737	Egr3	0.042601914
Mm.439670	Htr2c	0.042637052
Mm.277629	Rad9	0.04271045
Mm.392013	---	0.042722417
Mm.248647	Pi4k2b	0.042801382
Mm.261275	Als2cr4	0.042889635
Mm.4428	Prkrir	0.042920205
Mm.13445	Oxct1	0.043138803
Mm.182094	LOC100045031 /// Tceal8	0.043148996
Mm.254839	Abcb9	0.04325354
Mm.293378	Cdc42ep4	0.043263528
Mm.273768	Klhl7	0.043272219
Mm.9699	Pmm2	0.043352203
Mm.383185	Nfatc3	0.043426456
Mm.71633	---	0.043482301
Mm.182628	Rad21	0.043514806
Mm.57648	Mansc1	0.043710283
Mm.8294	Vbp1	0.043848686
Mm.286407	Sox9	0.04386319
Mm.451912	Srd5a1	0.043894079
Mm.25709	Ing1	0.044011918
Mm.14485	Tex9	0.044060125
Mm.280544	Ddx52	0.044081118
Mm.359408	Hmg1l1	0.044093666
Mm.334199	Acsm3	0.044169586
Mm.29497	Iscu	0.04425167
Mm.330785	2810408M09Rik	0.044365002
Mm.13445	Oxct1	0.044435384
Mm.3411	Orc2l	0.044538779
Mm.252695	D2Ertd750e	0.044767676

Table A.1 continued

Mm.159149	Gsdma2	0.044797135
Mm.2785	Dbi	0.044907072
Mm.252171	Snx2	0.044934393
Mm.297863	Megf10	0.045074818
Mm.219459	Sik3	0.045091831
Mm.28897	Ppa1	0.045112193
Mm.261676	Gm11277	0.045151573
Mm.12091	Rassf1	0.045170206
Mm.440339	Trpm3	0.045206974
Mm.23526	Cdca5	0.045282842
Mm.3552	Clock	0.045302089
Mm.272394	Cdkn3	0.04542359
Mm.262059	Cbx5	0.045468675
Mm.259026	2700078E11Rik	0.045470678
Mm.335237	Zwilch	0.045490906
Mm.3014	Ndufab1	0.045733578
Mm.18503	Ninj1	0.045737405
Mm.131038	Elf2	0.045761322
---	---	0.045791385
Mm.42203	Kif11	0.045815186
Mm.21687	Limd2	0.045839689
Mm.437411	---	0.045848196
Mm.439890	Trpm4	0.045912597
Mm.355614	Pde7a	0.045956887
Mm.478505	Gjc1	0.046032716
Mm.263913	Anp32b	0.046046191
Mm.331064	Schip1	0.046088241
Mm.296971	Ccdc41	0.046172587
---	---	0.046252172
Mm.166467	Pcyt1b	0.046296232
---	1810012K16Rik	0.046309942
Mm.273049	Ccnd1	0.046334904
Mm.428571	----	0.046442433
---	2810468N07Rik	0.046447174
Mm.63569	Chrna3	0.046641203
Mm.24202	Fzr1	0.04678937
Mm.479615	Ccdc30	0.047035683
Mm.249752	Pdss1	0.047053099
Mm.240336	Sptlc1	0.047327465
Mm.153963	Mlec	0.047500985
Mm.478293	Rfc5	0.047579206

Table A.1 continued

Mm.9916	Cep55	0.04775975
Mm.458619	---	0.04777942
Mm.160124	Phactr1	0.047803285
Mm.87773	Hsp90b1	0.047827771
Mm.136919	4930434E21Rik	0.047872854
Mm.22786	Trim32	0.047967243
Mm.24035	Ccdc52	0.048052205
Mm.27831	Pno1	0.048172274
Mm.104919	Bcas2	0.048209388
Mm.214530	Igsf9	0.04848252
Mm.148781	Ranbp9	0.048492275
Mm.89845	Cdc27	0.048534754
Mm.7320	Smad3	0.048613094
Mm.11333	Rtel1	0.048676279
Mm.478899	Pmepa1	0.04870265
Mm.34102	Odc1	0.048851032
Mm.155708	Etv5	0.048990735
Mm.204834	Slc1a3	0.049098014
Mm.212908	Zfp704	0.049160745
Mm.45602	Brd8	0.04924745
Mm.479548	Phf1	0.049286381
Mm.248827	Canx	0.049332202
Mm.273379	Snx5	0.049351442
Mm.327654	Lonrf3	0.049394455
---	---	0.049521736
Mm.263639	Stam2	0.049542052
Mm.251599	Zfp474	0.04969654
Mm.331129	Nes	0.04970591
Mm.21841	Sfrs2	0.049815517
Mm.476807	Mad2l1	0.049872989
Mm.297919	Zfyve26	0.049881996

Table A.2. Upregulated genes in selected N1-CKO cells versus selected WT cells

An unbiased search for significantly upregulated genes was conducted by comparing gene expression levels in cells classified as RPCs (WT cells 2-6, 8, 12) to those in cells classified as rod precursors (N1-CKO cells 1-10). T-test analysis ($p<0.05$) was performed to find significantly upregulated genes.

Table A.2 continued

UniGene ID	Gene Symbol	P-value
Mm.289915	Ddb1	0.00026739
Mm.235204	Atp1b2	0.001138192
Mm.38469	Apbb1	0.00114111
Mm.278865	Stxbp1	0.001696018
Mm.336955	Rpl10a	0.002245784
Mm.286394	Pcbp4	0.002293525
Mm.38469	Apbb1	0.002568509
Mm.1390	**Epha8**	0.002861742
Mm.4636	**Neurod1**	0.00334169
Mm.648	Prnp	0.003421822
Mm.240139	Tmprss11d	0.004231014
Mm.326167	Pkm2	0.00427551
Mm.30155	Atp6v0c	0.004515692
Mm.41758	Jam2	0.004529293
Mm.240627	Sox4	0.004993445
Mm.36726	Lad1	0.005663644
---	---	0.005710682
Mm.4636	**Neurod1**	0.005899267
Mm.205830	Gdi1	0.005959673
Mm.30155	Atp6v0c	0.00612077
Mm.444187	A330050F15Rik	0.006858951
Mm.460543	Gm3120	0.007702991
Mm.17185	Lgmn	0.007755552
Mm.180546	Ormdl3	0.008332806
Mm.300931	Col13a1	0.008684795
---	AA409368	0.009259921
Mm.30837	Ndrg1	0.009329179
Mm.4987	Ibsp	0.009353643
Mm.130362	Top2b	0.009640026
Mm.209041	Igdcc4	0.010233617
Mm.3746	Naca	0.010257474
Mm.210323	Acsl1	0.010675444
Mm.180003	Gm9354	0.010765376
Mm.2381	Aplp1	0.010798864
Mm.395281	Aff4	0.010826124
Mm.112933	Adamts5	0.010995183
---	6030422H21Rik	0.011285891
Mm.302754	1600002K03Rik	0.011366235
Mm.209041	Igdcc4	0.011798379

Table A.2 continued

Mm.379893	Glcci1	0.011894064
Mm.116802	Nfatc2	0.012640015
---	BC094435	0.013018896
Mm.259333	Pik3r1	0.013230788
---	---	0.01341365
Mm.784	Nbr1	0.01366448
Mm.10929	Fmo2	0.014062156
Mm.2395	Ccdc72	0.014084087
Mm.289707	Fscn1	0.015145813
---	9030407C09Rik	0.015336333
---	---	0.015594769
Mm.10695	**Neurod4 (Math3)**	0.015826691
Mm.30837	Ndrg1	0.016074927
Mm.270382	Yipf5	0.016238359
Mm.133083	Prss27	0.016304614
Mm.102470	Ankrd33b	0.01656729
Mm.280784	Ppp1cc	0.017479914
---	---	0.017493526
Mm.431334	Rpl18a	0.018151649
Mm.7821	Gm3258 /// Supt4h1	0.018379475
Mm.544	Pea15a	0.018405415
Mm.210787	Glcci1	0.018408025
Mm.274493	Vcpip1	0.018575996
---	4930544L18Rik	0.018775847
Mm.196595	Gc	0.019351606
Mm.75260	6430710C18Rik	0.019362348
Mm.285969	Armcx2	0.019586011
Mm.151293	Nlgn2	0.019718811
Mm.261984	Glo1	0.019765922
---	1700003I16Rik	0.019941546
---	1700016D18Rik	0.020018257
Mm.10510	Fcna	0.020030917
Mm.284811	Unc119	0.020052861
Mm.76694	1110067D22Rik	0.020336482
Mm.371590	Tpd52	0.020351458
Mm.6898	Naip1	0.02037353
Mm.458319	Ankzf1 /// Glb1l	0.020507645
Mm.400747	Epha4	0.020686211
Mm.76694	1110067D22Rik	0.021346021
---	---	0.021599416
Mm.218717	Vps26b	0.022144458

Table A.2 continued

Mm.229466	Macrod2	0.02221454
Mm.221298	Arf3	0.02249916
Mm.84774	4921501E09Rik	0.022749891
---	---	0.022883919
Mm.88349	Tmem50a	0.023198955
Mm.266611	Gpsm1	0.023422481
Mm.3503	Krtap8-2	0.02361533
Mm.245270	Rgl1	0.023809869
Mm.86541	BC094435 /// Ccrn4l /// Cog6 /// Gm4671 /// Sgip1	0.023847327
---	4930515G13Rik	0.023918411
Mm.441031	---	0.023974447
Mm.30038	Epb4.1	0.024023425
Mm.130752	Ash1l	0.024089851
Mm.9001	Nlk	0.024450641
Mm.10695	**Neurod4 (Math3)**	0.02469134
Mm.30155	Atp6v0c	0.02473745
Mm.207619	Iqgap1	0.024789748
Mm.361172	---	0.024807431
Mm.441340	Kif6	0.02486935
Mm.38578	BC024659	0.024893268
Mm.35803	Katnal2	0.025257514
---	4930542C12Rik	0.025376678
Mm.259260	Mxd4	0.025580572
Mm.146779	Srrm4	0.025966135
Mm.425294	Sh2b2	0.026130742
Mm.63068	Ss18l1	0.026298415
Mm.271724	Dtx3 /// LOC100045005	0.026449213
Mm.159149	Gsdma2	0.026700369
---	4833403J16Rik	0.026734876
Mm.213408	Ttc3	0.026738503
Mm.190	Xcl1	0.026965181
Mm.45953	Snap25	0.027661483
---	Mup4	0.027714472
Mm.444145	---	0.028114344
Mm.4800	**Prdm1 (Blimp1)**	0.028258839
Mm.252514	Kcnip1	0.028394761
Mm.5090	Tdgf1	0.028436284
Mm.159258	Clip3	0.02917019
Mm.252406	Fam161a	0.029524509
Mm.375091	Ncrna00081	0.029649039

Table A.2 continued

Mm.86507	Cog3	0.029691221
Mm.39739	Hspa12a	0.029725902
Mm.321312	Wdr70	0.029841688
Mm.218473	Serinc3	0.029871511
---	Gpr137b-ps	0.029926311
Mm.290655	Rasa4	0.029930625
Mm.200497	Hadha	0.030273672
---	1810012K16Rik	0.030538127
Mm.45274	Klb	0.030870157
Mm.20929	Herc2	0.030896579
---	4933440K10Rik	0.030904984
Mm.379269	Gpr137b /// Gpr137b-ps /// LOC100044979	0.031150656
---	6030458A19Rik	0.031310059
Mm.250641	Kidins220	0.031320413
Mm.265060	Slc19a1	0.031369202
Mm.103477	Npr2	0.031599038
Mm.430709	C430048L16Rik	0.031799694
Mm.80685	Crocc	0.031927822
Mm.219627	Pgam2	0.031935507
Mm.40298	Trib1	0.031947054
Mm.285969	Armcx2	0.032455613
---	5730405N03Rik	0.03247655
Mm.3644	Fabp7	0.032620629
Mm.260288	Ppp2ca	0.032670092
Mm.314056	Trim27	0.032774085
Mm.372826	Mbd6	0.032911781
Mm.379178	Btf3l4	0.033411371
Mm.270382	Yipf5	0.03352551
Mm.41969	Lce1a1	0.033615617
Mm.272794	Got1l1	0.033769308
Mm.297753	A4gnt	0.03388748
Mm.4406	Mmp9	0.03392681
Mm.17166	Arid2	0.03398543
Mm.205625	Atp13a2	0.034098191
---	AI849538	0.034177707
Mm.1860	Pitpnm1	0.034293578
Mm.40213	Lingo3	0.034521103
---	2010107H07Rik	0.034873147
Mm.295246	Os9	0.034958583
Mm.382099	---	0.034991198
Mm.441140	Proz	0.035028402

Table A.2 continued

Mm.198119	Rabif	0.035072162
Mm.41423	Endod1	0.035085917
---	Rmst	0.035258305
Mm.25856	Gtf3c3	0.035357624
Mm.2381	Aplp1	0.035722575
Mm.25788	Ccdc93	0.03576795
Mm.41903	1200014J11Rik	0.035861091
Mm.35483	Sbf1	0.036228449
Mm.265060	Slc19a1	0.036908744
Mm.329776	Tmem2	0.037168506
Mm.478296	Trib2	0.037343085
Mm.275158	Naa38	0.037613496
Mm.266611	Gpsm1	0.037761062
Mm.389334	Ddb2	0.037795988
Mm.29353	Higd2a	0.037851103
Mm.4465	Fbxw2	0.03793239
Mm.28349	Ndufv3	0.037947774
Mm.439921	Tnnc1	0.037955378
Mm.68889	Gnb3	0.038009277
Mm.439779	---	0.038021306
Mm.23488	Tmem161a	0.03809829
Mm.151308	Dpf3	0.038213261
Mm.119717	Btrc	0.038637343
Mm.479246	Mrvi1	0.038908
Mm.248779	Pop1	0.038939191
Mm.328602	Cxx1a /// Cxx1b	0.038951636
Mm.133301	Lrrc3	0.038969384
Mm.154358	Cyfip2	0.038977948
Mm.28357	Map1lc3b	0.039030513
Mm.259333	Pik3r1	0.039068887
Mm.293696	Glb1l2	0.039153989
Mm.28825	Pou6f1	0.039276761
---	4930483C01Rik	0.039342504
---	C78444	0.039583194
Mm.23010	Mrpl41	0.039614299
Mm.261218	Pcgf3	0.039693726
Mm.379227	Tubb2b	0.039712674
---	C030013G03Rik	0.039922389
Mm.371590	Tpd52	0.040036267
Mm.225649	Fam53b	0.040100119
Mm.332901	Ppp1r9a	0.040207121

Table A.2 continued

Mm.443421	Lce3b	0.040510651
Mm.159671	Edaradd	0.040716329
Mm.441911	**Crx**	0.040974006
Mm.259197	Rbm5	0.041039716
Mm.142843	Herpud2	0.041319722
Mm.222272	Clasp2	0.041391007
Mm.1605	Pdcd4	0.04149192
Mm.229141	Arfgef1	0.041598321
Mm.208919	Angptl2	0.041795402
Mm.142187	Ptms	0.041799488
Mm.261984	Glo1	0.041899147
Mm.257997	Igsf3	0.042010688
Mm.265060	Slc19a1	0.042338867
Mm.377079	Cyp11b2	0.0423647
Mm.205625	Atp13a2	0.04264654
Mm.439963	Lrrc17	0.042678796
Mm.235550	Esrrb	0.042779705
Mm.461107	Gm2164	0.042802212
Mm.389465	Cd1d2	0.042844035
Mm.131555	A630007B06Rik	0.043020727
Mm.4272	Snai2	0.043065721
---	4930403O18Rik	0.043104247
Mm.298728	Nisch	0.043322442
Mm.193539	Hist1h1c	0.043385214
Mm.463028	BC003883	0.043435961
Mm.2386	Scg3	0.043509765
Mm.478864	Impact	0.04363916
Mm.286394	Pcbp4	0.043639285
Mm.8655	Cfh	0.043780757
Mm.276063	Scyl1	0.043783946
Mm.159681	Rpap2	0.044189608
---	9430063H18Rik	0.044308773
Mm.441372	Papolb	0.044406557
Mm.86759	Mgat4b	0.044522964
Mm.86446	Klhl36	0.044695187
Mm.318042	Elavl2	0.044785547
Mm.255241	Chgb	0.044825605
Mm.17461	Stk16	0.045002329
Mm.44530	Kcnd3	0.045074722
Mm.98583	2210010C17Rik	0.045238754
Mm.157648	5730403B10Rik	0.04537022

Table A.2 continued

Mm.389330	Ubr1	0.045709472
Mm.141230	Agpat3	0.046031038
Mm.182377	B4galt4	0.046044311
Mm.446631	---	0.046054799
Mm.2560	Rundc3a	0.046064218
Mm.2180	Hsp90ab1	0.046216933
---	Ppp4r1l	0.046292312
Mm.277540	Exph5	0.046380416
Mm.375471	Gm10471 /// Speer4b	0.046457696
Mm.478340	Plaa	0.046625965
Mm.130610	Mfsd8	0.046844162
Mm.26147	Bach1	0.046949775
Mm.210323	Acsl1	0.047099109
Mm.259653	Rasa1	0.047507364
---	---	0.047617317
Mm.28908	Adam9	0.047678136
Mm.248296	Taok3	0.047714204
Mm.4128	Axl	0.047756263
Mm.155573	Wdr31	0.047962611
Mm.309526	Zfat	0.047986416
Mm.142187	Ptms	0.048287291
---	3110005L21Rik	0.048571644
Mm.142872	Hnrnpk	0.048628434
Mm.445781	Olfr66	0.048638297
Mm.10137	Il16	0.048693066
Mm.42829	Sepw1	0.048709556
Mm.330897	Hnf4g	0.048737401
Mm.76649	Vcam1	0.048817651
Mm.28219	Cdipt	0.048862681
Mm.379129	Eef1g	0.048863714
Mm.41075	Drd4	0.048923741
Mm.373919	---	0.04934486
Mm.272803	Pcbp3	0.049516433
Mm.284446	Aldh2	0.049691377
---	1700012O15Rik	0.04985789
Mm.478873	Cttnbp2	0.049968284

Table A.3. Gene identities

Affymetrix identifier, Unigene number, gene symbol, and gene title are listed for all genes depicted in heatmaps in Figures 2.3, 2.5, 2.6, 2.7.

Table A.3 continued

Probe Set ID	UniGene ID	Gene Symbol	Gene Title
1416776_at	Mm.9114	Crym	crystallin, mu
1417312_at	Mm.55143	Dkk3	dickkopf homolog 3 (Xenopus laevis)
1417506_at	Mm.12239	Gmnn	geminin
1417911_at	Mm.4189	Ccna2	cyclin A2
1417985_at	Mm.46539	Nrarp	Notch-regulated ankyrin repeat protein
1417999_at	Mm.4266	Itm2b	integral membrane protein 2B
1418054_at	Mm.10695	Neurod4 (Math3)	neurogenic differentiation 4
1418102_at	Mm.390859	Hes1	hairy and enhancer of split 1 (Drosophila)
1418304_at	Mm.156506	Cdhr1	cadherin-related family member 1
1418310_a_at	Mm.41653	Rlbp1	retinaldehyde binding protein 1
1418317_at	Mm.142856	Lhx2	LIM homeobox protein 2
1418376_at	Mm.3904	Fgf15	fibroblast growth factor 15
1418497_at	Mm.7995	Fgf13	fibroblast growth factor 13
1418558_at	Mm.478898	Rax	retina and anterior neural fold homeobox
1418705_at	Mm.441911	Crx	cone-rod homeobox containing gene
1419302_at	Mm.103615	Heyl	hairy/enhancer-of-split related with YRPW motif-like
1419324_at	Mm.250732	Lhx9	LIM homeobox protein 9
1419341_at	Mm.1390	Epha8	Eph receptor A8
1419628_at	Mm.4405	Vsx2	visual system homeobox 2
1419944_at	Mm.380027	Ccnb1	Cyclin B1
1420425_at	Mm.4800	Prdm1 (Blimp1)	PR domain containing 1, with ZNF domain
1420981_a_at	Mm.479165	Lmo4	LIM domain only 4
1421996_at	Mm.85544	Tcfap2a	transcription factor AP-2, alpha
1422694_at	Mm.29729	Ttyh1	tweety homolog 1 (Drosophila)
1423146_at	Mm.137268	Hes5	hairy and enhancer of split 5 (Drosophila)
1424103_at	Mm.29087	Atg4b	autophagy-related 4B (yeast)
1424118_a_at	Mm.272969	Spc25	SPC25, NDC80 kinetochore complex component, homolog (S. cerevisiae)
1424547_at	Mm.342160	Car10	carbonic anhydrase 10
1424944_at	Mm.440882	Pcp2	Purkinje cell protein 2 (L7)
1425041_at	Mm.386765	Lhx3	LIM homeobox protein 3
1425105_at	Mm.436622	Rbp3	retinol binding protein 3, interstitial
1425926_a_at	Mm.134516	Otx2	orthodenticle homolog 2 (Drosophila)
1426236_a_at	Mm.210745	Glul	glutamate-ammonia ligase (glutamine synthetase)
1426508_at	Mm.1239	Gfap	glial fibrillary acidic protein
1426681_at	Mm.297706	Unk	unkempt homolog (Drosophila)
1426817_at	Mm.4078	Mki67	antigen identified by monoclonal antibody Ki 67

Table A.3 continued

1427185_at	Mm.132788	Mef2a	myocyte enhancer factor 2A
1427482_a_at	Mm.119320	Car8	carbonic anhydrase 8
1429994_s_at	Mm.271190	Cyp2c65	cytochrome P450, family 2, subfamily c, polypeptide 65
1432466_a_at	Mm.305152	Apoe	apolipoprotein E
1433939_at	Mm.336679	Aff3	AF4/FMR2 family, member 3
1435021_at	Mm.8004	Gabrb3	gamma-aminobutyric acid (GABA) A receptor, subunit beta 3
1435670_at	Mm.137021	Tcfap2b	transcription factor AP-2 beta
1436205_at	Mm.326702	Nfasc	neurofascin
1436634_at	Mm.212826	Robo3	roundabout homolog 3 (Drosophila)
1436847_s_at	Mm.28038	Cdca8	cell division cycle associated 8
1436888_at	Mm.137286	Nhlh2	nescient helix loop helix 2
1437195_x_at	Mm.39253	Mapk10	mitogen-activated protein kinase 10
1437458_x_at	Mm.200608	Clu /// LOC100046120	clusterin /// similar to clusterin
1437828_s_at	Mm.2437	Wdr46	WD repeat domain 46
1438118_x_at	Mm.268000	Vim	vimentin
1438782_at	Mm.321683	Cntn4	contactin 4
1439377_x_at	Mm.289747	Cdc20	cell division cycle 20 homolog (S. cerevisiae)
1440487_at	Mm.167882	Dcc	deleted in colorectal carcinoma
1447676_x_at	Mm.331185	S100a16	S100 calcium binding protein A16
1447745_at	Mm.250786	Aqp4	aquaporin 4
1448314_at	Mm.281367	Cdk1	cyclin-dependent kinase 1
1448752_at	Mm.1186	Car2	carbonic anhydrase 2
1448996_at	Mm.426094	Rom1	rod outer segment membrane protein 1
1449145_a_at	Mm.28278	Cav1	caveolin 1, caveolae protein
1449159_at	Mm.68889	Gnb3	guanine nucleotide binding protein (G protein), beta 3
1449179_at	Mm.440883	Pdc	phosducin
1450920_at	Mm.22592	Ccnb2	cyclin B2
1450945_at	Mm.222178	Prkca	protein kinase C, alpha
1450946_at	Mm.20422	Nrl	neural retina leucine zipper gene
1451115_at	Mm.1635	Pias3	protein inhibitor of activated STAT 3
1451534_at	Mm.255667	Scgn	secretagogin, EF-hand calcium binding protein
1451582_at	Mm.42102	Tulp1	tubby like protein 1
1451826_at	Mm.103669	Cabp5	calcium binding protein 5
1451835_at	Mm.478420	Sox21	SRY-box containing gene 21
1452142_at	Mm.5260	Slc6a1	solute carrier family 6 (neurotransmitter transporter, GABA), member 1
1452240_at	Mm.266435	Celf4	CUGBP, Elav-like family member 4

Table A.3 continued

1453008_at	Mm.151594	Trnp1	TMF1-regulated nuclear protein 1
1455976_x_at	Mm.2785	Dbi	diazepam binding inhibitor
1457683_at	Mm.332838	Grik2	glutamate receptor, ionotropic, kainate 2 (beta 2)
1457946_at	Mm.134360	Sebox (Og9x)	SEBOX homeobox

Transcriptional role of cyclin D1 in development revealed by a genetic-proteomic screen

Frederic Bienvenu, Siwanon Jirawatnotai, Joshua E. Elias, Clifford A. Meyer, **Karolina Mizeracka,** Alexander Marson, Garrett M. Frampton, Megan F. Cole, Duncan T. Odom, Junko Odajima, Yan Geng, Agnieszka Zagozdzon, Marie Jecrois, Richard A. Young, X. Shirley Liu, Constance L. Cepko, Steven P. Gygi, Piotr Sicinski

Contributions: K.M. performed *in vivo* injections of NIN and NIN-NICD viruses into cyclinD1 null retinas and analyzed data. (Figure 4, a-c)

nature Vol 463|21 January 2010|doi:10.1038/nature08684

LETTERS

Transcriptional role of cyclin D1 in development revealed by a genetic–proteomic screen

Frédéric Bienvenu[1], Siwanon Jirawatnotai[1,5]*, Joshua E. Elias[2]*†, Clifford A. Meyer[3]*, Karolina Mizeracka[4], Alexander Marson[6], Garrett M. Frampton[6], Megan F. Cole[6], Duncan T. Odom[7], Junko Odajima[1], Yan Geng[1], Agnieszka Zagozdzon[1], Marie Jecrois[1], Richard A. Young[6], X. Shirley Liu[3], Constance L. Cepko[4], Steven P. Gygi[2] & Piotr Sicinski[1]

Cyclin D1 belongs to the core cell cycle machinery, and it is frequently overexpressed in human cancers[1,2]. The full repertoire of cyclin D1 functions in normal development and oncogenesis is unclear at present. Here we developed Flag- and haemagglutinin-tagged cyclin D1 knock-in mouse strains that allowed a high-throughput mass spectrometry approach to search for cyclin D1-binding proteins in different mouse organs. In addition to cell cycle partners, we observed several proteins involved in transcription. Genome-wide location analyses (chromatin immunoprecipitation coupled to DNA microarray; ChIP-chip) showed that during mouse development cyclin D1 occupies promoters of abundantly expressed genes. In particular, we found that in developing mouse retinas—an organ that critically requires cyclin D1 function[3,4]—cyclin D1 binds the upstream regulatory region of the *Notch1* gene, where it serves to recruit CREB binding protein (CBP) histone acetyltransferase. Genetic ablation of cyclin D1 resulted in decreased CBP recruitment, decreased histone acetylation of the *Notch1* promoter region, and led to decreased levels of the Notch1 transcript and protein in cyclin D1-null (*Ccnd1*$^{-/-}$) retinas. Transduction of an activated allele of Notch1 into *Ccnd1*$^{-/-}$ retinas increased proliferation of retinal progenitor cells, indicating that upregulation of Notch1 signalling alleviates the phenotype of cyclin D1-deficiency. These studies show that in addition to its well-established cell cycle roles, cyclin D1 has an *in vivo* transcriptional function in mouse development. Our approach, which we term 'genetic–proteomic', can be used to study the *in vivo* function of essentially any protein.

To study the molecular functions of cyclin D1 during development and in cancer formation, we generated knock-in mouse strains in which tandem (Flag and haemagglutinin (HA)) tags were inserted into the endogenous cyclin D1 (*Ccnd1*) locus through homologous recombination in embryonic stem cells. Tags were introduced into the amino terminus (*Ccnd1*^{Ntag} allele) or the carboxy terminus (*Ccnd1*^{Ctag}) of cyclin D1, and homozygous *Ccnd1*$^{Ntag/Ntag}$ and *Ccnd1*$^{Ctag/Ctag}$ mice were obtained (Supplementary Fig. 1). We reasoned that tagged knock-in mice would allow us to use sequential immunoaffinity purifications with anti-Flag and anti-HA antibodies, followed by repeated rounds of extensive, high-throughput mass spectrometry, to determine the repertoire of cyclin D1-interacting proteins in different mouse organs under normal conditions, or during tumorigenesis.

In tissues of knock-in animals, the expression of the tagged cyclin D1 mirrored the levels of wild-type cyclin D1 in control animals, and the tagged cyclin D1 retained the ability to interact with its known protein partners and to activate Cdk-kinase activity (Supplementary Fig. 2). Moreover, tagged cyclin D1 afforded normal development of cyclin D1-dependent compartments and restored normal breast cancer susceptibility in homozygous *Ccnd1*$^{tag/tag}$ animals, showing that the tagged protein is fully functional *in vivo* (Supplementary Fig. 3).

In proteomic analyses, we focused on embryonic brains, retinas, mammary glands of postpartum females and mammary carcinomas arising in *MMTV-ErbB2* females, as these compartments were shown to critically require cyclin D1 function[3–5]. We purified cyclin D1-containing complexes from these compartments (Fig. 1a), and the identities of cyclin D1-associated proteins were determined by exhaustive rounds of 'shotgun' liquid chromatography and tandem mass spectrometry (LC–MS/MS).

Among cyclin D1 interactors, we detected known cell cycle partners of cyclin D1, including the cyclin-dependent kinases Cdk4 and Cdk6, and cell cycle inhibitors from Kip/Cip and Ink families. We also observed interaction with Cdk1, Cdk2, Cdk5 and Cdk11, and found that the quantitative composition of these cyclin D1-containing complexes varies between organs (Fig. 1b, Supplementary Tables 1–3 and Supplementary Fig. 4a).

Screening the list of interactors for ontology categories showed enrichment for cell cycle ($P = 0.025$), as expected, but also for transcriptional regulation ($P = 0.040$) and apoptosis ($P = 0.084$) (Fig. 1c). Indeed, on the basis of *in vitro* and cell culture analyses, D-cyclins were postulated to have Cdk-kinase-independent functions in transcription by acting as molecular bridges between DNA-bound transcription factors and chromatin-modifying enzymes[6–8]. Cyclin D1 was shown to interact with these proteins through domains that are distinct from the one required for Cdk-binding and activation[9–11]. Our proteomic analyses suggested that cyclin D1 may indeed play a transcriptional function *in vivo*, during mouse development. For this reason, we decided to study the link between cyclin D1 and transcriptional machinery further.

We used chromatin immunoprecipitation coupled to DNA microarray analysis (ChIP-chip) to study the association of cyclin D1 with genomic DNA sequences. Because anti-Flag antibodies have been successfully used for ChIP-chip in several systems including murine cells[12], mice expressing tagged cyclin D1 provided us with a tool to query the association of cyclin D1 with the genome.

We immunoprecipitated cyclin D1, along with associated DNA sequences from embryonic day (E)14.5 tagged knock-in embryos using anti-Flag antibodies, and hybridized immunoprecipitated DNA onto

[1]Department of Cancer Biology, Dana-Farber Cancer Institute, and Department of Pathology, Harvard Medical School, [2]Department of Cell Biology, Harvard Medical School, [3]Department of Biostatistics and Computational Biology, Dana-Farber Cancer Institute and Harvard School of Public Health, [4]Department of Genetics, Harvard Medical School, Boston, Massachusetts 02115, USA. [5]Institute of Molecular Biosciences, Mahidol University, Salaya, Nakhon Prathom, 73170 Thailand. [6]Whitehead Institute for Biomedical Research and Department of Biology, Massachusetts Institute of Technology, Cambridge, Massachusetts 02142, USA. [7]Cancer Research UK-Cambridge Research Institute, Li Ka Shing Centre, Cambridge CB2 0RE, UK. †Present address: Stanford University School of Medicine, Stanford, California 94305, USA.
*These authors contributed equally to this work.

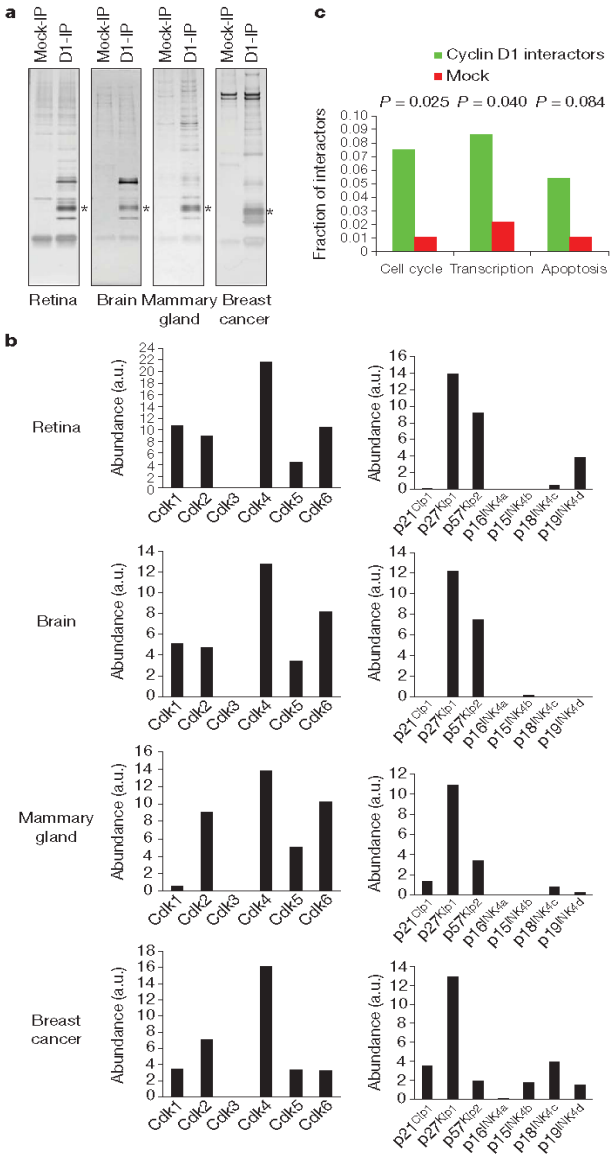

Figure 1 | Proteomic analyses of cyclin D1-associated proteins. **a**, Silver-stained gels with cyclin D1-containing complexes purified from indicated organs (D1-IP). Mock-IP, mock purification from organs of wild-type mice. Bands corresponding to cyclin D1 are marked by an asterisk. **b**, Relative abundance (arbitrary units, a.u.) of Cdks and cell cycle inhibitors in cyclin D1-containing complexes in different compartments. **c**, Fraction of proteins among cyclin D1 interactors and among 'mock' purified proteins classified to indicated Gene Ontology categories.

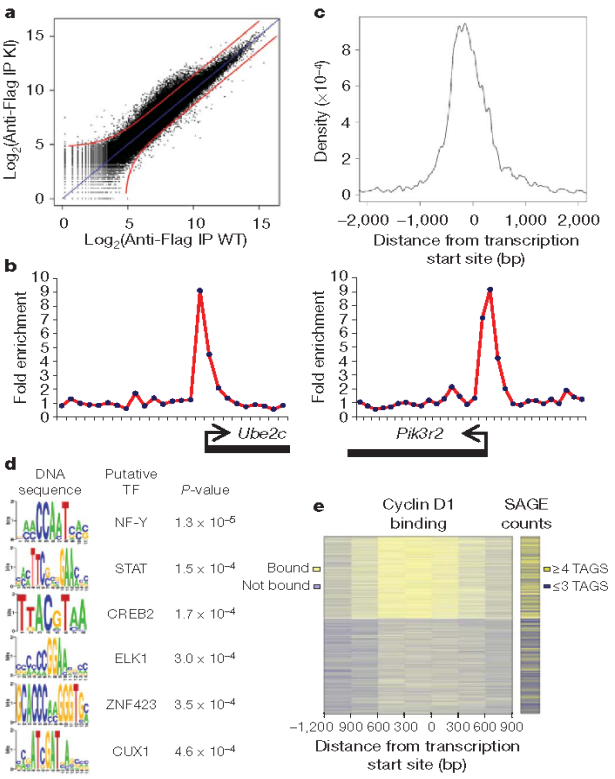

Figure 2 | Analyses of cyclin D1 interaction with the mouse genome. **a**, Scatterplot of chromatin immunoprecipitation with an anti-Flag antibody. Log_2 intensity values of immunoprecipitation from knock-in (KI) embryos are plotted against values from wild-type (WT) embryos. **b**, Examples of cyclin D1-bound regions. Plots show unprocessed ChIP-enrichment ratios for all probes within a genomic region. **c**, Location of cyclin D1-binding sites relative to transcription start sites of RefSeq genes. **d**, Conserved DNA sequence motifs identified among cyclin D1-bound regions. **e**, Left, unsupervised clustering of cyclin D1-binding events, identified in whole-embryo ChIP-chip. Each horizontal line represents one gene, centred around the transcriptional start site. Yellow and blue depict bound and not bound probes, respectively. Right, the number of tags observed for a given transcript (yellow: ≥4 tags; blue: ≤3 tags).

arrays. We detected binding of cyclin D1 to promoter regions (more than 900 at highest-stringency threshold, $P < 1 \times 10^{-4}$; Fig. 2a, Supplementary Fig. 5a, b and Supplementary Tables 4 and 5). Analyses of the exact location of cyclin D1 binding events showed that cyclin D1 interacts with DNA in close proximity to transcription start sites (in 79% of cases within 1 kb) (Fig. 2b, c). A bioinformatics search for conserved DNA sequence motifs among cyclin D1-bound genomic fragments identified six enriched ($P < 0.0005$) motifs that correspond to DNA-recognition sequences for transcription factors NF-Y, STAT, CREB2, ELK1, ZNF423 and CUX1 (Fig. 2d). Physical interaction of cyclin D1 with these transcription factors was verified using immunoprecipitation–western blotting (Supplementary Fig. 4b).

To study the transcriptional function of cyclin D1 at a mechanistic level, and to test its biological significance, we focused on developing retinas. This organ critically requires cyclin D1 function, as evidenced by severe retinal hypoplasia in cyclin D1-null mice[3,4]. We found an 80% overlap between cyclin D1 targets identified in the whole-embryo ChIP-chip versus targets identified in retinas (Supplementary Fig. 5c and data not shown).

Gene expression in developing mouse retinas had previously been profiled at several time points using serial analysis of gene expression (SAGE), thereby providing a quantitative measure of the levels of particular transcripts[13]. We queried retinal SAGE libraries (http://cepko.med.harvard.edu/) against our ChIP-chip data, to test the correlation between the binding of cyclin D1 to gene promoters and the abundance of these transcripts. We found that genes whose promoters are bound by cyclin D1 belong to the abundantly expressed genes ($P < 1 \times 10^{-15}$) (Fig. 2e).

Genes that are highly expressed in many tissues were shown to have a high content of CpG dinucleotides in their promoter regions[14]. We

performed a computational comparison of CpG content within cyclin D1-bound versus all other promoters. Cyclin D1-bound promoters were highly enriched for CpG dinucleotide ($P < 1 \times 10^{-15}$) (Supplementary Fig. 6a), further strengthening the notion that cyclin D1 occupies promoters of abundantly expressed genes.

We next asked whether in retinal cells cyclin D1 is brought to DNA by sequence-specific transcription factors. As mentioned earlier, we observed the enrichment of NF-Y DNA recognition sequences among cyclin D1-bound genomic fragments (Fig. 2d), and verified physical association of cyclin D1 with Nf-y (Supplementary Fig. 4b). We knocked-down the Nf-ya subunit in *in vitro* cultured rat retinal precursor R28 cells and found that this diminished the recruitment of cyclin D1 to several Nf-y target promoters (Supplementary Fig. 7). These findings indicate that cyclin D1 interacts with DNA through DNA-bound transcription factors.

To determine whether cyclin D1 functioned to positively or negatively regulate transcription of target genes *in vivo*, we compared gene expression profiles between wild-type and cyclin D1-knockout[4] retinas using microarrays (Supplementary Fig. 6b and Supplementary Table 6), and overlaid the data with ChIP-chip promoter-occupancy results. Among cyclin D1-bound genes, we observed genes with increased as well as decreased levels in *Ccnd1*$^{-/-}$ retinas (Fig. 3a, Supplementary Fig. 8 and Supplementary Table 7), suggesting that cyclin D1 can serve both to activate and downregulate gene expression.

Inspection of the list of genes bound by cyclin D1 and showing altered expression in cyclin D1-null retinas, revealed the presence of *Notch1*—an essential regulator of retinal progenitor cell proliferation[15,16]—along with several transcriptional regulators that probably contribute in this process (*Id3*, *Id1*, *Mrg1* (also known as *Meis2*) and *Tcf4*)[17–19]. We verified binding of cyclin D1 to upstream regulatory regions of these genes (Fig. 3b and Supplementary Fig. 9) and their altered expression in cyclin D1-null retinas (Fig. 3c and Supplementary Fig. 6c).

The rate-limiting role of Notch1 in retinal development is well-established, and retinal-specific ablation of the *Notch1* gene leads to a proliferative failure that resembles the cyclin D1-null phenotype[3,4,20]. Despite overall hypoplasia, *Ccnd1*$^{-/-}$ retinas display an excess of photoreceptor cells, with reduction of early-born horizontal and amacrine cells, again resembling fate-specification defects seen in Notch1-knockout retinas[20,21]. For this reason we investigated further the cyclin D1–Notch1 connection.

Activation of Notch1 during retinal development leads to upregulation of *Hes5*, which in turn represses the expression of proneural bHLH genes *Math5* (also known as *Atoh7*) and *Neurod1*. Consequently, in Notch1-knockout retinas, *Hes5* is downregulated, whereas *Math5* and *Neurod1* genes are de-repressed[22,23]. We found that in *Ccnd1*$^{-/-}$ retinas *Hes5* transcript levels were decreased, whereas *Neurod1* levels were increased, suggesting that Notch signalling is compromised in cyclin D1-knockout retinas (Fig. 3d). We also found that the levels of Notch1 protein were significantly decreased in cyclin D1-null retinas (Fig. 3e). Knockdown of cyclin D1 in rat retinal precursor R28 cells decreased the levels of Notch1 transcripts and protein, whereas cyclin D1 overexpression had the opposite effect (Fig. 3f). Collectively, these observations indicate that cyclin D1 transcriptionally upregulates the *Notch1* gene during retinal development. Consequently, Notch1 transcript and protein levels, as well as Notch-dependent signalling pathways are compromised in cyclin D1-null retinas.

We next asked whether increasing Notch1 signalling in *Ccnd1*$^{-/-}$ retinas would enhance progenitor cell proliferation. We injected a retroviral construct encoding the Notch intracellular domain (NICD, a constitutively activated allele of Notch1; Supplementary Fig. 10), into subretinal space of postnatal day (P) 0 cyclin *Ccnd1*$^{-/-}$ pups, and gauged the response after ten days. Expression of NICD in *Ccnd1*$^{-/-}$ retinas significantly increased *in vivo* proliferation of retinal progenitor cells (Fig. 4a–c). Hence, restoring Notch1 signalling in cyclin D1-null progenitor cells alleviates the phenotype of cyclin D1-deficiency.

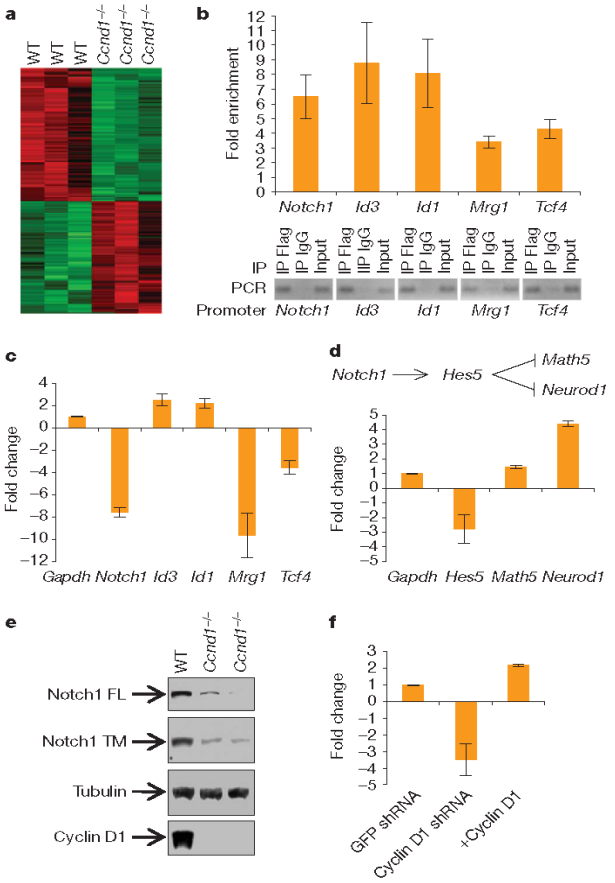

Figure 3 | Analyses of cyclin D1 transcriptional function in retina. **a**, Expression pattern of genes whose promoter regions were bound by cyclin D1, and which showed altered levels in *Ccnd1*$^{-/-}$ retinas. **b**, Binding of cyclin D1 to regulatory regions of indicated genes verified by targeted ChIP with anti-Flag antibodies (to bring down cyclin D1) using P0 retinas. **c**, **d**, Expression levels of indicated genes quantified in wild-type and *Ccnd1*$^{-/-}$ retinas by RT–PCR. Shown is the fold difference between wild-type and *Ccnd1*$^{-/-}$ retinas. **e**, Levels of Notch1 protein in retinas, determined by immunoblotting. FL, full length; TM, transmembrane. **f**, Levels of Notch1 transcripts in R28 cells, quantified by RT–PCR after knockdown of cyclin D1 (using short-hairpin RNA (shRNA)) or after overexpression of cyclin D1 (+cyclin D1). Shown is the fold difference compared to cells infected with control vector. GFP, green fluorescent protein. Error bars, s.d.

We addressed how mechanistically cyclin D1 acts on the *Notch1* promoter to increase Notch1 expression. Cyclin D1 was previously shown to physically bind histone acetyltransferases, and postulated to bring them to target promoters[7,24,25]. Indeed, our mass spectrometry analyses detected CBP acetyltransferase among cyclin D1 protein partners in developing retinas (Supplementary Tables 1 and 2); physical interaction of cyclin D1 with CBP was confirmed by immunoprecipitation–western blotting (Fig. 4d). Using targeted ChIP with anti-CBP antibodies, we determined that in developing retinas CBP binds the same upstream regulatory region of the *Notch1* gene as cyclin D1 (Fig. 4e, g and Supplementary Fig. 9). Co-localization of cyclin D1 and CBP on the *Notch1* gene regulatory region was also verified by ChIP with an anti-Flag antibody (to bring down cyclin D1) followed by re-ChIP with an anti-CBP antibody (Fig. 4e).

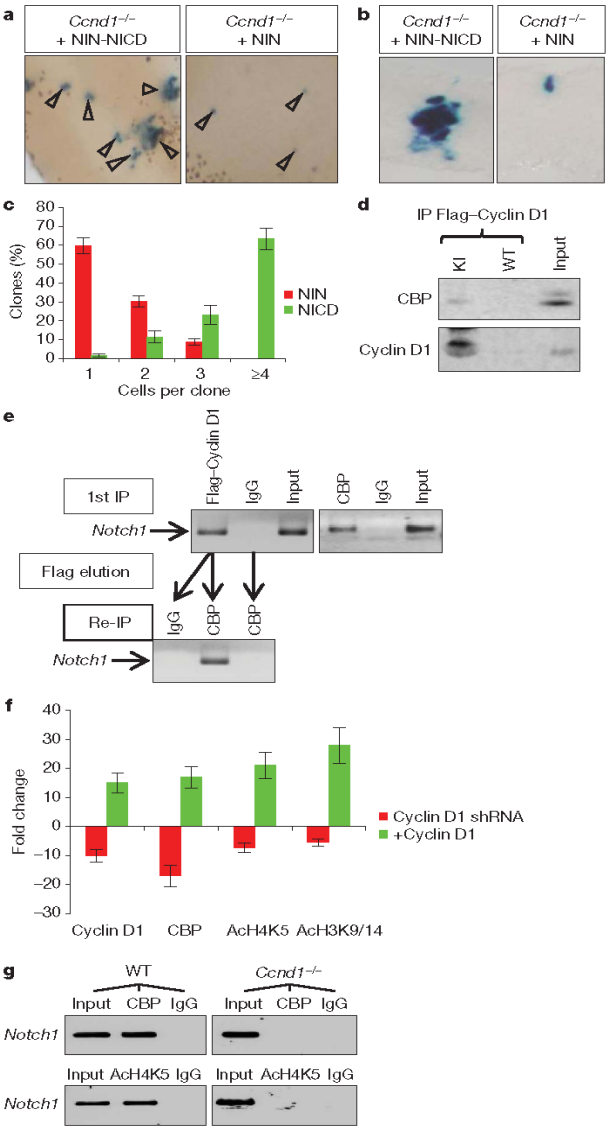

Figure 4 | *In vivo* and molecular analyses of the cyclin D1–Notch1 connection. **a**, Whole mounts of *Ccnd1*$^{-/-}$ retinas infected with viruses encoding activated Notch1 and β-galactosidase (NIN-NICD, see Supplementary Fig. 10) or with viruses encoding only β-galactosidase (NIN), stained with X-gal to visualize clones of infected cells (arrowheads). Original magnification, ×8. **b**, Higher magnifications (×20) of **a**. **c**, The percentage of β-galactosidase-positive clones composed of 1, 2, 3 and ≥4 cells. **d**, Cyclin D1 was immunoprecipitated using an anti-Flag antibody from P0 retinas and probed with indicated antibodies. **e**, Targeted ChIP on P0 retinas using anti-Flag (to bring down cyclin D1) or anti-CBP antibodies, followed by real-time PCR with *Notch1*-specific primers. Bottom panel, ChIP with anti-Flag followed by re-ChIP with anti-CBP antibodies and real-time PCR. **f**, Cyclin D1 was knocked down (cyclin D1 shRNA) or overexpressed (+cyclin D1) in R28 cells. ChIP with anti-cyclin D1, anti-CBP, anti-acetylated H4K5 (AcH4K5) or anti-AcH3K9/14 antibodies was followed by real-time PCR with *Notch1*-specific primers. The results show the fold difference compared to cells transduced with empty vectors. **g**, ChIP using anti-CBP and anti-AcH4K5 antibodies followed by real-time PCR with *Notch1*-specific primers using wild-type and *Ccnd1*$^{-/-}$ retinas. Error bars, s.d.

Knockdown of cyclin D1 in R28 cells decreased association of CBP with the *Notch1* gene. Conversely, overexpression of cyclin D1 increased binding of CBP (Fig. 4f). These results indicate that cyclin D1 functions to recruit CBP histone acetyltransferase to the *Notch1* upstream regulatory region. The Cdk4/6-inhibitor PD 0332991 had no effect on this process, suggesting a Cdk-independent function of cyclin D1 (Supplementary Fig. 11).

CBP activates gene expression by catalysing acetylation of histone residues[26]. We tested how manipulating cyclin D1 levels affects histone acetylation of the *Notch1* promoter. Knockdown of cyclin D1 in R28 cells decreased acetylation of histone H3 Lys 9/14 (H3K9/14), and H4K5 residues, whereas cyclin D1 overexpression increased their acetylation (Fig. 4f and Supplementary Fig. 9).

Furthermore, we examined molecular events within the *Notch1* gene in retinas of cyclin D1-deficient animals. We found that the recruitment of CBP to the *Notch1* gene regulatory region and acetylation of histone H4K5 on the *Notch1* promoter were diminished in cyclin D1-knockout retinas (Fig. 4g). Collectively, these analyses indicate that cyclin D1 controls expression of Notch1 in retinal progenitor cells by recruiting CBP to the *Notch1* upstream regulatory region. In the absence of cyclin D1, CBP recruitment is reduced, leading to impaired histone acetylation of the *Notch1* promoter region, and to decreased expression of the *Notch1* gene. This, in turn contributes to decreased retinal cell proliferation in cyclin D1-null animals.

The main finding of this work is the demonstration that cyclin D1 plays a transcriptional function in normal mouse development by acting at gene promoters. Although our mechanistic analyses focused on retinas, it remains to be seen whether this transcriptional function contributes to development of other cyclin D1-dependent compartments, such as mammary glands. It will be also of interest to determine whether this function of cyclin D1 contributes to cancer formation. Notch1 can function as an oncogene and several oncogenic pathways upregulate cyclin D1 (refs 27, 28). Our results indicate that cyclin D1 can serve not only as a downstream cell cycle recipient of oncogenic pathways, but also as an oncogene-activator. Of note, cyclin D1 was shown to upregulate Notch1 expression in ErbB2-positive breast cancer cells[29].

In this study, we designed a new system to study molecular functions of cyclin D1 in the mouse. We call this approach 'genetic–proteomic', because it combines genetic manipulations in the mouse germ line with proteomic mass spectrometry analyses. In the future this system can be applied to study tissue-specific functions of essentially any protein in mice and other model systems such as zebrafish or *Drosophila*, at any physiological or pathological state.

METHODS SUMMARY

Generation of tagged cyclin D1 knock-in mouse strains is described in the Supplementary Methods. For one purification round of cyclin D1-containing complexes, we used pooled 15 brains dissected E14.5 knock-in embryos, 40 eyes from P0 neonates, 5–6 mammary glands collected 1 day after delivery of pups, or 1–2 mammary adenocarcinomas arising in *MMTV-ErbB2* females. The same number of organs from wild-type mice was used for mock purifications. Details of protein purification, mass spectrometry and bioinformatics analyses are described in the Supplementary Methods. For ChIP-chip or targeted ChIP, cyclin D1 was immunoprecipitated using an anti-Flag antibody (M2 Sigma) from one-fifth of ten pooled E14.5 knock-in (or for control wild-type) embryos, or from one-fifth of 200 pooled retinas dissected from P0 neonates, and used for real-time PCR, or hybridized onto promoter BCBC 5A arrays (Beta Cell Biology Consortium) or hybridized onto tiled Agilent promoter arrays. Pooled retinas dissected from P0 wild-type or *Ccnd1*$^{-/-}$ neonates were used for targeted ChIP. Details and PCR primer sequences are described in the Supplementary Methods. For expression analyses, retinas were microdissected from P0 *Ccnd1*$^{-/-}$ or wild-type littermates. Total RNA was extracted from pooled 20 retinas using an RNeasy Mini Kit (Qiagen); biotinylated complementary RNA probes were prepared according to standard protocols, and hybridized to Affymetrix GeneChip Mouse Expression Set 430 2.0 arrays. Hybridizations were performed in triplicate. Reverse transcription real-time PCR (RT–PCR) to quantify transcript levels was performed as described in Supplementary Methods. The rat retinal precursor

cell line R28 was cultured as described[30]. *In vivo* retroviral infections were done as before[20] (see Supplementary Methods).

Received 18 June; accepted 18 November 2009.

1. Malumbres, M. & Barbacid, M. Cell cycle, CDKs and cancer: a changing paradigm. *Nature Rev. Cancer* **9,** 153–166 (2009).
2. Sherr, C. J. & Roberts, J. M. CDK inhibitors: positive and negative regulators of G1-phase progression. *Genes Dev.* **13,** 1501–1512 (1999).
3. Fantl, V., Stamp, G., Andrews, A., Rosewell, I. & Dickson, C. Mice lacking cyclin D1 are small and show defects in eye and mammary gland development. *Genes Dev.* **9,** 2364–2372 (1995).
4. Sicinski, P. *et al.* Cyclin D1 provides a link between development and oncogenesis in the retina and breast. *Cell* **82,** 621–630 (1995).
5. Yu, Q., Geng, Y. & Sicinski, P. Specific protection against breast cancers by cyclin D1 ablation. *Nature* **411,** 1017–1021 (2001).
6. Coqueret, O. Linking cyclins to transcriptional control. *Gene* **299,** 35–55 (2002).
7. McMahon, C., Suthiphongchai, T., DiRenzo, J. & Ewen, M. E. P/CAF associates with cyclin D1 and potentiates its activation of the estrogen receptor. *Proc. Natl Acad. Sci. USA* **96,** 5382–5387 (1999).
8. Fu, M. *et al.* Cyclin D1 inhibits peroxisome proliferator-activated receptor gamma-mediated adipogenesis through histone deacetylase recruitment. *J. Biol. Chem.* **280,** 16934–16941 (2005).
9. Adnane, J., Shao, Z. & Robbins, P. D. Cyclin D1 associates with the TBP-associated factor $TAF_{II}250$ to regulate Sp1-mediated transcription. *Oncogene* **18,** 239–247 (1999).
10. Inoue, K. & Sherr, C. J. Gene expression and cell cycle arrest mediated by transcription factor DMP1 is antagonized by D-type cyclins through a cyclin-dependent-kinase-independent mechanism. *Mol. Cell. Biol.* **18,** 1590–1600 (1998).
11. Zwijsen, R. M., Buckle, R. S., Hijmans, E. M., Loomans, C. J. & Bernards, R. Ligand-independent recruitment of steroid receptor coactivators to estrogen receptor by cyclin D1. *Genes Dev.* **12,** 3488–3498 (1998).
12. Marson, A. *et al.* Foxp3 occupancy and regulation of key target genes during T-cell stimulation. *Nature* **445,** 931–935 (2007).
13. Blackshaw, S. *et al.* Genomic analysis of mouse retinal development. *PLoS Biol.* **2,** e247 (2004).
14. Saxonov, S., Berg, P. & Brutlag, D. L. A genome-wide analysis of CpG dinucleotides in the human genome distinguishes two distinct classes of promoters. *Proc. Natl Acad. Sci. USA* **103,** 1412–1417 (2006).
15. Alexson, T. O., Hitoshi, S., Coles, B. L., Bernstein, A. & van der Kooy, D. Notch signaling is required to maintain all neural stem cell populations–irrespective of spatial or temporal niche. *Dev. Neurosci.* **28,** 34–48 (2006).
16. Jadhav, A. P., Cho, S. H. & Cepko, C. L. Notch activity permits retinal cells to progress through multiple progenitor states and acquire a stem cell property. *Proc. Natl Acad. Sci. USA* **103,** 18998–19003 (2006).
17. Flora, A., Garcia, J. J., Thaller, C. & Zoghbi, H. Y. The E-protein Tcf4 interacts with Math1 to regulate differentiation of a specific subset of neuronal progenitors. *Proc. Natl Acad. Sci. USA* **104,** 15382–15387 (2007).
18. Heine, P., Dohle, E., Bumsted-O'Brien, K., Engelkamp, D. & Schulte, D. Evidence for an evolutionary conserved role of homothorax/Meis1/2 during vertebrate retina development. *Development* **135,** 805–811 (2008).
19. Yeung, S. C. & Yip, H. K. Developmental expression patterns and localization of DNA-binding protein inhibitor (Id3) in the mouse retina. *Neuroreport* **16,** 673–676 (2005).
20. Jadhav, A. P., Mason, H. A. & Cepko, C. L. Notch 1 inhibits photoreceptor production in the developing mammalian retina. *Development* **133,** 913–923 (2006).
21. Das, G., Choi, Y., Sicinski, P. & Levine, E. M. Cyclin D1 fine-tunes the neurogenic output of embryonic retinal progenitor cells. *Neural Dev.* **4,** 15 (2009).
22. Hatakeyama, J. & Kageyama, R. Retinal cell fate determination and bHLH factors. *Semin. Cell Dev. Biol.* **15,** 83–89 (2004).
23. Yaron, O., Farhy, C., Marquardt, T., Applebury, M. & Ashery-Padan, R. Notch1 functions to suppress cone-photoreceptor fate specification in the developing mouse retina. *Development* **133,** 1367–1378 (2006).
24. Fu, M. *et al.* Cyclin D1 represses p300 transactivation through a CDK-independent mechanism. *J. Biol. Chem.* **280,** 29728–29742 (2005).
25. Ratineau, C., Petry, M. W., Mutoh, H. & Leiter, A. B. Cyclin D1 represses the basic helix-loop-helix transcription factor, BETA2/NeuroD. *J. Biol. Chem.* **277,** 8847–8853 (2002).
26. McManus, K. J. & Hendzel, M. J. Quantitative analysis of CBP- and P300-induced histone acetylations *in vivo* using native chromatin. *Mol. Cell. Biol.* **23,** 7611–7627 (2003).
27. Musgrove, E. A. Cyclins: roles in mitogenic signaling and oncogenic transformation. *Growth Factors* **24,** 13–19 (2006).
28. Ronchini, C. & Capobianco, A. J. Induction of cyclin D1 transcription and CDK2 activity by $Notch^{ic}$: implication for cell cycle disruption in transformation by $Notch^{ic}$. *Mol. Cell. Biol.* **21,** 5925–5934 (2001).
29. Lindsay, J. *et al.* ErbB2 induces Notch1 activity and function in breast cancer cells. *Clin. Transl. Sci.* **1,** 107–115 (2008).
30. Seigel, G. M. Establishment of an E1A-immortalized retinal cell culture. *In Vitro Cell. Dev. Biol. Anim.* **32,** 66–68 (1996).

Supplementary Information is linked to the online version of the paper at www.nature.com/nature.

Acknowledgements We thank T. Liu, Y. Ndassa-Colday, J. Marto, R. Bronson, B. Smith, E. Jacobsen, M. Brown and members of the Brown laboratory for help at different stages of the project, M. Ewen for p-Babe-puro-Cyclin D1 and cyclin D1(K112E) plasmids, G. Seigel for R28 cells, T. Volkert, J. Love and E. Fox for help with arrays, P. White and O. Smirnova for help with BCBC arrays. This work was supported by grants R01 CA108420, P01 CA080111 and P01 CA109901 (to P.S.), HG3456 (to S.P.G.), R01 EYO9676 (to C.L.C.), HG004069 (to X.S.L.), Cancer Research UK, European Research Council Starting Grant, and an EMBO Young Investigator Award (all to D.T.O.). P.S. is a Leukemia and Lymphoma Society Scholar.

Author Contributions F.B. and P.S. designed the study, analysed the data and wrote the manuscript. F.B. performed the experiments with the help of co-authors as detailed below. S.J. performed protein purifications. J.E.E. performed and together with S.P.G. analysed and interpreted mass spectrometry analyses. C.A.M. and X.S.L. contributed biocomputational analyses, K.M. and C.L.C. contributed *in vivo* transduction of cyclin D1-null retinas with Notch1, A.M., G.M.F., M.F.C., D.T.O. and R.A.Y. contributed to analyses of ChIP-chip and gene expression data, J.O., Y.G., A.Z. and M.J. helped with the experiments. P.S. directed the study.

Author Information The complete ChIP-chip and expression datasets have been submitted to the online data repository Gene Expression Omnibus (GEO; http://www.ncbi.nlm.nih.gov/geo/), under accession GSE13636. Reprints and permissions information is available at www.nature.com/reprints. The authors declare no competing financial interests. Correspondence and requests for materials should be addressed to P.S. (Peter_Sicinski@dfci.harvard.edu).